BEAM

Botanical Eradication and Management Machine

EEL 4915 | Senior Design 2 | Fall 2024 | Group 1

Authors:

TJ Jones

Electrical Engineering

Suhyun Hwang

Photonic Science Engineering

Daemy Luzardo

Electrical Engineering

Ryan Takiff

Electrical Engineering

Reviewer Committee:

Prof. Mark Maddox

Dr. Peter Delfyett

Dr. Mohsen Rakhshan

Instructors:

Dr. Chung Yong Chan

Dr. Wei Lei

Dr. Aravinda Kar

Chapter 1 – Executive Summary 1

Chapter 2 – Project Description 2

2.1 Background and Motivation 2

2.2 Goals/Objectives 3

2.2.1 Hardware Goals 4

2.2.1.1 Basic Goal 4

2.2.1.2 Advanced Goal 4

2.2.1.3 Stretch Goal 4

2.2.2 Software Goals 4

2.2.2.1 Basic Goals 5

2.2.2.2 Advanced Goals 5

2.2.2.3 Stretch Goals 5

2.3 Description of Features and Functionalities 5

2.3.1 Navigation 5

2.3.2 Rechargeable Power System 6

2.3.3 Weed Detection 6

2.3.4 Weed Elimination 7

2.3.5 Smartphone Application 7

2.4 Block Diagrams 8

2.4.1 Hardware 8

2.4.2 Software 9

2.5 Engineering Requirements Specifications 9

2.6 Past and Existing Projects' Comparison 10
2.7 House of Quality 13
Chapter 3 – Technology Research and Part Selection 14
3.1 Technologies 14
3.1.1 Microcontrollers 14
3.1.1.1 MCU 14
3.1.1.2 FPGA 15
3.3.1.2 MCU vs FPGA 16
3.1.2 Motors 17
3.1.2.1 DC Brushed Motors 20
3.1.2.2 Brushless DC Motors 20
3.1.2.3 Gear Motors 21
3.1.2.4 AC Motors 21
3.1.2.5 Stepper Motors 21
3.1.3 Motor Controllers 22
3.1.3.1 Pulse Width Modulation (PWM) 22
3.1.3.2 H-Bridge Motor Driver 23
3.1.4 Wheels 24
3.1.4.1 Mecanum Wheel 24
3.1.4.2 Omni Wheel 24
3.1.4.3 Orientable Wheel 24
3.1.4.4 All-Terrain Wheel 24

3.1.5 Batteries 25
3.1.5.1 Lithium Ion 26
3.1.5.2 Lead-Acid 27
3.1.6 Charge Controllers 27
3.1.6.1 Pulse-Width Modulation (PWM) 28
3.1.6.2 Maximum Power Point Tracking (MPPT) 29
3.1.7 Voltage Regulation 30
3.1.7.1 Linear Regulator 30
3.1.7.2 Buck Converter (Switching Regulators) 31
3.1.8 Solar Panels 32
3.1.8.1 Monocrystalline 32
3.1.8.2 Polycrystalline 33
3.1.8.3 Thin-Film 33
3.1.9 Laser Control System 33
3.1.9.1 Stepper Motors 33
3.1.9.2 Stepper Motor Drivers 34
3.1.10 Laser Diode 34
3.1.10.1 Laser Diodes VS LED 35
3.1.10.2 Laser Wavelength 38
3.1.10.3 Laser Temperature 40
3.1.11 Movement Control Sensors 44
3.1.11.1 Lidar 44

3.1.11.2 Sonar 45
3.1.12 Weed Identification Sensors 45
3.1.12.1 RGB Camera 45
3.2 Part Selection 46
3.2.1 Lithium Ion Battery 46
3.2.2 MPPT Charge Controller 47
3.2.3 Buck Converter (Switching Regulator) 47
3.2.4 Monocrystalline Solar Panel 48
3.2.5 Motors 48
3.2.6 Motor Control 50
3.2.7 Wheels 50
3.2.8 MCUs 51
3.2.8.1 Arduino MKR WAN 1300 (Specified for long range motor control and diagnostics) 51
3.2.8.2 Alternative to Arduino: ESP32-WROOM-32 board 52
3.2.8.3 Raspberry Pi 4 Model B (Specified for Object Detection and Computer Vision) 52
3.2.9 Movement Control Sensors 53
3.2.9.1 Lidar 54
3.2.10 Weed Identification Sensors 55
3.2.10.1 RGB Camera 55
3.2.11 Laser Diode 56
3.2.12 NEMA 17 Stepper Motor 58

3.2.13 Stepper Motor Driver 58
Chapter 4 – Design Constraints and Standard 59
4.1 Design Constraints 59
4.1.1 Environmental Constraints 60
4.1.2 Economic Constraints 62
4.1.2.1 Market and Competition 62
4.1.2.2 Reducing Costs in Labor and Pesticides 63
4.1.3 Manufacturability Constraints 64
4.1.4 Health and Safety Constraints 64
4.2 Industrial Design Standards 65
4.2.1 Standards for Lithium-Based Batteries 65
4.2.2 Standards for Charge Controllers 65
4.2.3 Standards for Solar Panels 66
4.2.4 Standards for Motors 66
4.2.5 Standards for Motor Controllers 67
4.2.6 Standards for Laser Safety 68
4.2.7 Standards for MCU 69
Chapter 5 – Comparison of Chat GPT and Similar Platforms 70
5.1 Chat GPT Pros 70
5.2 Chat GPT Cons 77
Chapter 6 – Hardware Design 81

6.1 Hardware 81
6.1.1 Materials and Design 81
6.1.2 Electrical Power System and Power Delivery 81
6.1.2.1 FET Selection Criteria 83
6.1.3 Motor Control 86
6.1.4 MCU ESP/Raspberry Pi Plugin 89
6.1.5 Laser System 89
6.1.5.1 Lens 90
6.1.5.2 Intensity of Laser Beam 97
6.1.5.3 Beam Waist 98
6.2 Breadboard Testing 103
6.2.1 DRV8255 and NEMA 17 Stepper Motor Testing 104
6.2.2 Laser Diode Testing 105
6.2.3 DC Motors 105
Chapter 7 – Software Design 107
7.1 Object Detection 112
7.2 ROS and Micro-ROS 114
7.3 SLAM Mapping, Lidar, and Gazebo 115
Chapter 8 – System Fabrication/Prototype Construction 116
8.1 Beam Dimensions and Levels 116
8.2 PCB 116

Chapter 9 – System Testing and Evaluation 122
9.1 Navigation Motor Control Testing 122
9.2 Object Detection Testing 122
9.3 Power System Testing 123
9.4 Laser System Testing 124
9.5 DC Motor Testing 124
9.6 Laser Testing 126
Chapter 10 – Administrative Content 131
10.1 Budget and Financing 131
10.2 Project Milestones 133
10.2.1 Senior Design I 133
10.2.2 Senior Design II 134
10.3 Distribution of Workload 134
10.3.1 Senior Design I 135
10.3.2 Senior Design II 136
Chapter 11 – Conclusion 138
Appendix A - References 139
Appendix B – Copyright Permissions 157
Appendix C – Software Code 157

List of Figures

Figure 1 - Hardware Graphic 6

Figure 2 - Cartesian System for Laser Control 7

Figure 3 - BEAM Hardware Diagram 8

Figure 4 - BEAM software diagram 9

Figure 5 - Carbon Robotics LaserWeeder [9]. 11

Figure 6 - Tertill Weeding Robot [14] 12

Figure 7 - Motor Part-Load Efficiency [24] 19

Figure 8 - PWM Duty Cycle [28] 23

Figure 9 – H-Bridge Circuit [29] 23

Figure 10 - Battery 3-stage charging (bulk, absorb, float) [42] 28

Figure 11 - © Wikimedia Commons / Daniele Pugliesi, M0tty 40

Figure 12 - Average Temperature by Month [67] 42

Figure 13 - Orlando Humidity by Month [67]. 61

Figure 14 - Original Image 'a' inserted to MATLAB 76

Figure 15 - Code applied to MATLAB 76

Figure 16 - Fourier Transformed Image 77

Figure 17 – Buck converter circuit diagram 85

Figure 18 – Navigation Motor Control Schematic (SDI) 87

Figure 19 - DC Motor Driver PCB (SD2) 88

Figure 20 - MCU/PCB Connections Schematic (DATA PINS ONLY) 89

Figure 21 - 3DOptix Simulation with One Focus Lens 93

Figure 23 - 3DOptix Simulation with Two Focus Lenses 94

Figure 22 – Laser Beam Alignment Diagram 94

Figure 24 - Schematic of Two Lenses 96

Figure 25 – 3D Scchematic of Beam Expander Lenses 97

Figure 26 Characteristics of Gaussian Beam Waist w(z) 99

Figure 27 - Characteristics of the Gaussian Beam Radius of Curvature 100

Figure 28 – Lens System with a Single Thin Lens 102

Figure 29 - Horizontal & Vertical Beam Diameter over Treatment Distance 102

Figure 30 – Laser Control System Schematic Diagram 103

Figure 31– DRV8255, Arduino Uno, and Stepper Motor Connections [147] 104

Figure 32 – DC Motor Driver Breadboard Test 106

Figure 33 - Raspberry Pi Object Detection Workflow 107

Figure 34 - MCU to PBC Flowchart 108

Figure 35 - ESP32 Motor Control Flowchart 109

Figure 36 - LCS Flowchart 110

Figure 37 - Raspberry Pi Application Interaction Flowchart 111

Figure 38 – Labels for Object Detection 112

Figure 39 – Object Detection Model Set 113

Figure 40 – BEAM Level Diagram 116

Figure 41– Power Regulator PCB 117

Figure 42 - MCU PCB 118

Figure 43 – Navigation Motor Control PCB 119

Figure 44- DC Motor Driver PCB (SD2) 120

Figure 45 – Overall Schematics for BEAM..... 121

Figure 46 – DC Motor PCB Test 125

Figure 47 – PWM signal from ESP for four motors. 125

Figure 48 - DC motor setup 126

Figure 49 - Horizontal & Vertical Beam Diameter over Treatment Distance 127

Figure 50 - *Relationship Between Laser Intensity and Distance for Weed Burning* 128

Figure 51- Laser Setup..... 129

Figure 52 - *Weed Treatment Before & After*..... 129

Figure 53 - Appearance of Treated Weeds After 1 Day (Left) & 2 Day (Right) 130

List of Tables

Table 1- Engineering requirements and specifications..... 10

Table 2 - Marketing requirements..... 10

Table 3 - House of quality 13

Table 4 - House of quality correlation matrix..... 13

Table 5 - MCU Vs FPGA Comparison..... 17

Table 6 – Motor Vocabulary..... 18

Table 7 - Battery Terminology [34]..... 25

Table 8 - Battery comparison [35]..... 26

Table 9 – Charge controller comparison..... 27

Table 10 - Voltage Regulator Comparison [49] 30

Table 11 – Solar Panel Comparison..... 32

Table 12 - Optics Terminology..... 35

Table 13 – Comparison of LEDs and Laser Diodes (reprinted with permission) [60]..... 36

Table 14- Difference between Chlorophyll A VS B [64]..... 39

Table 15 - Orlando Monthly Temperature [67]..... 42

Table 16 - Weather Factors in Orlando [68]..... 43

Table 17 - 5W Laser Diode Specifications..... 44

Table 18 - Peak Power Information per Component..... 46

Table 19 - Battery Selection Comparison..... 47

Table 20–MPPT Charge Controller Selection Comparison..... 47

Table 21 – Buck Converter Selection..... 48

Table 22– Solar Panel Selection..... 48

Table 23-Brushed DC Motors Comparison..... 49

Table 24 – H-Bridge Motor Driver Comparison..... 50

Table 25 – All-Terrain Wheels Comparison..... 51

Table 26 – MCU Feature Comparison..... 53

Table 27 – Table of Movement Control Sensors..... 54

Table 28 – Table of LIDAR Options..... 55

Table 29 - Comparison Table of RGB Cameras..... 56

Table 30 - 1-2 W Blue Laser Diode Comparison..... 57

Table 31 - 5W Laser Diode Specifications..... 57

Table 32 - 2W Red Laser Diode Specifications..... 58

Table 33 – NEMA 17 Stepper Motor Selection 58

Table 34 – Stepper Motor Driver Selection 59

Table 35 – TPS40200-Q1 Design Parameters 82

Table 36 – FDC654P MOSFET Information 83

Table 37 – FET Selection Equation List and Definitions 84

Table 38 - Beam Divergence Angle 92

Table 39 - Collimating Lens Specification 92

Table 40- Focus Lens Specification [142] 93

Table 41 - Beam Expander Lenses 95

Table – Budget 132

List of Equations

(1) Total Torque Formula 18

(2) Angular Velocity Formula 19

(3) Power Formula for Rotational Motion 19

(4) Current Formula 19

(5) Battery Capacity Formula 20

(6) - Linear Regulator Power Dissipation 31

(7) – Power Efficiency 82

(8) – Power Loss 82

(9) – DC Conduction Loss 83

(10) – Minimum Inductance for FET 84

(11) – Voltage Ripple Equation 85

(12) Numerical Aperture of Laser Diode [141] 91

(13) Distance between Two Lenses 95

(14) Magnification Factor 96

(15) Light Intensity 97

(16) Intensity of Laser Beam 98

(17) Radius of a Gaussian Beam 98

(18) Rayleigh Range 99

(19) Beam Divergence Angle 99

(20) - Current limit for stepper motor 104

(21) Area of an Ellipse 127

Chapter 1 – Executive Summary

The Botanical Eradication and Management Machine (BEAM) project was created to address the significant challenge of weed control in agriculture, specifically the overuse of dangerous chemical pesticides, by developing a solar-powered autonomous robot equipped with object detection and laser technology. Weeds pose a major threat to crop health by competing for essential resources like nutrients, water, and sunlight. Traditional weed control methods, including manual weeding, mechanical removal using other large machines, and especially chemical herbicides. All of these have notable drawbacks such as high labor costs, environmental toxicity, and potential harm to non-target plants as well as soil health.

The BEAM project aims to help revolutionize weeding industry through an environmentally friendly, and precise method of weed removal. The robot is designed to navigate agricultural fields automatically, utilizing high-resolution cameras and machine learning to accurately detect and identify weeds. Once identified, a high-power laser diode targets and eliminates the weeds, effectively neutralizing them without harming surrounding crops or the environment. Additionally, the BEAM project's integration of a real-time monitoring and data collection system through a smartphone application will empower farmers with valuable insights into weed control and crop health, facilitating the farmers best informed decision-making and improved agricultural practices.

The hardware and software components of BEAM have been carefully selected and integrated to achieve an efficient performance, as well as overall reliability, and safety for the overall design but especially when implementing the use of laser-diodes to achieve the eradication of weeds. The BEAM project offers a sustainable solution to weed management that promotes better soil health and reduces negative environmental impact from agriculture. Overall, we aim to not only enhance the efficiency and effectiveness of weed control but also contribute to the broader goals of sustainable agriculture. This report details the design, development, and implementation of the BEAM robot, highlighting its potential impact on the agricultural industry.

Chapter 2 – Project Description

Our goal is to clarify the reason behind this project's concept and objectives, we outline the challenges we seek to address, accompanied by descriptions of the features of the various systems involved. This includes BEAM's specific goals concerning electrical and optical components, as well as a general comparison with past and existing projects. Additionally, we detail the engineering requirements and specifications that guide our approach along with the chosen specifications to demonstrate.

2.1 Background and Motivation

The agriculture industry and all related industries in the US accounts for approximately the 5.6% of the Gross Domestic Product (GDP) and 10.34% of U.S employment [1]. Although, its significance might not seem much, production agriculture is the leading source of economic activity in numerous counties spread throughout the country, but they concentrate in the Great Plains states towards the Midwest. The Midwest is renowned for fertile soil, a temperate climate, and plenty of water resources like rivers and aquifers which are essential for irrigation and sustaining crop growth [2]. With our project, we aim to aid in the crop production yield of farms to fight the loss of direct employment and lower than average wage in rural areas, and to make it easier for farmers, both big and small, to diversify their production since research show that it has a direct correlation with a decrease in population [3].

In agriculture, one of the the largest inhibitors of plant growth are weeds. Weeds can be any plant that grow in places humans don't want them to grow. These invasive plants can spread rapidly through fields, becoming very tedious and difficult to remove. Weeds will often grow "too well", and outcompete desired crops for nutrients, water, and sunlight [4]. This can cause great economic loss for a farm. Monitoring and controlling weed growth can greatly benefit commercial crops, and there are only a few ways to handle this problem. So far, the strategies most used by commercial farmers are manual weeding, which is paying workers to pull weeds, mechanical weeding, using a machine pulled by a tractor to uproot weeds, or chemical weeding, using pesticides to kill weeds [5].

Chemical herbicides are one of the most common tools used to remove weeds, but along with the benefits of weed removal come disadvantages from their toxicity to the environment and human health. These herbicides can be extremely toxic to livestock, fisheries, natural predators, soil microbiomes, native plants, crops, and humans [6]. The many disadvantages of chemical herbicides should outweigh the benefits, but it is still a popular technique in many countries. Our project aims to revolutionize weed removal through a combination of object recognition and lasers. The use of light radiation to burn weeds is more environmentally friendly and will promote overall crop health, prevent the destruction of soil and water microbiomes, and decrease human contact with toxic chemicals.

2.2 Goals/Objectives

The goal of our project was to build a solar-powered vehicle-type robot that uses object detection to recognize weeds and then uses a laser to remove them. The main goals and objectives are listed below.

Overall Goals

- Build a robot that is suitable for navigating a field.
- Build a laser system capable of burning weeds.
- Provide farmers with an environmentally friendly weed control method that minimizes impacts on other vital plants.

Advanced Goals

- Keep track of number of weeds lasered.
- Have a reasonable data refresh rate for the application.

Stretch Goals

- Build on the application to add a user-friendly GUI used to monitor the robot's progress.

Robot Objectives

- Be able to navigate a field without getting stuck or becoming lost.
- Be able to charge the system battery using sunlight.
- Create a simple application that keeps track of weed statistics.

Laser System Objectives

- Achieve a high-power output from the laser diode to ensure efficient moisture evaporation, allowing for quick and effective weed control.
- Design the system to be lightweight, compact, and portable for the robot, allowing it to navigate various terrains and locations with ease.
- Integrate safety features into the robot's design to prevent accidents and ensure safe operation in proximity to humans and other objects.
- Achieve acute control of the laser position for weed removal.

2.2.1 Hardware Goals

These are the goals that we wanted to be able to accomplish with the BEAM's hardware setup. These goals were divided into basic, advanced, and stretch goals.

2.2.1.1 Basic Goal

Our project's overall engineering goal was to find and identify weeds using a vehicle robot that could navigate its surroundings without becoming lost or stuck. It was also essential that our robot did not become stuck in the wet soil while navigating its area. It was designed for moderate to mild conditions, and not built for extremely muddy conditions to protect the hardware. To ensure that our robot did not become stuck in the soil or mud, we equipped the chassis with quality tires and strong motors.

2.2.1.2 Advanced Goal

An advanced hardware goal for the BEAM project was to add a sufficient cooling system for all the electronics on board. The robot was to operate outside in hot temperatures, and it was important to ensure that these components remained at an appropriate temperature during operation, as overheating could negatively impact the performance of the electronics and inhibit the robot's overall performance.

2.2.1.3 Stretch Goal

The BEAM robot was tested in Florida, where it was both hot and humid, and as such, it was important that the components onboard were appropriately sheltered and protected from rapid changes in weather conditions. The hardware stretch goal of the BEAM project was to make the robot highly water-resistant, create proper housing for each component, and modify the chassis to prevent water from penetrating the robot's infrastructure.

2.2.2 Software Goals

To obtain accurate weed identifications, we fed our object detection system many images for comparison with real plants. The data used to train the system was essential for the correct identification of crops versus weeds. The navigation system utilized mapping to ensure that the robot did not get lost or wander aimlessly. We employed a lidar system to map out the area and used coding logic to assist the robot in making navigation decisions. The start-up method we implemented for the robot involved having it map out the entire area, after which it proceeded to identify weeds and note treated locations.

2.2.2.1 Basic Goals

The basic software goals for the BEAM project included establishing direct communication between the navigation system and the motors to pilot the robot to its desired locations. This also involved communication between the weed location sensors and the laser positioning system to accurately target the correct areas beneath the robot.

2.2.2.2 Advanced Goals

An advanced goal of our project was to create a 3D active map model of the area the robot is in. This not only helps with navigation but allow for path planning and accurate location tracking for weed treatments. The 3D active map allows for enhanced spatial awareness like obstacle detection and depth perception. This is important on a farm plot with uneven surfaces and crops in the way. Using simultaneous localization and mapping (SLAM) techniques, our robot will be able to build and update maps in real-time while monitoring its location. This allows for improved route planning, and adaptability for changes in the environment such as terrain changes or moving objects.

2.2.2.3 Stretch Goals

An application for the robot would let users monitor the progress of weed removal in their field and document weed location so the user would know where problem areas are located. It would also show battery life and current location of the robot. The app would increase the amount of data provided to the user about their field, allowing them to make more informed choices about how to provide proper care for crops.

This application would let users navigate a graphical user interface allowing for easy user interaction between menus and systems. Additionally, the application allows for real time monitoring to allow the user to track the robot in action. The application should allow for a reliable communication link between the robot and itself, allowing the user to momentarily take tele-present control remotely move the robot.

2.3 Description of Features and Functionalities

In this sub-chapter discussed the robot's features such as navigation, power system, weed detection, weed elimination, and smart phone application.

2.3.1 Navigation

LiDAR technique was used to help the robot navigate by emitting laser pulses to create detailed 3D maps of their surroundings. This enabled accurate environmental mapping, obstacle detection, and avoidance. The technique supported simultaneous localization and mapping. It allowed the robot to track its position while building maps. LiDAR data

facilitated efficient path planning and dynamic path adjustments in real-time, ensuring safe and autonomous navigation in both indoor and outdoor settings.

2.3.2 Rechargeable Power System

Our outdoor robot was powered by a solar-charged power system, featuring solar panels connected to a high-capacity battery. Designed for field operations, this system used solar energy to keep the robot charged and operational throughout the day, ensuring continuous performance without the need for external power sources or overnight charging.

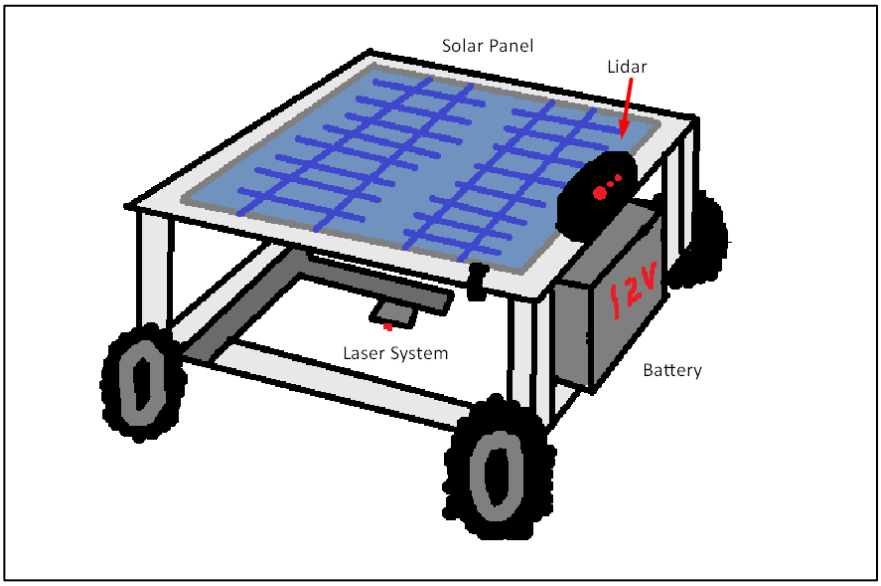

Figure 1 - Hardware Graphic

2.3.3 Weed Detection

The weed detection process began with high-resolution cameras mounted on the robot capturing images of the field. These images were then processed using machine learning algorithms to identify weeds based on their visual characteristics. Machine learning models trained on weed and crop datasets classified the objects in the images. Weeds were identified by their size, shape, color, texture, and other features. Once the weeds were detected, their positions were calculated relative to the robot's location. This information was used to precisely target and activate the laser beam onto the detected weeds for effective weed-killing. By utilizing cameras and machine learning algorithms, the robot was able to accurately detect weeds in real-time, enabling targeted weed control without harming surrounding plants.

2.3.4 Weed Elimination

To eliminate weeds effectively, we used laser diodes to evaporate plant moisture. Numerous studies and experiments had been conducted on weed elimination by cutting their stems using lasers, but Mathiassen et al. [7] introduced another way to eradicate weeds by increasing the temperature of the moisture in the plant cells to eventually delay or stop its growth. Laser diodes with different wavelengths were tested: blue, green, red, and infrared. Focusing on the objective of minimizing harm to essential plants and reducing environmental contamination, we aimed to use high-power lasers that were strong enough to heat weeds. Laser diodes enabled precise transfer of radiation energy, offering advantages for weed control such as weather-independent operation near crops and customizable dosing capabilities.[8].

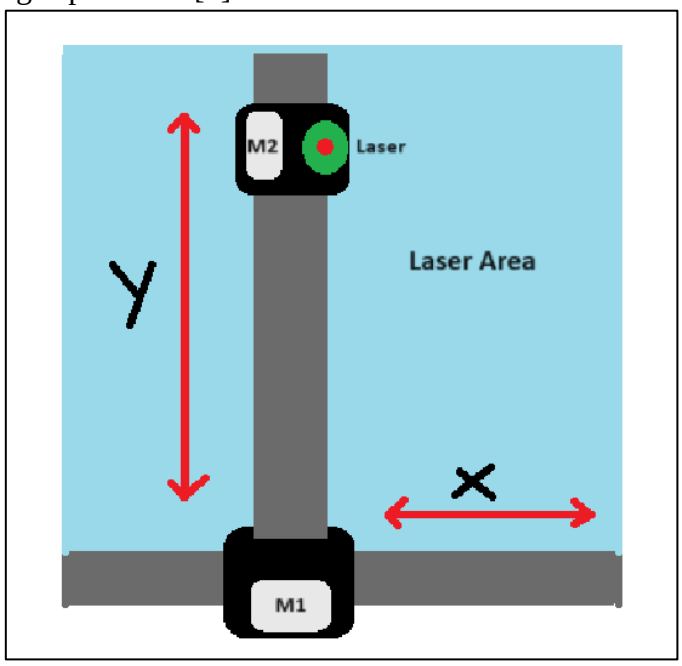

Figure 2 - Cartesian System for Laser Control

2.3.5 Smartphone Application

The application was designed to provide users with more information about weed treatment and problem areas in their field. This application was intended to be hosted on a web interface that would run on a web server. The server was planned to allow the user to control the Raspberry Pi's GPIO pins and read information from sensors through a web browser. The code to read the data from the robot's external sensors was to be executed via a Python script interacting with the MCU. This information was then to be displayed on the web server through a user interface written in Java or HTML.

2.4 Block Diagrams

The hardware and software diagrams were created to help further understanding of how all systems come together in the BEAM robot to allow for the functionality and features we want to have.

2.4.1 Hardware

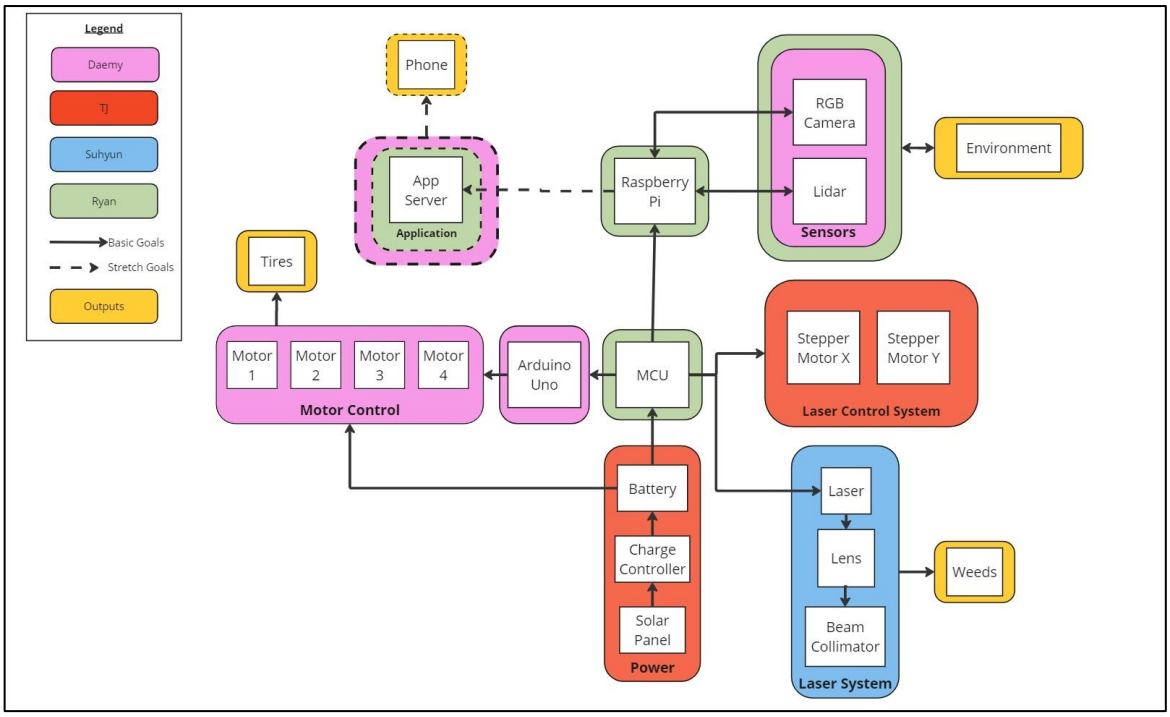

Figure 3 - BEAM Hardware Diagram

The BEAM project was divided into 6 sections: Motor control, Power management, sensors, laser system, laser control system, and the application. Daemy and Ryan worked together on the motor control system and sensors, along with the communication pathway between the Raspberry Pi, MCU, sensors, and application. TJ worked on the power management system involving the solar panel, charge controller, and battery that powered the robot. TJ also worked closely with Suhyun to calibrate the laser system and laser control to effectively target and laser weeds. Suhyun designed the laser system to find the most efficient way to evaporate water from the leaves of the weeds. As the main components of the BEAM system came together, we intended to work on the communication pathway between the application and the server.

2.4.2 Software

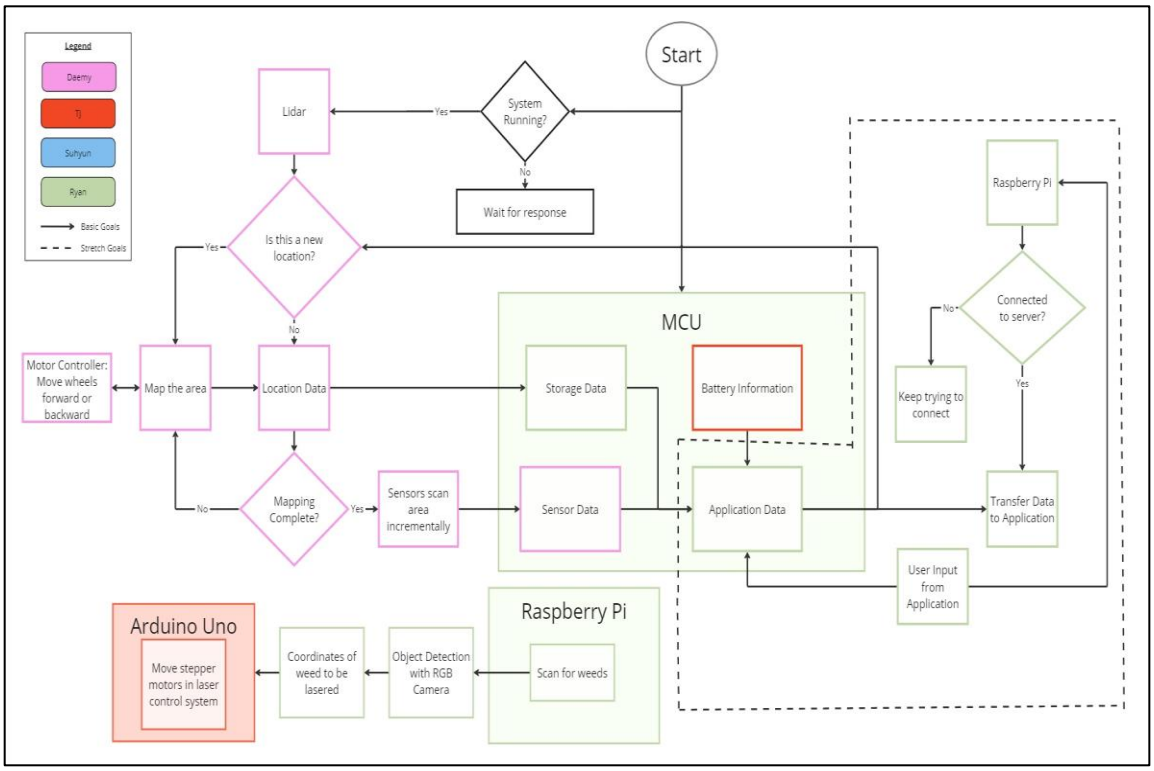

Figure 4 - BEAM software diagram

As shown in Figure 4 - BEAM software diagram, the software portion of the BEAM project was divided into mapping and location, laser control system coordination, and application information transfer. The system first determined if it needed to map an area, and then proceeded to record location information for mapping if it was in a new area. Once the mapping was complete, visual sensors like the RGB camera were used via the Raspberry Pi to detect weeds underneath the robot. The Raspberry Pi then transferred the coordinates of the weeds to the Arduino Uno so the laser control system could reposition itself to lase them. As part of our application, the weed location data corresponded to a location on the robot's mapping system so the user could track treated areas. The Raspberry Pi functioned as a server for an application to connect to, allowing data to be quickly transferred between the robot and the application.

2.5 Engineering Requirements Specifications

Demonstratable specifications are highlighted in yellow.

BEAM Engineering Requirements	
Chassis	
Length x width x height	TBD
Weight	TBD
Material	Aluminum
Solar Panel	
Max Power	6 W
Maximum Voltage	15 V
Battery	
Maximum Lifespan	10 Ah
Maximum Voltage	12.8 V
Laser Source	
Wavelength Range	450 – 550 nm
Optical Power	1000 – 5500 mW
Laser System	
Location accuracy	≤ 1 cm
Weed Treatment	
Treatment Time	≤ 30 seconds
Treatment Distance (Laser Pointer End to Plant)	3 – 4 cm
Weed Identification Efficiency	Expected at 70-85%

Table 1- Engineering requirements and specifications

Marketing Requirements
1. The Rover should not exceed the proposed object (not including replacements). 2. The Rover should accurately identify weeds. 3. The Rover should be easy to use. 4. The Rover should withstand weather changes. 5. The Rover should have low maintenance. 6. The Rover should have high performance. 7. The Rover should have moderate power consumption.

Table 2 - Marketing requirements

2.6 Past and Existing Projects' Comparison

Previously existing products and related work, like our project, include:

Carbon Robotics is a leading organization within the agricultural technology industry. Their particular niche is laser weeding technology. Their autonomous robot weeder is diesel-powered and equipped with multiple high-resolution cameras and an AI-powered

computer to aid in autonomous features. The robot is estimated to eliminate around 200,000 weeds per hour without disrupting the soil. [9]

EcoRobotix is a Swiss corporation that has developed a solar-powered weeding robot that uses cameras and GPS guidance to navigate and detect weeds. Instead of a laser, the robot targets and applies microdoses of herbicides to the individual identified weeds. The idea is to use these precisely targeted microdoses to significantly reduce overall chemical usage. This robot adapts its operation speed to the size of the field it is working on as well as the overall weed density in a given area, allowing it to remain power-efficient in most situations. [10]

LettuceBot, created by Blue River Technology, uses computer vision and image recognition to identify weeds and spray them with a precision dose of herbicide. The idea is similar to that of the EcoRobotix robot, if the weeds can be found much easier and sprayed with much higher precision with much less use of these herbicides, reducing the overall impact over time. [11]

WeedBot, based in Lavata, is planning to launch its own laser weeding robots. These aim to provide a less harmful alternative to traditional herbicides, offering precise weed control using an AI-backed algorithm for weed and crop recognition. After detection, the weeds are quickly eliminated with minimal disruption of other organic material and soil. [12]

Autonomous Diode Laser Weeding Robot, A project led by the West Central Research and Outreach Center collaborated with the University of Minnesota to develop a laser weeding robot designed specifically for use in cotton fields and to utilize deep learning for weed detection. Combining a GPS-based navigation system with visual serving allows the robot

Figure 5 - Carbon Robotics LaserWeeder [9].

to precisely target and eliminate weeds using diode lasers. Another project aims to reduce the reliance on chemical herbicides as well as improve overall sustainability. [13]

The Tertill Weeding Robot, produced by the company Tertill and developed by the inventor of Roomba, is a small weeding robot made for gardens. It is solar powered and weather resistant and uses specially designed wheels to kill emerging weeds. It also comes with a small trimmer to chop sprouted weeds and an app for users to monitor their weeding bot. [14]

Figure 6 - Tertill Weeding Robot [14]

2.7 House of Quality

The house of quality takes the information from the engineering requirements (Table 1- Engineering requirements and specifications) and the marketing requirements (Table 2) from the section 2.5 and provides matrices of correlation between them. Below there's a legend that describes what each correlation means and their polarity.

Correlation Matrix	
↑↑	Strong Positive
↑	Positive
↓	Negative
↓↓	Strong Negative
	Not Correlated

Positive Polarity	+
Negative Polarity	-

Table 4 - House of quality correlation matrix

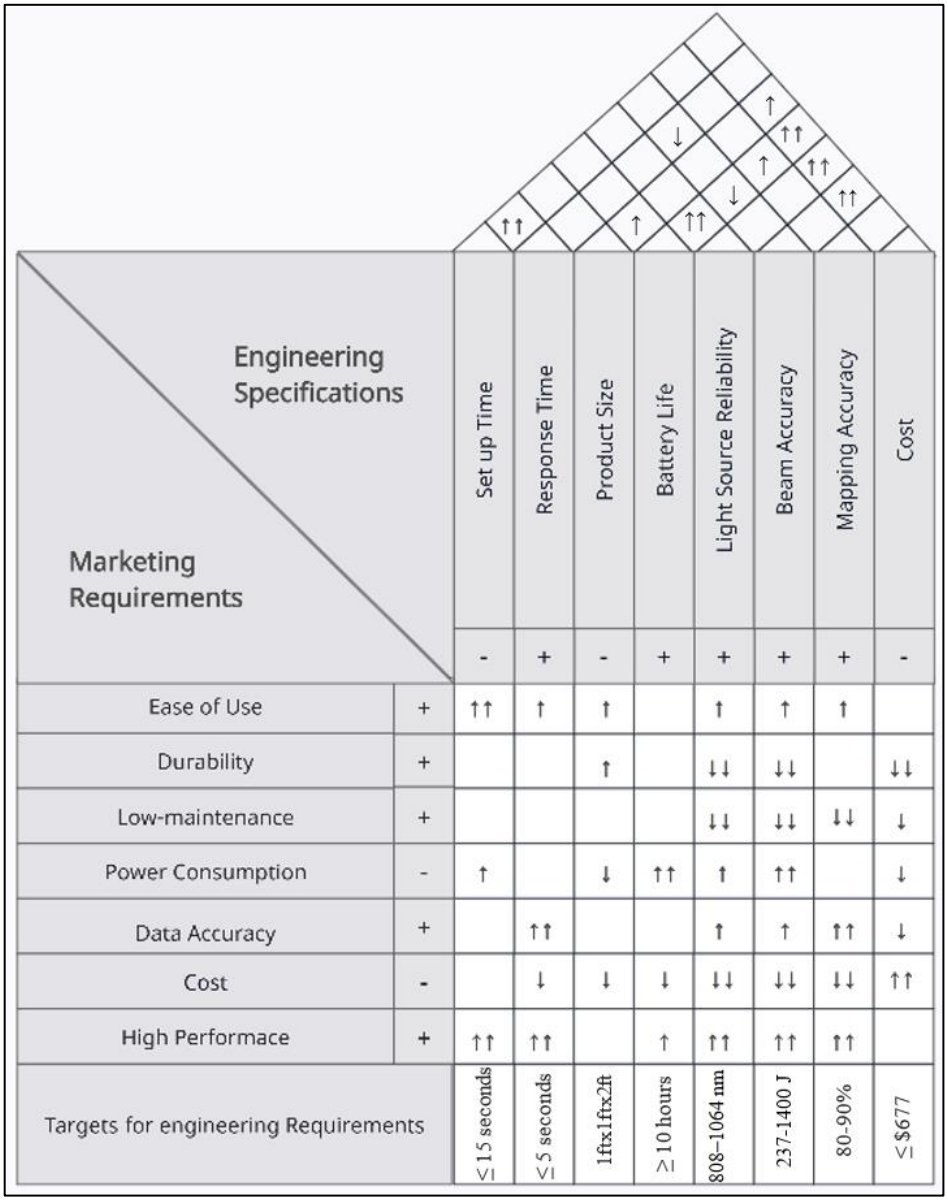

Table 3 - House of quality

Chapter 3 – Technology Research and Part Selection

By conducting side-by-side assessments, we analyzed how each technology aligns with our project goals and requirements. This includes both a general overview of the systems in place and a detailed comparison that informs our decision-making process where we selected the most appropriate technology, maximizing benefits while minimizing costs wherever possible whenever possible.

3.1 Technologies

The BEAM project required the integration of advanced technologies to ensure precise, efficient, and sustainable weed management. Key components of this system included microcontrollers, which served as the brain of the robot, coordinating actions and processing data from multiple sensors. Motors and motor controllers were essential for precise movement and control of the wheels, allowing the robot to navigate diverse terrain. Reliable energy sources, facilitated by batteries, charge controllers, and solar panels, enabled stable operation and extended operational time in the field. The core functionality of weed removal was accomplished by the advanced laser control system and laser diodes, which targeted weeds with high accuracy. Movement control sensors allowed the robot to map its surroundings and avoid obstacles, while weed identification sensors detected and differentiated weeds from crops. Researching and selecting the optimal components for these categories was crucial to enhancing the BEAM robot's efficiency, accuracy, and overall performance in the field, making it a viable solution for modern agricultural problems.

3.1.1 Microcontrollers

The microcontroller was a critical component of the project since it served as the main processing unit that could be programmed for various tasks. It was essential to consider a wide range of characteristics when choosing the correct microcontroller, as different models came with a variety of existing platforms and resources for easier programming. Additionally, it could reduce the need for additional components, simplify circuit design, and lower the overall cost of the project.

3.1.1.1 MCU

Microcontroller Units (MCUs) are circuit chips designed to execute on specific control tasks within integrated embedded systems. They usually consist of a CPU, memory, as well as programmable I/o peripherals and ports. They are used widely in various applications due to their overall low cost, ease of use, availability, and energy efficiency.

Most MCUs are designed for low power consumption making them the ideal choice for systems that need to be battery operated. They offer a myriad of power options to allow for

sleep, standby, or various other low power modes tailoring to the users' needs whenever necessary. [15] MCU's typically support multiple communication protocols and come equipped with integrated peripherals like ADCs and DACs as well as supporting I2C, UART, and other types of communication interfaces. MCUs are generally much lower cost, and compact, which is very beneficial to people looking for low cost and cost-efficient solutions for various applications it would benefit. [16] MCUs are known to support real-time processing, however it should be noted that their capabilities are limited in comparison to FPGAs, while this is the case MCUs are able to support and are suitable for many real time control applications. Most industrial MCUs are available and usable for applications requiring operating the robot or MCU in various harsh environments, obviously greater shielding and placement withing the robot may further benefit an MCU. MCUs are much easier to develop for and program with then FPGAs, this is due to the use of higher-level programming languages like C or C++, this also allows for a much greater amount of support, as these languages are much more popular and have more documentation, allowing for greater ease in troubleshooting then with any FPGA. [17] Some of the advantages an MCU helped serve our purposes are the overall ease of use and cost effectiveness compared to most other FPGAs, as well as the compact size, On-Chip integrated peripherals, as well as its low power consumption make it an easy choice for our purposes. An MCU was the type of processor we used as the main brain of the robot. However, some disadvantages we needed to tackle were the overall lack of flexibility in customization and various optimizations that FPGAs are overall better at achieving. As well as the overall limited processing power, we needed to make adjustments in the code in order to overcome these limitations.

3.1.1.2 FPGA

Field Programmable Gate Arrays or FPGAs are devices that consist of an array of logic blocks that are programmable and interconnected by routing resources. One of the key characteristics of FPGAs that differentiate them from MCUs is the ability to excel in parallel processing. Along with an overall higher performance than an MCU, this makes them very suitable for handling real time data and complex calculations. [18] These gate arrays are highly customizable, enabling them to be tailored for a myriad of applications. With the proper protection, they are suitable for industrial applications and can be configured to perform a wide variety of tasks, making them a versatile and powerful tool. Many applications that FPGAs are used for are in industrial automation. FPGAs are also widely used in the telecommunications industry as they typically require high speed data processing and transfer. [19] They are great for industrial automation applications that require custom hardware and fast performance and are beneficial to advanced robotics applications that require real time control. This also includes other weed killing robots in the industry.

FPGAs are ideal for tasks that have excessive parallelism as well as require high speed processing, as well as data encryption. FPGAs would potentially suit our purposes better

than an MCU, however due to certain flaws, they are unlikely to be applicable to this project. While it has been established that FPGAs have much higher processing speeds and are well suited to applications in real time systems, this comes at the expense of much higher power consumption than MCUs, making them less suited to battery operated robots or other applications. [20] Additionally, FPGAs have a much more complicated programing and development cycle then an MCU. Requiring an expertise in HDLs and other specialized development tools would prove to be complicated and stop us from taking full advantage of these resources. Another major disadvantage our project would incur if we decided to use an FPGA would be its much higher initial cost in hardware. These processors usually take up more space, which would had affected our PCB design as we would have needed to compensate for the space somewhere in the design. The increase in the cost alone would normally disqualify it from use from our project, and especially considering a lot of the other disadvantages, FPGAs while incredibly useful, was not the right processor for the BEAM project.

3.3.1.2 MCU vs FPGA

When deciding on the specifications of a project's hardware, it is likely that the discussion between FGPAs and MCUs and their corresponding advantages and disadvantages take place. Without this context, the reason for deciding between the two may become muddied and confusing. To start, one of the main advantages FPGAs have over MCUs is their ability to do parallel processing. This makes tasks that would otherwise take a much longer time easily processed in a much faster time than a regular MCU would be able to. Additionally, the FGPA's must use more complicated programming languages like Verilog, which provide quite a steep learning curve. This is directly opposed to the MCU's ease of use in programming languages such as C or C++. [20] While these are not easy to program with, the documentation and resources available to help navigate difficult debugging questions are much easier to describe and diagnose than with another less documented and more complicated programming language, such as Verilog.

Another major comparison between the two is the power consumption of both processor types. Generally, the power consumption of the FPGA is much higher than that of the MCU. This is due to the parallel processing mentioned before; the FPGAs have high-speed clocks and can often operate at much higher frequencies, which typically results in decreased overall power consumption. [21] This may be advantageous for certain applications, due to the limited power supply as well as the dynamic power generated by the solar panels. It was better for our purposes to use an MCU, as the MCU was designed for more portable, battery-powered machines. This is due to its overall power efficacy, offering low power modes and dynamic power management features. For these reasons, we feel as if an MCU was a better choice of processor than the FPGA alternatives. Some qualities to consider when picking out the correct MCU needed for the job go as follows: processing power, overall complexity, peripheral support, memory, communication interfaces, environmental

tolerances, and real-time processing. These are the metrics to which the MCUs will be compared and contrasted; multiple tables are provided at the end for viewing convenience.

MCU Vs FPGA [22]		
Parameter	MCUs	FPGAs
Processing Power	Moderate, typically up to 480 MHz	High, excellent for parallel processing and high-speed tasks
Power Consumption	Low, suitable for battery-operated devices	Higher, generally higher power consumption
Peripheral Support	Extensive integrated peripherals (ADC, DAC, timers, communication interfaces)	Highly customizable, flexible peripheral integration
Memory	Varies (e.g., up to 2 MB Flash, 1 MB RAM)	Depends on design, typically large capacity
Communication Interfaces	Supports multiple protocols (I2C, SPI, UART, CAN)	Supports multiple protocols, customizable
Environmental Tolerance	Industrial-grade versions available	Suitable for outdoor use with appropriate enclosures
Real-time Processing	Limited real-time processing capabilities	High, ideal for minimal latency and precise control
Development Complexity	Easier to program (C/C++), extensive development tools and libraries	Complex to program (HDLs like VHDL or Verilog), steeper learning curve
Cost	Lower cost	Higher initial cost, both in hardware and development

Table 5 - MCU Vs FPGA Comparison

3.1.2 Motors

A motor is a machine that converts electric energy into mechanical energy by the interaction of the field current and the magnetic field, making the armature rotate (this will be joined to the wheels). There are several different types of motors that can be subdivided into many categories, however, to decide which one is better suited for our project we must look into distinct aspects such as weight capacity, size, torque, etc.

The first step was to calculate some of the motors' specifications, RobotShop Community [23] offers a tool designed to give you some of the basic outputs desired for your motor depending on the following:

Input	Outputs
a = acceleration = 0.2 m/s^2	T = total Torque
g = acceleration due to gravity = 9.8 m/s^2	W = angular velocity
θ = degrees on the incline = 20°	P = total power
M = total mass of the robot = 9.071 kg	I = Maximum current
R = radius of wheels = 0.0635 m	c = battery pack capacity
N = number of drive motors = 4	
v = speed = 0.2 m/s	

Table 6 – Motor Vocabulary

They take the inclined plane formula, torque formula, and calculate for the total Torque.

$$T = \frac{(a + g * \sin(\theta)) * M * R}{N}$$

(1) Total Torque Formula

$T = \frac{(.2+9.8*\sin(20^\circ))*9.071*0.0635}{4} = 511.466 * 10^{-3}\ Nm$ This answer provides the torque at a 100% efficiency, however, motors can't work at full efficiency so we that took into account. According to the figure below, a motor working at optimum efficiency can range from 60 to 80 %, so we chose to calculate the total torque of each motor at 65% efficiency to have little room to spare when it comes to the workload or mass of the motor.

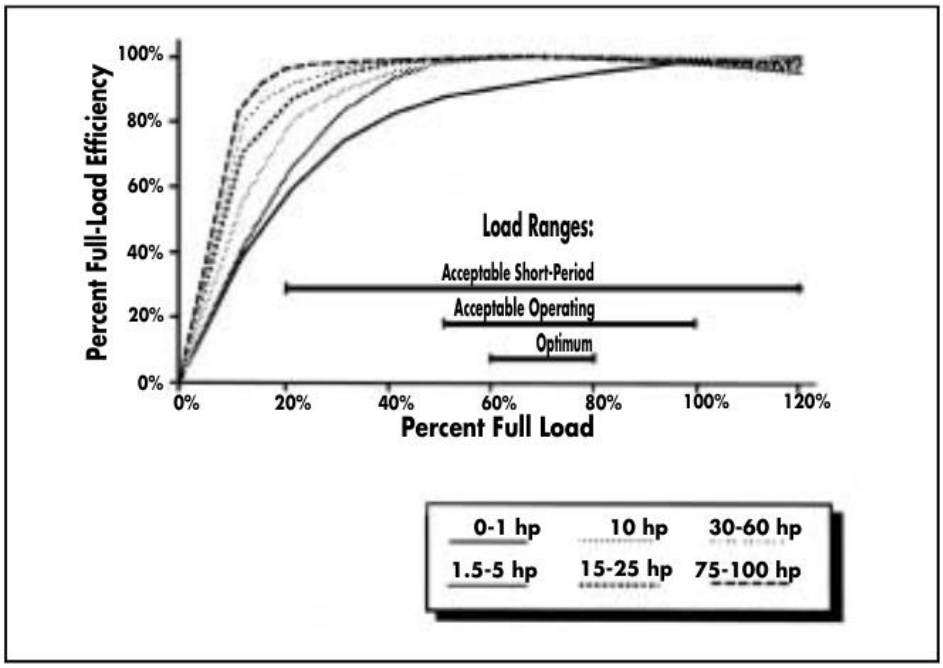

Figure 7 - Motor Part-Load Efficiency [24]

At 65% efficiency T=(100/65)($511.466 * 10^{-3}$)= $786.871 * 10^{-3} Nm$.

$$\omega = \frac{v}{r}$$

(2) Angular Velocity Formula

The angular velocity obtained with the formula was be used to calculate the angular velocity, $\omega = \frac{0.2}{0.0635} = 3.1496\, rad/s$.

$$P = T * \omega$$

(3) Power Formula for Rotational Motion

Afterwards, we took the torque and angular velocity previously calculated to determine the power needed. $P = 786.871 * 10^{-3} * 3.1496 = 2.4783\, W$.

$$I = \frac{P}{V}$$

(4) Current Formula

From the power calculated, we can divide it by the supplied voltage to get the maximum current allowed, $I = \frac{2.4783}{12} = 0.2065\ A$.

$$c = I * t$$

(5) Battery Capacity Formula

We used the battery capacity formula to calculate the minimum battery pack capacity per motor needed with our specifications, $c = 0.2065A * (3h * 4) = 2.478\ Ah$.

3.1.2.1 DC Brushed Motors

DC motors have two main types, brushed and brushless, a brushed motor consists of a rotor containing current-passing coils, which is encapsulated by a permanent magnet or electromagnet. To keep rotation, it is imperative that the current is constantly reversed, this is achieved by the use of mechanical brushes and a commutator that switch the current direction in the windings, transferring electrical power from the brushes to the windings which generates the magnetic field necessary for motion. DC Brush motors are one of the most commonly used types of motors, they are characterized by a simple design that doesn't require a high initial cost for its construction, they also have a higher reliability compared to other types of motors, offer a simple motor speed control, and they have higher torque characteristics. However, they tend to have a higher maintenance due to the use of brushes, which require the change of the worn-out brushes, they also have a lesser efficiency rate due to the loss of energy from friction and heat because of the brushes and commutator, and they have a higher noise production making them not ideal for certain applications.

3.1.2.2 Brushless DC Motors

As opposed to brushed motors, in a brushless DC motor, instead of using brushes and a commutator, the permanent magnet is attached to the rotor while the coils are fixed in the outer shell, since the permanent magnet is the one that is constantly rotating it makes the use of brushes unnecessary. Advantages of brushless DC motors include higher efficiency due to reduced energy loss from friction and heat, a longer lifespan and lower maintenance due to the lack of brushes, and a reduced noise production. Although they provide many benefits, they have a higher initial cost in comparison with other types of motors since they implement the use of a controller to monitor different axes, in addition, they have a generally more complex speed control and require more sophisticated algorithms for better performance.

3.1.2.3 Gear Motors

Gear motors is a term used to refer to the combination of a gearbox and an electric motor, which can use either AC or DC as a power supply, it serves as speed reducer and a torque multiplier to the output shaft, making them enticing when needed to reduce power for a heavier load. Different combinations are possible depending on intended use, all aspects are needed to be known to maximize the operation and are customizable. They also offer a precise and optimal speed control, a high torque, higher efficiency, and are adaptable to different environments and load conditions given the proper gear ratio is selected.

A couple of drawbacks are the higher complexity on design, the larger size in comparison with simpler motors making them have limited applications due to size constraints, the high initial cost of the specific design, and that performance is affected by different factors such as hosing design, lubrication, gear type, bearings.

3.1.2.4 AC Motors

AC motors are electric machines that converts alternating current to mechanical power, similar to DC motor, they can be brushed or brushless, but most of them are brushless. They offer a high versatile range of applications from industrial to residential that can be further specified by their different types, such as induction or synchronous motors. AC motors are characterized by their robust and reliability making them suitable for various environments, they have a longer lifespan than DC motors, they have a lower maintenance since most models are brushless, they have a lower cost due to their standardized manufacturing processes and have a higher efficiency particularly when operating at their rated load [25]. Some of their disadvantages include a low starting torque compared to DC motors or other types of motors, these motors have a more complex speed control for adjustments, they tend to have fluctuations in voltage and frequency that affects their performance when not regulated, and they suffer a slowing down due to the Back-Electromagnetic Field, not practical for portable applications [26].

3.1.2.5 Stepper Motors

They are electrical motors that are characterized by moving in precise steps and to facilitate this they convert digital pulses into motions. They are mostly used in applications that require accurate positioning and control without the need of feedback since they moved in a fixed number of degrees counting the number of steps taken. They can not only move continuously in a forward or reverse direction like most motors, but they can also rotate in steps and hold its position, offering a higher precision control. Some of their advantages include precise positioning without the use of sensors, higher torque at low speeds, high mechanical stability making them more useful in automation. However, the selected torque must be precise since having it too high or too low can make it miss a step, meaning it can no longer accurately count the steps to know the position of the motor. These motors have

generally low torque, emit a higher noise than other types of motors at high speeds, they're more complex when it comes to a smooth motion control that requires a specific algorithm. Stepper motors also have a higher power consumption because of high currents draws at high speeds, and they can be heavier than other types of motors and can also overheat while providing low efficiency [27]. While stepper motors are not the best option for movement control for the BEAM navigation system, it is a great option for the controlling the precise movements of the weeding laser, which is discussed in more detail later in section 3.1.9 Laser Control System.

3.1.3 Motor Controllers

Motor controllers are electronic devices that manage the operation of electric motors, they can regulate the speed by adjusting the input voltage supplied, control the direction allowing the motors to drive forward and backwards, depending on the controller chosen it can regulate the torque output of the motor, it can also control the acceleration and deceleration profiles of the motor, and provide feedback by using a closed-loop control system.

3.1.3.1 Pulse Width Modulation (PWM)

PWM is a technique used to control electric motors by using a comparator with a sawtooth wave and a modulating signal as inputs and generating a modulated pulse signal as an output. Instead of being continuously ON or OFF, it works by switching between these two states for a certain amount of time that is determined by the duty cycle of the PWM [28], expressed as a percentage. This technique has a low cost for implementation, it helps to generate maximum torque for the motors at lower speeds, it is easy to implement and adapt to different conditions, it provides a fast response time and offers precise control of a motor without considerable overheating. However, the PWM frequency and switching losses have a direct relationship, meaning that as frequency increases the switching losses also rises, they can also produce Radio Frequency Interference and voltage ripple, and have a complex design that require timing and control algorithms.

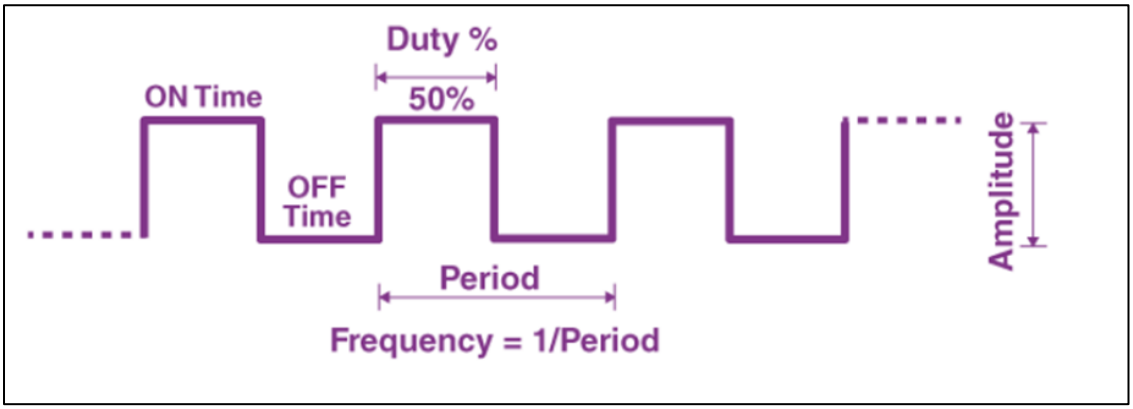

Figure 8 - PWM Duty Cycle [28]

3.1.3.2 H-Bridge Motor Driver

Another widely used approach is an H-bridge motor driver that allows a DC motor to be driven in a forward and backwards directions by swapping the polarity of the supply to the motor. They are composed of four switches that are arranged in an H-shape where the two top switches on both sides are connected to positive supply voltage while the bottom two switches are connected to ground.

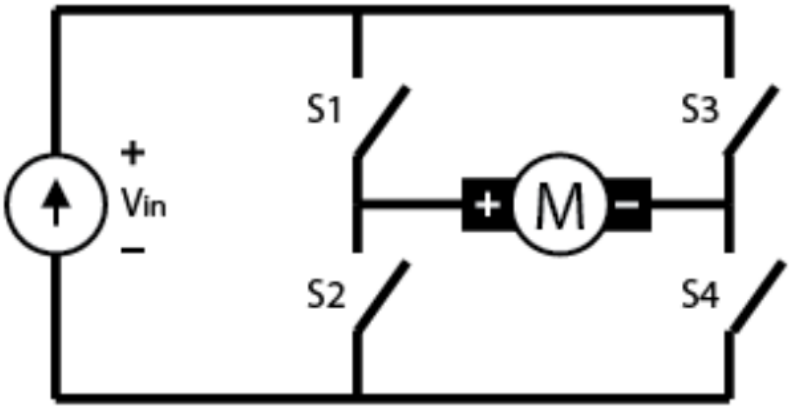

Figure 9 – H-Bridge Circuit [29]

The direction of the motor is chosen by activating a pair of diagonally opposed switches, for example, to go forward switch one and four needs to be activated and for reverse switches two and three would need to be activated [29]. This motor driver provides a flexible way to precisely control the direction and speed of the motors, it also has a compact design that usually includes a protection features and limits current. However, they might require a more complex design for implementation depending on the features wanted,

special attention to the voltage and current ratings are needed to match those of the motor, and it can generate heat especially at high frequencies.

3.1.4 Wheels

Wheels are a key component for the BEAM project because they affect the speed of the robot, center of gravity, and impact the overall performance of the robot. To choose the right type of wheels we needed to know the environment the robot was going to be operating in, the size and weight of the project, and the desired function.

3.1.4.1 Mecanum Wheel

Unlike a standard/fixed wheel, the driving force of these wheels comes at a 45° angle because of the rubber rollers placed along its circumference with the same angle that allows an increase of the range of movements, not only including the standard forward and backward motion but side to side, diagonal motion, and rotation around a fixed axis [30]. They provide these motions without sacrificing the simplicity of the speed and direction control; however, they can be slightly more expensive to produce due to their complex design and have less traction due to the angled rollers.

3.1.4.2 Omni Wheel

Omni wheels are a bit similar to the Mecanum except that their movement is achieved by having the rollers along its circumference at a 90° angle [31], they can achieve the same wide range of motion at lower cost, they have a high efficiency ratio, are simple to control, and have a high maneuverability making them easy to use in robotics. Despite this, they have a higher manufacturing complexity, they can affect the weight distribution of the robot, and have limited traction on uneven terrain.

3.1.4.3 Orientable Wheel

Orientable wheels use a mechanism where the wheels are mounted to a fork instead of directly to the robot to better balance it, because of this, they're rarely used for driving. There are two types of orientable wheels, centered and off-centered, the former has the vertical axle pass through the center of the wheels while the latter one doesn't have the vertical axle through the center of the wheel, allowing it to have 360° of freedom [32], this can prove as a disadvantage when lifted off the ground since the wheel can be in an off-position when landing.

3.1.4.4 All-Terrain Wheel

Just like the name implies, an all-terrain wheels are meant to withstand rugged terrain and uneven surfaces [30], they provide higher tractions compared with other types of wheels

by having specialized pattern-treads, they're great for outdoor applications since most are made from rubber or reinforced plastic, they also provide stability while being reliable. Some drawbacks of using these wheels are the limited speed due to the tread patterns, they tend to be heavier and larger that can affect the weight and maneuverability of the robot, and they can be more expensive.

3.1.5 Batteries

The difference between charging capabilities of primary and secondary batteries needs to be explained before delving into the various types of batteries. Primary batteries are "single use" and cannot be recharged and must be discarded after they runs out of energy. Meanwhile, secondary batteries are rechargeable and reduce the need for frequent replacements. Typically, secondary batteries more expensive than primary ones because of the cost of materials, safety features, and performance [33]. The BEAM robot will use a secondary battery because it needs to be able to recharge itself using solar energy while it navigates its target region. There are many specifications for secondary batteries that need to be considered, such as specific energy, cycle life, charge time, overcharge tolerance, charge/discharge temperature, maintenance requirements, and more. The necessary values we need to compare are explained in Table below.

Battery Terminology		
Terms	Definition	Significance
Specific Energy	The amount of energy a battery can store per unit weight (watt-hours per kilogram).	Higher specific energy means the battery can store more energy for its weight.
Cycle life	The number of complete charge and discharge cycles a battery can complete before its charge capacity starts to decrease.	Longer cycle life means a more durable battery and less battery replacement.
Charge/Discharge Temperature	The optimal range within which a battery can be charged and discharged safely.	Batteries need to operate in specific temperature ranges to maintain performance and safety.

Table 7 - Battery Terminology [34]

Battery Comparison						
Specifications	Lead Acid	NiCd	NiMH	Li-Ion	Cobalt Phosphate	Manganese
Specific Energy (Wh/kg)	30-50	45-80	60-120	150-250	100-150	90-120
Cycle Life	200-300	1000	300-500	500-1000	500-1000	1000-2000
Charge Time	8-16h	1-2h	2-4h	2-4h	1-2h	1-2h
Self-discharge per month	5%	20%	30%	<5%		
Cost (per kWh)	$150-200	$300-500	$400-800	$100-300		

Table 8 - Battery comparison [35]

3.1.5.1 Lithium Ion

Lithium-ion (Li-ion) batteries use ions to store energy and create electric potential differences between two poles. They are widely used in consumer and commercial electronics, and are well renowned for their recharge capacity, charge storage, and size. These batteries also vary in the materials used, such as lithium cobalt oxide and graphite, lithium manganese oxide, and lithium phosphate oxide. Li-ion batteries are one of the highest energy dense batteries in commercial use and can come close to 300 Wh/kg depending on the type [36]. These batteries also vary in size and can be small, like smartphone batteries, or large, like batteries in vehicles or ships.

There are several advantages that make lithium-ion batteries a great choice for the BEAM robot. Two of the main benefits are the high energy density and cycle life. BEAM is a moderate-energy consuming robot that needs a lightweight, yet powerful battery to navigate its difficult terrain. The battery needs to be able to be charged and discharged whenever necessary, so having a high cycle life is very advantageous as it will contribute to the overall cost-effectiveness over time. Li-ion batteries also have a very low self-discharge rate which allows them to retain charge when not being used. This was very beneficial to the battery life during and after scheduled weed treatments.

Li-ion batteries do have some disadvantages that should be noted. They can be sensitive to temperature extremes, which can impact their operation and durability. This battery is almost always manufactured with protection circuits to maintain safe operation because overcharging, extreme discharging, and high temperatures can cause the battery to give off immense heat and possibly catch fire. Li-ion batteries are often still the most expensive type of battery when compared to other commercial batteries [37].

3.1.5.2 Lead-Acid

The lead-acid battery was the first secondary battery to be invented for commercial use. It is still very popular today and in wide use as a cost-effective battery for vehicles, backup power supplies, and energy storage systems. The lead battery uses a combination of lead alloy and sulfuric acid to charge and discharge, and it is heavy and bulky due to the lead content.

Lead-acid batteries have several advantages when compared to other batteries on the market. They are cost-effective, often cheaper than NiCd, NiMH, and Li-ion batteries, they can deliver high surge currents for more power, they can operate in a wide span of temperatures, and they are very reliable having been in use for over a century. Though with these advantages come several disadvantages such as the battery having a shorter cycle life, the charge time is very long (8-16h), the battery has a smaller specific energy, and the lead is also very toxic to humans and the environment [38].

For the intended purpose of the BEAM robot, the specific energy and cycle life of the lead-acid battery did not suit the project's needs. The battery is very heavy, and not intended to be recharged constantly and at multiple intervals. While some of the advantages are appealing, like the cost and operational temperature range, the lead-acid battery would not be the most efficient power storage unit for this project.

3.1.6 Charge Controllers

Charge controllers are a necessary component of a solar power system, providing electrical protection for both the battery and solar panel. They perform three main functions: suppling adequate voltage for the battery, regulating charging current, and preventing battery overcharge [39]. In addition, depending on the charge controller, it can also regulate voltage differences between the solar panel and battery. There are several factors to consider when choosing a charge controller, such as voltage compatibility, maximum current rating, display monitoring, temperature compensation, efficiency, and cost.

Charge Controller Comparison		
Specifications	PWM	**MPPT**
Voltage Compatibility	Fixed voltage Battery = Panel	Wide range of voltages
Displays	Basic LCD or LEDs	Advanced displays and detailed monitoring
Efficiency	70-85%	95-99%
Cost for small systems	$10-60	$100-200

Table 9 – Charge controller comparison

3.1.6.1 Pulse-Width Modulation (PWM)

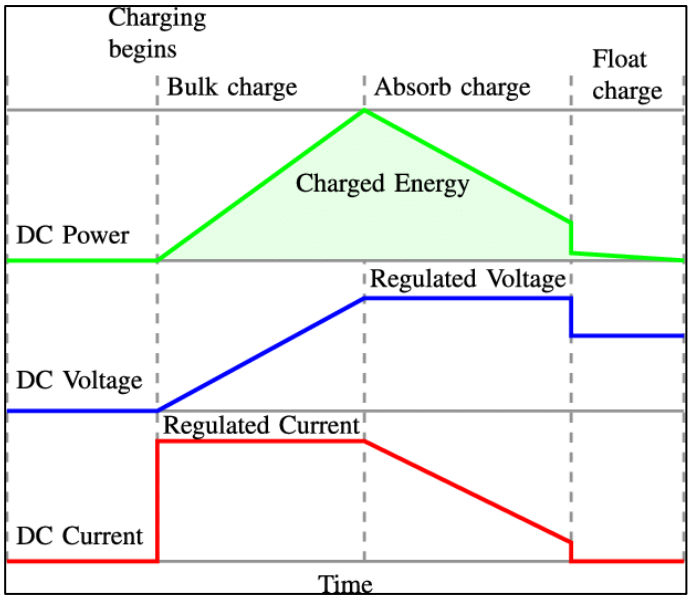

Figure 10 - Battery 3-stage charging (bulk, absorb, float) [42]

Pulse-width modulation is a method of representing a signal as a square wave for a certain frequency per duty cycle. This method is used in the algorithms inside some solar charge controllers, which is why they are called PWM solar charge controllers. Batteries need to be charged with the right level of voltage, and a PWM charge controllers helps facilitate this by modifying the voltage that exits the solar panel and preparing it to be absorbed by the battery input [40]. This controller can help prevent a battery from overcharging by decreasing the current that flows into it as the charge increases. There are three main charging stages for PWM controllers on lead-acid batteries: bulk charging, absorption charging, and float charging. Bulk charging is the initial stage in a battery where the charge controller fully opens the connection between battery and solar panel and allows the maximum current to leave the panel and enter the battery. This stage is meant to bring the battery up to 80-90% charge and is usually used when the battery is low or close to zero charge. The next stage is absorption charging, where the charge controller starts to slowly decrease the current flow so the battery can start to approach full capacity at 98% or higher. Usually during this stage, the voltage is constant and regulated as to prevent the battery from overcharging. The final stage is float charging, where the PWM further reduces the current to an extremely low level. This current only provides enough power to keep the battery full, and to compensate for any self-discharged energy. The voltage in the float stage is typically lowered even more so than the absorption voltage to ensure that the battery does not overcharge [41] [42].

The three charging stages for lead-acid batteries are slightly different when it comes to PWM charge controllers and lithium batteries. Lithium-ion batteries still go through the bulk and absorption charging phases, but both the bulk and absorption voltages are usually

lower for Li-ion during these stages. As for the float stage, Li-ion batteries do not require this stage because it can be detrimental to the battery to leave it at a constant high voltage. Typically, if a PWM charge controller has adjustable settings for lithium batteries, it will stop charging once the battery reaches full charge. This is due to the lithium batteries having an extremely low (close to zero) self-discharge rate [43].

Lithium batteries are more widely used with MPPT solar chargers, but it is possible to use them with PWM chargers if a Li-ion compatible charger is used. There are several factors to take into consideration when choosing a PWM controller for a Li-ion battery, such as voltage range, current rating, safety features, and more. If a noncompatible PWM charger is used with a Li-ion battery, it could cause the battery to fail or overheat and catch fire. It is important to use a PWM that has a temperature monitor to adjust charge rates, charge current selection to reduce excess heat generation, and voltage monitoring to prevent overcharging. These safety measures were essential when choosing a PWM charge controller to provide efficient power transfer between the BEAM solar panel and battery, and also protect both components from damage [44] [45].

3.1.6.2 Maximum Power Point Tracking (MPPT)

Maximum power point tracking is another algorithm used in photovoltaic systems that help account for factors that impact solar panels like variable sunlight, temperature, and battery load [46]. The “maximum power point” (MPP) is the point where current and voltage production is maximized for a solar panel. This point varies based on sunlight intensity and temperature, and it is monitored by the MPPT algorithm by varying the resistance seen by the panel then measuring the power output [47]. MPPT charge controllers adjust the current leaving the solar panel to keep the system running close to peak power point of the panel.

An important part of the MPPT system is the buck/boost DC-DC conversions that allow the system to convert between higher and lower currents and voltages. The boost conversion will increase the power from the solar panel to match that of the battery, so if the panel outputs 6V and the battery needs 12V, the boost converter will increase the voltage exiting the panel to 12V. This is the opposite for the buck conversion which decreases the voltage from the panel to match the battery. If the panel outputs 24V and the battery needs 12V, then the buck converter will decrease the panel output to 12V. This buck/boost conversion allows for high power transfer, compatibility between different panels and batteries, and flexibility in panels for different applications [48].

When considering MPPT charge controllers for the BEAM project we needed to take into consideration the type of battery and solar panel that would suit the project the best. However, the type of battery typically takes precedence when considering what type of charge controller to use, so in this case we focused on how the MPPT charge controller could benefit our project when used in combination with a lithium-ion battery. MPPT charge controllers can provide more power during varying weather conditions, voltage

match and compensate for inconsistencies between battery and panel and provide more precise charge control to prevent overcharging the battery. MPPT charge controllers are also more widely used with lithium-ion batteries because of their ability to precisely regulate the voltage and current between panel and battery. A lithium-ion battery needs to have stable and constant charge to achieve peak performance, so a MPPT charge controller was a great choice over PWM for this project.

3.1.7 Voltage Regulation

The BEAM power system needs a voltage regulator to step down the battery's 12V to 5V to power the electronics guiding the system. The Raspberry Pi 4 needs 5V/3A to operate, and the Arduino can handle 7-12V/1A, so our system needed to be able to bring down the voltage to prevent damage to these components. The two options for a voltage regulation system are a linear regulator or a buck converter. Both options are cost effective, reliable circuits that have been tested and compared by reputable companies such as Texas Instruments.

Voltage Regulator Comparison		
Specifications	Linear Regulator	Buck Convertor
Cost	$2-5	$5-15
Voltage Output Ripple	1-50 mV	10-100mV
Full-Load Efficiency	15-20%	65-80%
Circuit Complexity	3-5 Components	6-11 Components
Power Loss[1]	2W	0.1W

Table 10 - Voltage Regulator Comparison [49]

3.1.7.1 Linear Regulator

Linear regulators are very reliable and have been in production for over 50 years. They have been widely used in industrial circuits because they are simple and can provide voltage conversions for a wide range of voltages. These regulators are typically less complex, requiring less components, but they often require more space to provide proper thermal relief. This regulator works by using a voltage-controlled current source to set a fixed voltage across a load resistor. This load resistance is connected to the voltage output of the regulator, and so sets the output to the desired voltage. A control circuit/feedback loop is used to monitor the voltage output and adjusts the current source based on the load to keep the voltage consistent [50]. For large voltage differences, the linear regulator tends

[1] The power loss shown in the table comes from a study completed by Texas Instruments [49]. Its purpose in the table is to show that linear regulators typically have a very large power loss when compared to buck converters.

to have large power losses that ends up dissipating as heat in the system. This is because of the power dissipated, given by Equation (6) - Linear Regulator Power Dissipation, where if Vin is larger than Vout and the current needed across the load is also large, then P will also be quite large.

$$P_{dissipated} = (V_{in} - V_{out}) * I_{Load}$$

(6) - Linear Regulator Power Dissipation

This power loss also leads to the linear regulator having poor power efficiency because over half of the power going into the circuit is wasted as heat energy. This would force us to design a circuit that provides maximum heat dissipation and invest in heat sinks or cooling fans.

A benefit of the linear regulator is the low voltage ripple, which leads to overall less noise in the system. This would be beneficial to prevent disturbances in signal integrity for our sensing equipment. Another benefit is the low cost of a linear regulator, when reviewing a report written by Texas Instruments (TI), they found out that a linear regulator circuit ($0.32) cost more than five times less than a buck converter circuit ($1.80) [49]. This decrease in cost would allow us to spend more towards a cooling system, potentially making the linear regulator a viable option for a voltage regulator.

3.1.7.2 Buck Converter (Switching Regulators)

Buck converters, also known as switching regulators, are newer than linear regulators and widely used in industrial voltage regulation systems for its efficiency and simplicity. The buck converter controls voltage transfer through switches, inductors, diodes, capacitors, and sometimes MOSFETs. The switches are used to control the flow of current through the inductor which charges the output capacitor and powers the load. When the switches are turned off, the stored energy is released and current continues to flow into the load. Similarly to the linear regulator, the output voltage is monitored using a feedback system that compares the output to a voltage reference [51]. Buck converters are typically more complex than linear regulators because they use more external components and can be more complicated to design. Unlike linear regulators though, buck converters can take up less space because they do not need to spread out components for adequate heat dissipation. Buck converters are extremely efficient when compared to linear regulators, and have very minimal power loss, resulting in little heat generation. These regulators even excel at preventing power loss when using increased load currents and tend to perform better with higher currents over 1A [49].

There are some manageable downsides to using buck converters, such as higher voltage ripple and noise production. These regulators generate more noise and voltage ripple due to switching on and off to regulate the output voltage, which can lead to interference in sensitive digital circuits. We knew that if this regulator was implemented, proper circuit

design and filtering would need to be used to mitigate interference with other sensitive components [52]. With proper implementation, the benefits of using the buck converter outweighed the disadvantages. The buck converter had many benefits over the linear regulator that were desirable for the BEAM project, such as low heat generation for large voltage conversions, high power efficiency for large load currents, and less design space required for circuit board layouts.

3.1.8 Solar Panels

For the BEAM project, solar panels were used to power the electronics on board and keep the system's battery charged. There are three popular types of solar panels used for industrial, residential, vehicular, and personal applications: monocrystalline, polycrystalline, and thin-film photovoltaics. It is important to compare the specifications between these three panels, specifically cost, energy efficiency, and temperature performance. The BEAM project required a solar panel with high energy efficiency, low temperature performance, and at a reasonable cost.

Solar Panel Comparisons			
Specifications	Monocrystalline	Polycrystalline	Thin-Film
Efficiency	≥ 23%	≤ 20%	7-18%
Cost per Watt [53]	$1 – 1.50	$0.90 – 1.50	$0.50 – 1.50
Color Hue	Black	Blue	Blue
Temperature Performance [54]	0.38 - 0.44%	0.44 - 0.50%	0.20%
Lifespan (years) [55] [56]	25+	25+	10-20

Table 11 – Solar Panel Comparison

3.1.8.1 Monocrystalline

Monocrystalline solar panels, also known as single-crystal panels, are made from a single silicon crystal that is then divided into wafers. Monocrystalline panels can reach power efficiencies of over 23% [56].The efficiency of these cells are due to the increased electron flow of the single crystal. While these panels are well-known for being the most efficient in power collection, they are also the most expensive. The monocrystalline panels have a good performance in high temperature conditions due to the single crystal and with proper housing can be waterproof. The lower temperature coefficient, high energy efficiency, and durability made the monocrystalline solar panel a great option for the BEAM robot. While the monocrystalline solar panels are typically the most expensive, they have also been very popular in personal applications. There are several affordable and reasonably sized panels available that met the BEAM project's needs.

3.1.8.2 Polycrystalline

Polycrystalline solar panels are made from multiple silicon crystals melted together. This process of creating wafers is less complex than that of the monocrystalline wafers, making these solar panels have a cheaper price, but also a lower efficiency [56]. Polycrystalline solar panels also have a higher temperature coefficient when compared to monocrystalline because of the structure of the wafer, making it less desirable than the single-crystal panels. While both polycrystalline and monocrystalline panels are widely available on the market at various voltages and power ranges, a polycrystalline panel was a less suitable choice when compared to monocrystalline.

3.1.8.3 Thin-Film

Thin-film panels are created by placing layers of photovoltaic material onto a conductive substrate, allowing them to be lightweight and flexible. Solar cells for thin-film panels can be made from amorphous silicon (a-Si), cadmium telluride (CdTe), or copper indium gallium selenide (CIGS). These panels can be the same thickness as silicon-based mono/polycrystalline panels, or up to 350 times thinner [55]. A great benefit of thin-film panels is that they are extremely insensitive to high temperatures and even resilient against moisture, making them great for humid climates. This proved extremely beneficial to the BEAM project because it can be tested and conditioned to work in Florida, which is both humid and hot. Another benefit of thin-film photovoltaics is the cost when compared to crystalline panels. Thin-film is lighter because of how it is manufactured, and requires less material, and so is less expensive. Thin-film was not be the best option for the BEAM project because the energy efficiency is very low when compared to other photovoltaic panels. There are also not many thin-film solar panels available on the market at specific voltages and powers, whereas compared to the more popular crystalline panels, there are many options to choose from. It was more expensive to request a custom thin-film panel from a manufacturer than find an available crystalline one on the market.

3.1.9 Laser Control System

The laser control system was necessary to efficiently cover all areas within the monitoring region that needed to be treated by the laser. The control system motors functioned on a railed cartesian system, allowing the laser to move along the XY plane to the coordinates specified by the object detection system. This system allowed BEAM to function with not only accuracy, but also precision while treating weeds. A sketch of the control system is shown in Figure 2.

3.1.9.1 Stepper Motors

As previously discussed in section 3.1.2.5 Stepper Motors, these motors are used in applications that require accurate positioning and control without the need of feedback.

This was extremely useful for fixed cartesian systems because it eliminated the need for limit switches if the length and height of the plane are known. The system needed two motors, one for each axis, and will be controlled by gcode that was be produced after the target area underneath the robot is scanned by the object detection system. In Senior Design 2, our team did end up incorporating the use of limit switches to add homing sequences and movement accuracy to the software.

3.1.9.2 Stepper Motor Drivers

Motor drivers are essential to power the motors and convert digital signals from the control system into power signals for the motors. These drivers are important for direction and speed control and provide valuable protection for the motors themselves. To improve the performance of motion and provide a higher precision, some stepper motors have microstepping capabilities that allow them to divide each motor step into smaller steps. This is accomplished by using PWM voltage control to manage the current in the motor windings, resulting in reliable torque and better motion control, especially at slower speeds [57].

3.1.10 Laser Diode

Lasers are considered one of the most effective light sources for targeting weeds [58]. Laser is an acronym for "light amplification by stimulated emission of radiation," which refers to a device that emits light through the optical amplification process, which is based on the stimulated emission of electromagnetic radiation. Prior to detailed information about laser diode, Table 12 explains some important optics terms, such as wavelength, refractive index, stimulated emission, spontaneous emission, and waveguide. They will help readers gain a better understanding of different optical concepts.

A laser diode emits a beam from an active layer located either on the surface or embedded within a non-active bulk material. The active layer has two facets: front and back. The front facet of the active layer is uncoated with a natural approximate reflectivity of 0.3 while the back facet is high-reflection (HR) coated. A lasing cavity is created by these two facets. A laser diode with this type of cavity is referred to “Febry-Perot” laser diode, which differs from laser diodes with other types of cavities. The refractive index of the active layer is higher than that of the bulk inactive material around the layer and it serves as a waveguide. Upon the injection of electrical current into the active layer, electrons and holes combine together, resulting in photon emission. The photons emitted here bounce back and forth between the two facets of the active layer. This process is called lasing. Since the active layer has an indirect relationship with the lasing efficiency, it has a thickness of only a few microns to maximize the efficiency. Only a minor portion of the laser energy is confined within the active layer, and part of this laser energy is called the confinement factor. The active layer can be widened to several hundred microns to enhance the laser power output [59].

Optics Terminology		
Terms	Definition	Significance
Wavelength	The distance between corresponding points of two consecutive waves	It directly relates to several key properties of waves: frequency, wave behavior, wave types, and wave propagation
Refractive Index	The measure of the bending of a ray of light when passing from one medium to another	Higher refractive index indicates stronger light bending and slower light speed in the material
Stimulated Emission	The amount of energy a battery can store per unit weight (watt-hours per kilogram).	Higher specific energy means the battery can store more energy for its weight.
Spontaneous Emission	The number of complete charge and discharge cycles a battery can complete before its charge capacity starts to decrease.	Longer cycle life means a more durable battery and less battery replacement.
Waveguide	Any device that confines and directs the propagation of electromagnetic waves, including radio waves, infrared rays, and visible light	Waveguides come in various shapes and forms, such as hollow metallic tubes, coaxial cables, and optical fibers

Table 12 - Optics Terminology

3.1.10.1 Laser Diodes VS LED

Another optical energy source used for weed control is LED, which stands for light-emitting diode. Table 13 shows comparison data over some key parameters of LEDs and laser diodes. Unlike lasers, LED is an incoherent light source and operates based on spontaneous emission of photons. LEDs can typically be operated at higher currents, are more cost-effective, consume less power, feature larger emitting areas, and have longer lifespans. Unlike LEDs, lasers do not operate below a threshold current; they only begin lasing once this threshold current is reached. Both LEDs and laser diodes are sensitive to temperature, affecting their overall lifetime. For instance, operating a laser diode just 10°C above its rated temperature can halve its lifespan, and lasers typically cease functioning at 100°C.

Although LEDs are more affordable, have lower power consumption, and have longer lifespan, laser diodes were utilized in this project based on some considerations. First, laser diodes are capable of operating at higher intensities. High-power lasers provide the necessary energy to effectively target and destroy weeds. They can penetrate deep into

plant tissues, causing thermal damage that leads to the immediate death of the weed or severely hinders its ability to recover and grow. This ensures that the treatment is both rapid and effective, reducing the likelihood of regrowth [7]. Moreover, the precision of high-power lasers allows for targeted weed control. This means that the robot can selectively target weeds without damaging the surrounding crops, which is particularly beneficial in mixed or densely planted fields. This level of precision minimizes collateral damage and helps maintain the health and productivity of the crops [58]. High-power lasers also offer the advantage of reducing the need for chemical herbicides [7].

Comparison of LED and Laser Diode		
Specifications	LEDs	Laser Diodes
Particle Phase	Incoherent	Coherent
Radiative Recombination	Spontaneous Emission	Stimulated Emission
Direction	Random	Linear
665 nm	GaAsP	GaAlAs
800-930 nm	$Ga_{1-x}Al_xAs$	$Ga_{1-x}Al_xAs$
1300, 1550 nm	InGaAsP	InGaAsP
Output Power	10 – 50 µW	1 – 1000 mW
Rise Time	1 to 100 ns	< 1 to 10 ns
Temperature Effects	Increases wavelength by .6 nm/ °C	Wavelength varies by .25 nm/ °C Threshold current rises by .5mA/ °C
Significant Parameters	BW vs Power BW increases at the expense of power	Threshold current, Index guided: 10 to 30 mA Gain guided: 60 to 150 mA

Table 13 – Comparison of LEDs and Laser Diodes (reprinted with permission) [60]

By providing a non-chemical method of weed control, the robot can help mitigate the environmental impact associated with herbicide use, such as soil and water contamination and harm to beneficial insects and other wildlife. Additionally, the use of high-power lasers enhances the efficiency and speed of weed control operations. Lasers can operate continuously and effectively in various weather conditions, unlike some mechanical or chemical methods that may be hindered by rain or wind. This reliability ensures consistent weed management and can lead to a reduction in labor costs and time spent in the field. In overall, to eliminate weeds effectively by raising their temperature, a high-power light source is necessary. In his research group, Rakhmatulin built a weed controlling device that uses laser beams and showed a laser with power less than 1W was not enough to damage crop plants in a short time [61].

Another consideration is that using laser diodes reduces treatment time. The project utilizes a chassis with four wheels for traversing the wide field. Consequently, minimizing treatment time significantly enhances efficiency, allowing it to cover larger areas in a shorter period. This is especially important in agricultural settings where timely weed control is essential to prevent competition for resources between weeds and crops. By minimizing the treatment time, the robot can address weed growth more effectively and promptly, reducing the likelihood of weeds reaching a stage where they can severely impact crop yield. Additionally, shorter treatment times mean that the robot can operate more frequently or attend to multiple fields within a given timeframe, thereby maximizing the utility and cost-effectiveness of the technology. Faster operations also reduce the energy consumption per unit area treated, contributing to the sustainability of the farming practices. Moreover, by quickly eliminating weeds, the robot helps maintain optimal growing conditions for crops, which can lead to better crop health and higher productivity. Overall, short treatment times enhance the robot's effectiveness in managing weeds, supporting agricultural productivity, and ensuring more efficient use of resources.

An experiment conducted at University of Georgia had two types of weeds growing in the pots that underwent laser treatment using laser diodes placed approximately 5 cm away and perpendicular to the weed stems to minimize the treatment time. This experiment followed a factorial design involving 2 laser output powers, 3 treatment durations, and 2 weed species, resulting in a total of 12 treatments. Each treatment combination was replicated 5 times. The laser powers were 5.1 W and 6.1 W, respectively, while treatment durations varied between 0.5, 1, and 1.5 seconds. As a result the 5.1 W diode laser showed an overall effectiveness of 66.67% (kill/stunt) across all treatment durations. On the other hand, the 6.1 W diode laser exhibited 80% effectiveness for treatment durations of 0.5 s and 1 s, and 100% effectiveness for the 1.5 s duration [58]. This experiment presents a direct relationship between laser power and treatment time. Applying the experimental findings to our project, we intend to utilize a high-power laser while minimizing treatment duration. However, considering laser safety concerns, it's crucial to note that when a laser beam contacts a surface, it converts into heat energy. High-energy lasers have the potential to ignite materials and inflict thermal injuries [62]. Employing diode lasers with lower output power has fewer operational risks compared to high-powered CO2 and fiber lasers, which are more complex. However, even low-output diode lasers can pose risks to the eyes upon exposure, necessitating the use of protective eyewear [62]. Therefore, we plan to still maintain high laser power and low treatment intensity while ensuring optimal safety measures.

Furthermore, laser diodes have narrow beams, which are critically important for a weed control robot because they significantly enhance precision, safety, and energy efficiency in the weed control process [8]. By focusing the laser energy on a very small, specific area, narrow beams allow the robot to target weeds with high accuracy, ensuring that only the unwanted plants are affected and minimizing the risk of damaging valuable crops [58]. This precise targeting is especially beneficial in fields where crops and weeds are closely spaced. Additionally, the concentrated energy of narrow beams maximizes the intensity at

the target point, leading to more efficient use of power and reducing overall energy consumption, which extends the robot's operational time. Furthermore, the focused heat minimizes the spread of thermal damage to surrounding areas, protecting nearby crops and soil microorganisms from unintended harm [58]. Narrow beams also provide better control over the depth and extent of laser penetration into the weed tissues, allowing for effective destruction of various types of weeds without unnecessary damage to the soil. Moreover, the precision of narrow beams enhances safety by reducing the risk of accidental exposure to humans, animals, or unintended parts of the field [8]. For robots equipped with advanced machine vision systems, narrow beams complement high-resolution imaging and identification, enabling the targeting of even the smallest weeds at an early growth stage. Overall, narrow beams are essential for achieving efficient, effective, and safe weed control, significantly improving the performance and reliability of the weed control robot in agricultural fields.

3.1.10.2 Laser Wavelength

Choosing the correct laser diode wavelength is critical for weed control because different wavelengths affect how quickly the temperature of the plant leaves rises or how efficiently they dry out. Essentially, the wavelength of light plays a vital role in how plants absorb light. To effectively remove moisture from plants, it's necessary to use a laser with the right wavelength. To gain a rough idea of which wavelengths are most effective in this regard, we need to understand how plants derive their energy and absorb light.

Plants perform photosynthesis, which is the major function of converting solar energy into chemical energy to synthesize their food source and storing that chemical energy for later use. (The important role of photosynthesis, 4/9, 2013, Michigan State university Extension, Bill Cook) Photosynthesis occurs in specialized regions of the cell known as chloroplasts. Photosynthesis relies on light sources, with the intensity and spectral distribution of light exposure significantly impacting the rate of photosynthesis. The spectrum characteristics of light, including light quality, play a crucial role in the rate of photosynthesis [63].

Two primary pigments located in chloroplasts are involved in plants' photosynthesis: Chlorophyll A and B. For this project, we are going to target these pigments since they are parts that allow plants to absorb light to provide for their energy. Chlorophyll A is the green pigment responsible for absorbing light and providing energy for oxygenic photosynthesis. It is present in all plants, green algae, and cyanobacteria, and plays a pivotal role in photosynthesis by acting as the primary electron donor in the electron transport chain. On the other hand, chlorophyll B collects light energy and transfers it to chlorophyll A. The structure of Chlorophyll B closely resembles chlorophyll A. Chlorophyll B is present in plants and green algae. Figure 7 shows the absorption spectrum of chlorophyll A and B. Observing, the peak absorption coefficient for each chlorophyll, chlorophyll A most effectively absorbs light at wavelengths of 429 nm and 659 nm, corresponding to the violet-blue and orange-red parts of the spectrum, respectively while chlorophyll B absorbs light

most effectively at wavelengths of 455 nm and 642 nm, corresponding to violet and red colors, respectively, and reflects a yellow-green color. [64]

Difference Between Chlorophyll A VS B		
	Chlorophyll A	Chlorophyll B
Role	The main pigment that absorbs sunlight	The auxiliary pigment that captures sunlight and transfers it to chlorophyll A
Absorbed Light Wavelength	430 – 660 nm	450 – 650 nm
Absorption Peak	430 nm & 662 nm	470 nm
Absorbed Light	Violet-blue & Orange-red	Orange-red
Color Reflected	Blue-green	Yellow-green
Organism Types	all plants, algae, and cynobacteria	All plants and green algae
Proportion in Total Chlorophyll in Plants	$^{3}/_{4}$	$^{1}/_{4}$

Table 14- Difference between Chlorophyll A VS B [64]

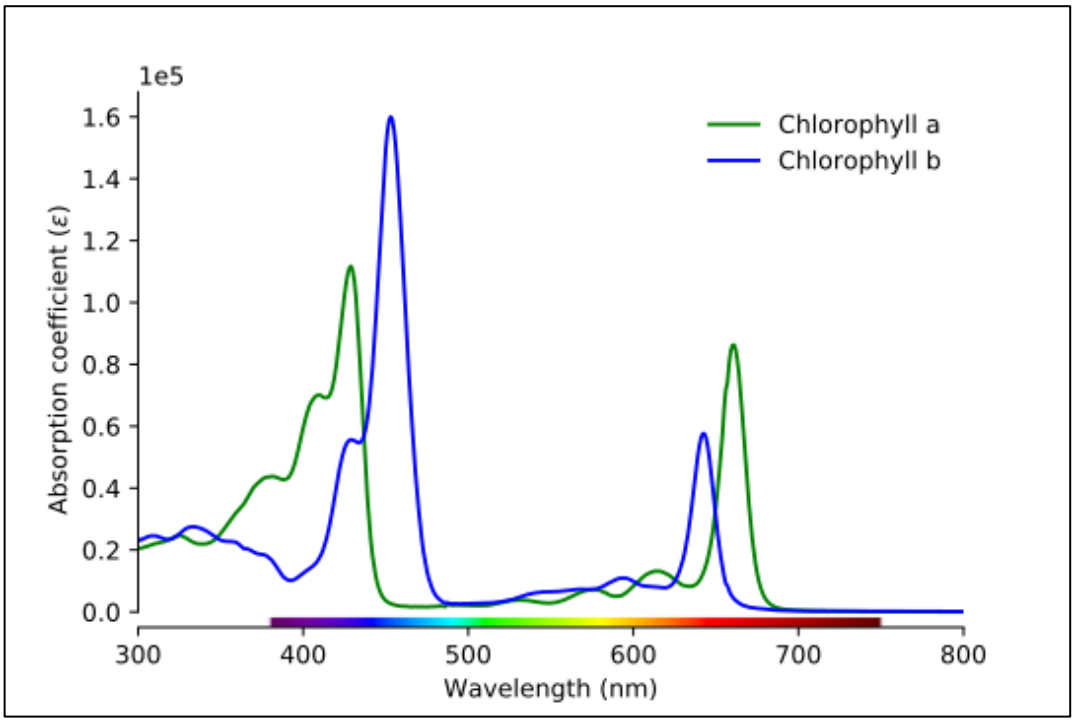

Figure 11 - © Wikimedia Commons / Daniele Pugliesi, M0tty

3.1.10.3 Laser Temperature

Setting the right temperature for a laser and considering the environmental temperature are crucial for effective weed control. Heat stress impacts plant growth at all stages of development, though the heat threshold level varies significantly across these stages. For example, high temperatures during seed germination can slow down or completely inhibit the process, depending on the plant species and the intensity of the heat stress. In later stages, high temperatures can negatively affect photosynthesis, respiration, water relations, and membrane stability, as well as alter hormone levels and the production of primary and secondary metabolites. Additionally, throughout a plant's development, increased expression of various heat shock proteins, other stress-related proteins, and the production of reactive oxygen species (ROS) are key responses to heat stress [65]. The laser temperature needs to be high enough to cause fatal damage to the weed's tissues, ensuring that the plant is killed efficiently. If the laser temperature is too low, it may only stress the plant without killing it, allowing it to recover and continue growing. On the other hand, if the laser temperature is too high, it could lead to unintended damage to surrounding plants, soil, or beneficial organisms. Additionally, environmental temperature plays a significant role in the effectiveness of the laser treatment. In hotter conditions, the initial temperature

of the weeds is higher, meaning less energy is required to reach a lethal temperature. Conversely, in cooler conditions, more energy might be needed, which could affect the efficiency and speed of the treatment. Understanding and adjusting for these factors ensures that the laser weed control method is both effective and environmentally safe.

An experiment conducted at the Department of Plant Biology at Carnegie Institution of Washington measured the amount of emitted fluorescence at 77 K (-196 °C) from Siratro and found out that the plant exhibits a special protective mechanism called paraheliotropic leaf movement (PLM) to reduce exposure to intense sunlight when the water shortage becomes severe. Chlorophyll fluorescence is a technique used to measure the efficiency and health of photosynthetic systems. By measuring fluorescence emission kinetics at 77 K (a very low temperature), researchers can assess how well the photosynthetic machinery is functioning under stress conditions. The experiment further showed that the photosynthetic system of the plant started to get damaged even in darkness when the leaves were exposed to a temperature exceeding 42°C and leaf death was observed at 48°C. Heat damage severity increased with increased time exposure between 42°C and 48°C, although moderate damage recovery took several days. As the temperature range ideal for plant growth increased, the threshold temperature for direct heat damage increased, regardless of water-stress history or current leaf hydration levels. Below 42°C, there was no direct heat damage. However, plants that had inadequate water availability or drought conditions experienced more suppression in their photosynthesis between 31–42°C of leaf temperature with increasing photon flux density up to values equivalent to full sunlight [66].

Similarly, for effective weed control specifically in Orlando, we examined a climate graph displaying monthly temperatures in the area. Understanding Orlando's climate conditions was crucial for targeting plants that grow there, as it helps identify the optimal temperatures for plant eradication as the information given above for Siratro and informs our laser settings. Additionally, because temperatures vary across different seasons and months, we aim to develop a solution that accounts for these changing conditions. Based on the average monthly data on the temperature of Orlando from 1991 to 2021, it is noticeable that Florida experiences less temperature fluctuation throughout the year compared to other regions, with average temperatures ranging from 50 to 80°F. From January to February, temperatures typically remain below 65°F, which is relatively cool compared to other months. This trend continues into March, with temperatures still below 70°F. By April, temperatures begin to rise, marking the transition to the peak season (May - September), where temperatures range from 75 to 80°F. In October, temperatures start to cool as the cold season begins, typically falling below 70°F.

For the experiment, we were given August to November as our timeframe, which we consider optimal since this period allows us to conduct treatments during the peak temperatures of 87 to 90°F in August and September, followed by the transition season in October as temperatures begin to cool. We observed the effects of the treatment during November, which represented the onset of the colder season.

Orlando Temperature by Month			
	Average Temperature (°F)	**Min Temperature (°F)**	**Max Temperature (°F)**
January	59.5	51.8	69.6
February	62.6	54.7	72.7
March	66.6	57.8	77.1
April	71.7	62.8	81.9
May	76.7	68.1	86.4
June	79.9	73.6	88.2
July	80.8	75.1	88.6
August	80.9	75.5	88.5
September	78.8	73.7	86
October	74	67.8	81.8
November	67.2	60.2	76.2
December	63	56	72.4

Table 15 - Orlando Monthly Temperature [67]

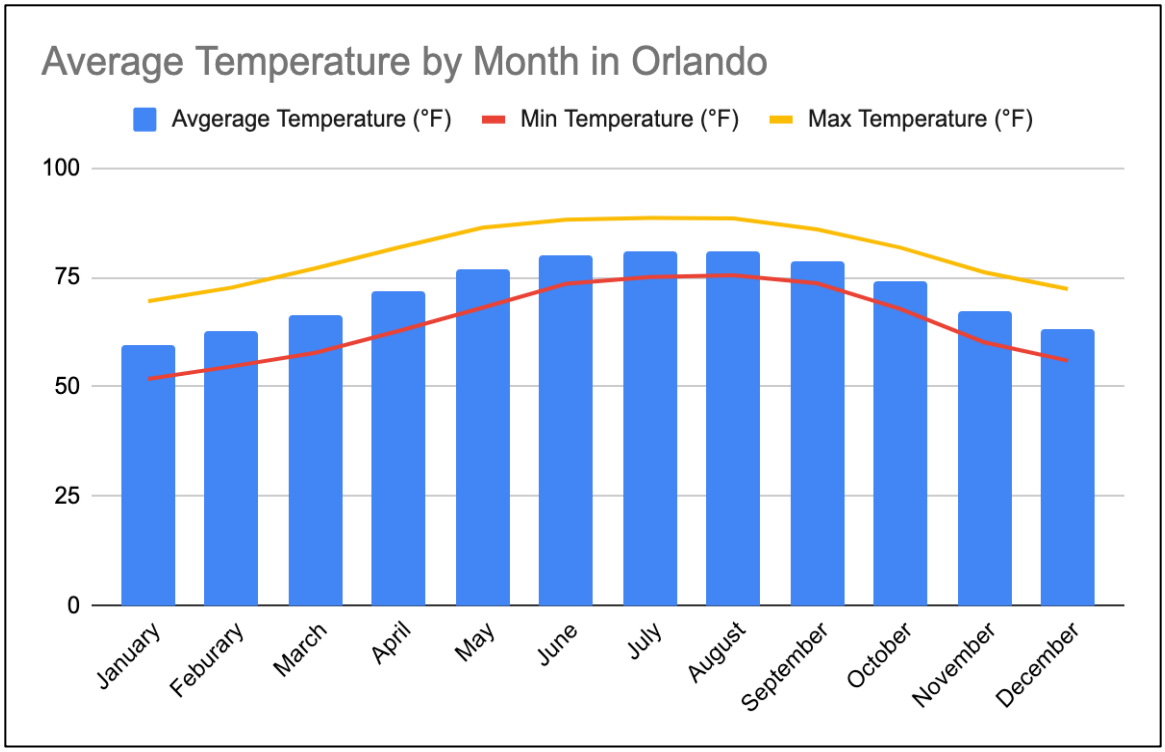

Figure 12 - Average Temperature by Month [67]

For other consideration factors, there are humidity, rain days, precipitation depth, and average sun hours. Analyzing the climate data for Orlando, we observed that humidity levels vary throughout the year, with the highest levels recorded in July and August at 80%. These months, coupled with June and September, also experience the highest rainfall, ranging from 142 mm to 170 mm, and have the most rain days (14-17 days). Conversely, the humidity is lowest in April and May at 64-65%, and these months, along with November, have the least rainfall (36 mm to 70 mm) and fewer rain days. Sunlight hours peak in May and June, averaging around 10.2 to 10.3 hours per day, providing the most sunlight exposure, while the shortest sunlight hours occur in December with 6.5 hours.

For the project, which involves using high-power lasers to dry and kill weeds, the ideal periods were April, May, October, and November. During these months, the combination of lower humidity, moderate rainfall, and adequate sunlight hours enhances the effectiveness of the laser drying process. In contrast, the months from June to September posed significant challenges due to high humidity, frequent rainfall, and slightly reduced sunlight hours, making these periods less suitable for the weed control method. Therefore, targeting the drier and sunnier months will maximize the efficiency of the laser treatment, while the rainy and humid summer months may hinder its performance.

Orlando Temperature by Month				
	Humidity (%)	**Rain days (d)**	**Precipitation / Rainfall (mm)**	**Average Sun Hours (hours)**
January	71	5	58	6.9
February	68	5	52	7.1
March	65	5	64	8.5
April	64	5	55	9.5
May	65	7	70	10.2
June	75	14	157	10.3
July	79	16	158	10.3
August	80	17	170	9.6
September	80	14	142	8.7
October	73	8	69	7.9
November	71	4	36	7.1
December	73	4	51	6.5

Table 16 - Weather Factors in Orlando [68]

For Model PLPT9 450LB, given with output power, operation current, I_{op}, and threshold current, I_{th}, we can use the equation below to calculate the expected output power.

$$\eta_s = \frac{P_{out}}{I_{op} - I_{th}}$$

Hence, we get

$$\eta_s = \frac{5}{3 - 0.29} = 1.845\ W/A$$

Table 17 - 5W Laser Diode Specifications

3.1.11 Movement Control Sensors

Motion control sensors were a crucial part of the robot's performance by allowing it to precisely control, navigate, and interact with the chosen environment, they provided feedback related to the robot's movement, orientation, and position. That's where these feedback from a closed-loop control systems of the sensor comes in considering the BEAM project relies heavily on precise movements to effectively perform tasks. Given that the setting is uneven terrain, they aided in the overall safety of the robot by preventing any collisions and by avoiding obstacles. Finally, they increased the energy efficiency of the robot by optimizing movement patterns and reducing unnecessary movements once it maps out an area.

3.1.11.1 Lidar

A type of motion control sensor is Lidar, short for Light Detection and Ranging, a method where the sensor emits a light in the form of a pulsed laser to measure the surface of earth and the distance of objects. It provides a highly accurate rendition of the environment, 3D mapping, including the distances of the objects in real or near real-time which helps in fast decision making when it comes to navigation. Depending on the type of Lidar used, the range for object detection can go from a few meters to over hundreds of meters and has versatile applications across different industries. They can also operate in a variety of weather condition, such as rain, fog, and even in darkness since they rely on the emitted pulses and are not greatly affected by environmental changes. However, the environment where they are operating needs to be taken into consideration since highly reflective surfaces can affect its performance affecting the data acquisition, they can also be very expensive compared to other sensors and similar technologies because of their complexity when it comes to calibration, processing of large volumes of data, and synchronization with other sensors.

3.1.11.2 Sonar

Another type of motion control sensor is Sonar, short for Sound Navigation and Ranging, a technique used to detect the distance, direction, and shape of objects by listening to the echoes of sound waves. There are two types of sonar; passive sonar refers to the usage of specialized listening devices to pick up the sound waves in the environment without emitting any signals and determine the size and distance of objects from these waves, active sonar on the other hand refers to the usage of a sound pulse emitter device and determining the distance of objects from listening to the echoes with a receiver. Their application ranges from civilian use in robotics to military use in submarines, both types have their advantages, passive sonar is great for detecting objects without giving away position and active sonar is great for detecting objects that are too quiet for passive [69]. Although sonar is great for real-time monitoring, is more resistant to weather changes, and depending on the sonar implemented it can have a long-distance range for object detection, it can have limited resolution of sonar data compared with lidar, it is also susceptible to noise that can be generated by other machines or wildlife, and it requires a sophisticated signal processing and interpretation.

3.1.12 Weed Identification Sensors

The BEAM project required the identification of different plants including weeds, which in these context means any undesired plant, to determine which kind to eliminate. To accomplish this, we needed to first need to create a comprehensive data set, which was used to train the object detection algorithm and enables the robot to recognize and classify various plant species effectively. By processing real-time data, the robot made immediate decisions, allow for precise and efficient weed control. Our robot utilized a RGB camera connected to a Raspberry Pi 4 to accurately detect and differentiate between weeds and crops. This feature emphasized the importance of accurate data preparation, algorithm training, and real-time processing, and allowed our robot to achieve optimal performance for supporting sustainable agricultural practices.

3.1.12.1 RGB Camera

An RGB camera is an imaging device that captures images or video using three sensors to process the wavelengths for red, blue, and green colors. It replicates the human perception of color by combining these three colors with the information received. They usually have image sensors to capture light, a color filter array, and an image processing algorithms for the image quality and color balance. They have a wide range of applications from simple photography in consumer cameras or implemented in smartphones, security systems, to medical imaging to monitor and diagnose. Depending on the RGB camera chosen they can be great at accurately reproducing color, they have different price ranges to choose from, and they are easy to use and interpret the data. However, they can present different performance limitations when operating in low-light conditions because they can struggle

to capture clear images or reproduce the same color, and they don't provide depth information.

3.2 Part Selection

In this section, we identified and evaluated the specific components that were used in our project, focusing on overall design requirements and their compatibility with the chosen technology, this process was vital for optimizing the efficiency and effectiveness of our final product. We considered factors such as voltage and power, performance, cost, availability, and ease of integration. By selecting the right parts, we ensured that our system not only meets its functional goals but also adhered to project timelines.

Peak Power Information per Component			
Components:	Quantity	Input Voltage (V)	Peak Power Input (W)
Motor Controller	1	5V Logic	5W
ESP32	1	3.3V	0.825W
Raspberry Pi 4	1	5V	15W
Laser Diode	1	1.7V	4.25W
Lidar	1	5V	5-15W

Table 18 - Peak Power Information per Component

3.2.1 Lithium Ion Battery

The BEAM robot required a secondary battery to power all electronics and motors onboard. This battery needs to be lightweight, compatible with a MPPT charge controller, have good temperature ratings, be 12-12.8V and have at least 10-amp hours.

Battery Selection Comparison			
Brand	**Eco-Worthy** [70]	Nermak [71]	XZNY [72]
Voltage	12.8V	12.8V	12.8V
Amp Hours	10Ah	10Ah	10Ah
Battery Type	LiFePO4	LiFePO4	LiFePO4
Discharge Temperature Rating	-20－55℃	-20 – 60℃	-20 – 60℃
Weight	2.46 lbs	2.64 lbs	2.43 lbs
Dimensions	5.9 x 2.6 x 3.7 in	5.94 x 2.56 x 3.71 in	5.94*2.56*3.7 in
Price	$49.99	$35.99	$36.99
Charging Requirements	14.4 – 14.6V CC, ≤10A	14.4 – 14.6 V CC, ≤6A	14.6V CC, ≤10A

	Yes BMS	Yes BMS	Yes BMS

Table 19 - Battery Selection Comparison

3.2.2 MPPT Charge Controller

The BEAM robot required a Maximum Power Point Tracking (MPPT) charge controller that was compatible with lithium battery. It was crucial that the charge controller had a 14.4–14.6V range output for charging the lithium battery, accepted solar power input DC 15–30V, had an output current of 8-12A for rapid charging to reduce downtime and enhance operational efficiency, in addition, it needed to offer protection features from over charging, over voltage, over temperature, etc. To enhance the robot's mobility, it was beneficial for the charge controller to be lightweight, minimizing any additional load on the robot. Finally, a charge controller with some degree of water resistance provided added protection against environmental elements and increased the durability.

MPPT Charge Controller Selection Comparison			
Brand	Powerwerx [73]	**Bateria Power** [74]	Voltset [75]
Input Voltage	16-25 V	15-30 V	≤ 30 V
Output Current	12 A	10 A	10 A
Max Power	150 W	144 W	144 W
Price	$29.99	$36.99	$39.99
Protections[2]	SC, OT	OC, OT, OV, SC	OC, OT, OV, SC
Operating Temperature	N/A	-20－45℃	N/A
Weight	0.25 lbs	0.32 lbs	0.375 lbs
Dimensions	2.3 x 1.6 x 0.9 in	3.75x2.42x1.06 in	6.69"L x 4.72"W x 1.3"H
LCD	No	Yes	Yes

Table 20–MPPT Charge Controller Selection Comparison

3.2.3 Buck Converter (Switching Regulator)

The buck converter was essential for dropping voltage for the electronic components that needed 3.3V or 5V. The buck converter needed to handle a voltage drop of 12V to 3.3V and have good heat dissipation. The TPS40200QDRQ1 had programmable short-circuit

[2] Overcharge (OC), Over Temperature (OT), Over Voltage (OV), Short Circuit (SC)

protection, a current output of up to 3A, overcurrent recovery, and undervoltage lockout. Only short-circuit current limiting was available for the MC34063ADR, so more protective circuit design needed to be applied when using that regulator. The TPS40200QDRQ1 also included a very detailed datasheet that provided layout guidelines, power supply recommendations, and application information. This information was extremely useful for the design portion of the project.

Buck Converter Selection		
Specs	**TPS40200QDRQ1** [76]	MC34063ADR [77]
Voltage Input (Vin)	4.5 – 52 V	3 – 40 V
Voltage Output	0.7 – (Vin-10) V	1.25 – 40 V
Maximum Current Out	3 A	1.5 A
Power Efficiency [78] [79]	≤ 94%	≤ 87.7%
Price	$2.48	$0.70

Table 21 – Buck Converter Selection

3.2.4 Monocrystalline Solar Panel

The power system for the BEAM project ran off a 12.8V battery that required 14.4–14.6V to charge. Typically, solar panels rated for 12V produced a range of 18–22V, so a charge controller was necessary to provide the correct voltage. The robot required a weather-resistant solar panel that not only provided the voltage for charging but also was a suitable size (≤1.5 ft) to be secured to the roof of the machine. All solar panels listed in the table below were rated 12V and waterproof. Eco-Worthy was a reputable energy storage brand, and their 25W solar panel was the perfect fit for the BEAM's power system because of its price, size, charging power, and high user approval rating.

Solar Panel Selection			
Specs	OYMSAE [80]	**Eco-Worthy** [81]	SOLPERK [82]
Power	20W	25W	25W
Size (inches)	14.4 x 13.6 x 0.8	16.5 x 12.6 x 0.7	16.3 x 13.19 x 0.67
Price	$49.99	$35.99	$59.99

Table 22– Solar Panel Selection

3.2.5 Motors

AC motors have a lower initial cost and high efficiency rates compared to other types of motors; however, they present certain trade-offs, factors such as a lower starting torque and the need for adjustments due to their complex speed control were carefully considered. Because of the commonness of brushless motors in AC configurations, they have a low maintenance which makes them ideal for outdoor applications, however, the need of

alternating current to be powered, whether single-phase or three-phase, presents a challenge as our project setup doesn't accommodate this. Since gear motors are characterized for their optimal speed control, they initially seemed to be a good addition to our project, however, the high initial cost coupled with the fact that this project has a low use demand for heavy load made the implementation of gear motors unfavorable. Stepper motors would be a great addition to the project when it comes to the navigation system of the robot because of their inherent ability for counting steps which makes them not require feedback to always know their position, despite their advantages, we ended not going this route because they tend to have a low torque and require a specific algorithm for motion control. The low maintenance of the brushless DC motors and its high efficiency made it a great candidate to implement it in our project, however, its high cost and the complexity associated with its speed control made us ultimately not select it as an option. Although Brushed DC motors require a higher maintenance in comparison to brushless motors and have a lower efficiency rate, we ended up choosing them for the navigation system because of their low initial cost, high reliability, and simple motor control system.

When it comes to choosing a motor, we referred to the values for Torque, angular velocity, power, current, and battery capacity previously calculated on section 3.1.2 Motors to serve as initial criteria for researching the specifications for brushed DC motors.

Brushed DC Motors Comparison				
Motor	E-S Motor 555 Size DC [83]	**Mabuchi RS-555SH** [84]	E-S Motor 775 DC Motor [85]	OSEPP Electronics R540 6-12V [86]
Nominal Voltage	12 V	12 V	12 V	6 V
Torque	400 g-cm	420 g-cm	2 kg-cm	-
Dimensions	77mm x 36mm[3]	3.035"x1.48"[3]	91mm x 42mm[3]	50mm x 35.8mm[3]
No-load Speed	8000 RPM	5100 RPM	4000 RPM	16700 RPM
Weight	-	0.45 lbs.	-	160g
Cost	$14.50	$9.99	$11.78	$14.25
Rated Current	3.5 A	2.83 A	1.5 A	2.5 A

Table 23-Brushed DC Motors Comparison

[3] Motor Dimensions include shaft Dimensions.

The first motor we compared was an E-S motor that features integrated a cooling blade and a dual-channel encoders with hall power of ± (5 V/3.3 V), it has high torque and when tested it proved to last more than 1000 operational hours, in addition, it has stable power and balanced heat dissipation. The second one is a Mabuchi motor that has as key features high torque with high-efficiency, a wrap-around shield that reduces electrical interference, and a speed of 5100 RPM. The third motor is also an E-S Motor that offers high torque and low noise, it has a cooling fan and five group winding at voltages 6/12/24 V. The last motor to consider is an OSEPP Electronics motor that has a no load speed of 16700 RPM with a 10% margin error, a voltage range of 6-12 V but a nominal voltage of 6V, and a no load current maximum of 2.5 A.

3.2.6 Motor Control

We decided to go with the H-bridge driver as the main driver of the motors for the navigation system because it allows for bidirectional control of motors, they usually provide a wide supply voltage range and are highly efficient when driving different types of motors.

Motor Driver	**L293D Quadruple Half-H Drivers** [87]	DRV8870 Brushed DC Motor Driver [88]	TB6612FNG [89]	A5950GLPTR-T [90]
Supply voltage	4.5-36 V	6.5-45 V	15 V	5.5-40 V
Number of DC motors	2[4]	1[4]	2[4]	2[4]
Peak Output current	1.2 A per channel	3.6 A	3.2 A	3A
Size	19.80 mm × 6.35 mm	4.90 mm × 6.00 mm	0.220", 5.60mm Width	0.173", 4.40mm Width
Cost	$8.11	$2.13	$2.93	$2.14

Table 24 – H-Bridge Motor Driver Comparison

3.2.7 Wheels

The wheels chosen for the BEAM project were the all-terrain because the intended setting is on a farm where the soil is uneven and these wheels provided improved traction because of the tread patterns along their surface, in addition, they could withstand rough

[4] The number of motors correlates to bidirectionality functionality.

terrain without excessive wear and tear, and they enhanced the overall stability of the robot and maintained balance.

Wheels	T Tulead Tire Wheels [91]	All Terrain Robot Wheel [92]	All-Terrain Robotics Wheel Set [93]	**DC12V DIY Encoder Gear Motor** [94]
Dimensions	66 x 51.8mm	130 x 59mm	125 x 47.1mm	65 x 10mm
Weight	11.7 oz	173 g	-	-
Shaft hole width	3.66 mmm	6mm	15mm	4mm
Material	Plastic, Rubber	Rubber	Rubber	Plastic, Rubber
Cost	~$2	$16.5	~$10	~$5

Table 25 – All-Terrain Wheels Comparison

3.2.8 MCUs

The MCU's are the heart and central control of all of the robot's processes. It is responsible for task management. Managing and executing multiple tasks simultaneously, ensuring that complicated systems with lots of moving parts, are operated smoothly. For real time systems like ours, the MCU was also responsible for decision making, allowing for real time control to actuators and other necessary peripherals. Along with this, our project needed to connect various different interfaces through methods such as I2C, SPI, UART, and others. In addition, our robot needed to collect, process, and transmit visual information and data from various connected devices. An essential part of our design was based in the relatively low power consumption required as our robot will be continuously powered by solar panels and will be required to go long distances while maintaining functionality. The MCUs picked from are all designed to operate efficiently, often enabling low power modes and come with low power requirements, making them ideal for battery powered devices like ours.

3.2.8.1 Arduino MKR WAN 1300 (Specified for long range motor control and diagnostics)

1st pick is the Arduino MKR WAN 1300 LoRA board. This board provides 32-bit computation similar to other higher end MCU boards on the market, sporting a SAMD21 Cartex-M0+ Microcontroller on board leaves it a suitable candidate for complicated applications that require real time processing speeds. It has a power supply options of a regular USB stick as well as battery powered options, allowing for AA or AAA options. This allows for a much more flexibility in our design options when it comes to supporting our electronics efficiently. One of the defining features of this board ins it CMWX1ZZABZ Radio Module, allowing for long range, low power wireless communications between applicable technologies and applications. This board has been used in other applications

including environmental monitoring, market agriculture, energy monitoring, as well as other IoT applications that would require low power consumption and long-range communications. This made the Arduino MKR WAN 1300 LoRA board a suitable pick for an MCU specialized for the Motor Controllers. [95]

3.2.8.2 Alternative to Arduino: ESP32-WROOM-32 board

Our alternative MCU pick was the ESP32-WROOM-32 board. This board provides powerful 32-bit computation, making it also comparable to other high-end MCU boards on the market. It features a dual-core processor running at 160 MHz, which makes it suitable for complex applications requiring efficient processing speeds. This board offers built in Wi-Fi and Bluetooth connectivity, essential for modern IoT applications. This board is used for various IoT applications, home automation, remote monitoring, as well as other projects requiring high processing power and energy efficiency. Both of these boards provide versatile, powerful, and energy-efficient solutions for a wide array of applications. Specifically, dealing with embedded systems along with IoT applications. After considerations and discussions with advisors and staff, we decided to go with the ESP32-WROOM-32 over the Arduino due to its overall ease of use and to avoid potential issues of compatibility. [96]

3.2.8.3 Raspberry Pi 4 Model B (Specified for Object Detection and Computer Vision)

The Raspberry Pi development boards are capable of handling tasks like object recognition and are able to capable communicate with other boards. Our primary choice would be the Raspberry Pi 4 Model B, equipped with a Quad- Core Cortex A72 (Arm v8) running at 1.5Ghz, as well as up to 8GB of RAM, providing an ample amount of processing power. Available in multiple memory options allowing for more flexibility within our budget. It is able to be connected directly to ethernet, and comes with Wi-Fi capabilities, sporting a Dual-Band 2.4/5.0 GHz IEEE 802.11ac wireless connector, as well as Bluetooth 5.0. It also boasts a wide range of connectivity options and allows for seamless integration with various actuators and peripherals. These boards support I2C, SPI, and UART protocols, allowing them to effectively communicate with other development boards. The board also provides a 40-pin GPIO header to help enable direct hardware connections for external device communication and control. All of these aspects and specifications enable the Raspberry Pi 4 Model B to be made available for real-time object recognition using available software curated by the extensive community support behind the Raspberry Pi development boards. [97]There have been libraries created specifically for the Raspberry Pi that provide tools necessary for computer vision and machine learning models for object recognition and detection. A comprehensive table with all of the researched specifications are available in the chart below.

MCU Feature Comparison [96]					
Feature	Arduino Nano 33	**esp32-wroom-32**	Arduino MKR WAN 1300	Franzininho Board	**Raspberry Pi 4 Model B**
Microcontroller	SAMD21 Cortex M0+	Dual-core @ 240 MHz	ARM Cortex-M0+	ATTiny84	Broadcom BCM2711
Clock Speed	48 MHz	240 MHz	48 MHz	20 MHz	1.5 GHz
Flash Memory	256 KB	4 MB	256 KB	8 KB	microSD
SRAM	32 KB	520 KB	32 KB	512 B	2/4/8 GB LPDDR4
GPIO Pins	14	34	22	12	40
Analog Inputs	8	18	7	8	-
Digital I/O Pins	14	34	22	12	40
Wi-Fi	Yes	Yes	Yes	No	Yes

Table 26 – MCU Feature Comparison

3.2.9 Movement Control Sensors

Movement control sensors were essential for BEAM, as movement control sensors are crucial for ensuring that a robot can navigate its environment efficiently, if necessary, and perform all of its tasks accurately. Their sensors provided the necessary feedback to the control system. This allowed for precise movement and operation of the robot. Here are some key reasons why: First and most important are position tracking and object detection. These features assisted in path planning as well as providing real-time data on the robot's position and orientation, which were crucial for maintaining the correct path and reaching the robot's intended destination without any unnecessary distractions. Secondly, the motor control sensors allowed and provided architecture for a feedback loop, allowing the control system to adjust the motor output continuously, ensuing stable and controlled movement. This is particularly important for tasks that would require higher precision, such as burning weeds with a laser-guided robot or rover.

Table of Movement Control Sensors [98] [99] [100]			
Feature	**Adafruit 9-DOF IMU Breakout**	AMS AS5048B Magnetic Encoder	HC-SR04 Ultrasonic Distance Sensor
Degrees of Freedom	9 (Accelerometer, Gyroscope, Magnetometer)	Not applicable	Not applicable
Measurement Range	360-degree motion tracking	0 to 360 degrees	2 cm to 400 cm
Accuracy	High precision	14-bit resolution	±3 mm

Scan Rate/Update Rate	High-frequency sampling	Up to 5 kHz	-
Interface	I2C, SPI	I2C	Digital
Special Features	Comprehensive motion sensing	High-resolution position feedback	Effective obstacle detection
Best For	Navigation, stabilization, precise motion tracking	Position tracking, motor control	Obstacle detection, basic navigation

Table 27 – Table of Movement Control Sensors

After consideration of these aspects, extensive research was made, and the Adafruit 9-DOF IMU Breakout Sensor was chosen for some specific reasoning. First and foremost, the sensor provides comprehensive motion tracking. Combining an accelerometer, gyroscope, and magnetometer allows the sensor to provide complete motion-sensing capabilities in three dimensions and a total of 9 degrees of freedom, as the sensor name would suggest. This makes it a suitable choice for a wide range of applications, including navigation, stabilization, and precise motion tracking—all things that would be very helpful for an autonomous robot. [98] Confidently and equally as important, it boasts high resolution motion data, enabling the precise control and adjustment of the robot during navigation and operation. Additionally, the gyroscope and accelerometer data help to minimize any potential drift. Finally, the Adafruit 9-DOF IMU Breakout is easily integrated with compatible interfaces such as I2C and SPI, making it much easier to interface with Raspberry Pi and Arduino platforms and development boards. Including an almost excessive amount of documentation and support, allowing and facilitating us for an overall straightforward implementation process. We have also provided a table below with our other considerations for this part for your viewing convenience.

3.2.9.1 Lidar

Our design requires the implementation of a LIDAR. This will be crucial, as our robot needed to be able to map and navigate the environment. LIDAR provided the robot with the ability to create a detailed 3D map of the environment, allowing it to understand and navigate its surroundings effectively and efficiently. Not to mention, object detection and avoidance were paramount. We may deploy in a large field with few possible interruptions; however, in order for our robot to be as versatile as we desire, we believe it is an important feature to make sure the robot has. After extensive research, we have concluded that the Slamtec RPLIDAR A1. The primary reasons for this are due to its ease of integration with both Raspberry Pi and Arduino development boards. Connecting via USB or with UART, there are a lot of resources and documentation available to assist with the setup of the LIDAR. [101] The Slamtec RPLIDAR A1 also provides 360-degree scanning, which would be crucial for a comprehensive environmental mapping and navigation system.

Table of LIDAR Options [101] [102] [103]			
Feature	**Slamtec RPLIDAR A1**	TFMini-S-Micro LiDAR	TF-Luna LiDAR
Measurement Range	0.15 to 12 meters	0.1 to 12 meters	0.2 to 8 meters
Scan Rate	5.5 Hz (default) to 10 Hz (max)	100 Hz	Up to 250 Hz
Interface	UART, USB	UART, I2C	UART
Special Features	360-degree scanning	Compact size, versatile connectivity	High sampling rate
Best For	Comprehensive environmental mapping	Compact designs, budget-sensitive	High update rate applications

Table 28 – Table of LIDAR Options

The Slamtec RPLIDAR A1 offers a measurement range of 0.15 to 12 meters. This also includes accuracy within 1% error within a 6-meter range. This accuracy and range was sufficient for our purposes, including navigation and obstacle avoidance. We have provided a table with some useful comparisons between the other LIDARs we were considering.

3.2.10 Weed Identification Sensors

In order to properly identify which plants are "weeds" and be able to differentiate that with the rest of a field, will require an advanced object detection algorithm. It will also require a high-quality image feed to constantly update the computer vision and object detection. Ideally achieving a detection success rate of around 75% in proper lighting conditions. This will require the use of a high quality RGB camera enabled to be integrated with one or multiple of our MCUs.

3.2.10.1 RGB Camera

After researching many possible candidates for an RGB camera the conclusion came down to the Raspberry Pi Camera Module V2, equipped with a 8 MP Sony IMX219, allowing for high resolution and superior image quality, crucial for accurate object recognition. This being Raspberry Pi's own camera module it has native and well supported compatibility backed by documentation from the Raspberry Pi community, below is a table with other considered camera modules along with some of the features [104]

Comparison Table of RGB Cameras [104] [105]

Feature	**Raspberry Pi Camera Module V2**	Raspberry Pi High Quality Camera	Arducam Pivariety Camera	Arducam IMX219 Camera Modules
Sensor	8 MP Sony IMX219	12.3 MP Sony IMX477	Sony STARVIS CMOS	8 MP Sony IMX219
Resolution	3280 x 2464	4056 x 3040	Varies based on model	3280 x 2464
Lens Options	Fixed lens	C- and CS-mount lenses	Fixed and variable options	Fixed, NoIR, Wide-angle, Fisheye
Special Features	None	Adjustable focus, high quality	Ultra low light performance	NoIR, Wide-angle, Fisheye options
Dimensions	25 x 23 x 9 mm	38 x 38 x 18.4 mm	Varies	25 x 24 x 9 mm

Table 29 - Comparison Table of RGB Cameras

3.2.11 Laser Diode

In our selection process for laser diodes, we carefully considered models emitting in red and blue wavelengths, as these colors are most effective in the photosynthesis spectrum. This choice is pivotal since the wavelengths closely align with the light absorption peaks of chlorophyll, which is crucial for our application of evaporating water from weed leaves. To optimize the performance of our robotic system, we conducted detailed experiments with laser diodes operating at power levels of 1, 2, and 5 watts. This range allowed us to assess the effectiveness of different power outputs and determine which level provides the most efficient evaporation of water while minimizing energy consumption. Our experiments focused on evaluating both the impact of power output on performance and the energy efficiency of the diodes. In addition to performance, we also emphasized selecting laser diodes that offer high operational efficiency and cost-effectiveness. We aimed to balance performance with economic considerations to ensure that the final design is not only effective but also competitively priced. High-efficiency diodes contribute to lower energy consumption, which is crucial for both reducing operational costs and enhancing the sustainability of the system.

1-2 W Blue Laser Diode Specifications		
Model	LT-LD-450-1600M-FS	**M140-M-Type**

Output Power	1100 - 1600 mW	1200 - 1400 mW
Wavelength Range	440 – 455 nm	435 -455 nm
Peak Wavelength, λ_p	450 nm	445 nm
Operation Current, I_{op}	1.7 A	1 - 1.7 A
Threshold Current, I_{th}	80 – 220 mA	0.29 – 0.45 A
Operation Voltage, V_{op}	3.7 – 5.5 V	3.7 – 5.5 V
Module Diameter	9 mm TO9	5.6 mm TO18
Slope Efficiency, η_d	1.0 – 2.0 W/A	1.845 W/A
Cost	$59.00	$10.95

Table 30 - 1-2 W Blue Laser Diode Comparison

5W Blue Laser Diode Specifications			
Model	LT-LD-455-5000M-C [106]	PLPT9 450LB [107]	**GH04C05B9G** [108]
Output Power	5000 mW	5000 mW	5000 mW
Wavelength Range	448 – 462 nm	440 – 455 nm	430 - 450 nm
Peak Wavelength, λ_p	455 nm	450 nm	440 nm
Operation Current, I_{op}	-	3 – 3.8 A	2.24 – 2.28 A
Threshold Current, I_{th}	220 – 420 mA	0.29 – 0.45 A	0.25 – 0.33 A
Operation Voltage, V_{op}	3.6 – 4.8 V	-	4.8 – 5.6 V
Forward/Reverse Voltage	-	4.3V~5V (Forward)	
Module Diameter	-	9mm TO-5	9.0 mm
Slope Efficiency, η_d	1.8 W/A	1.845 W/A	2 W/A
Cost	$42.00	$48.32 (Amount:2)	$29.50

Table 31 - 5W Laser Diode Specifications

2W Red Laser Diode Specifications		
Model	**ML562G85-02**	665A-110-2-1.5-TO9
Output Power	2100 mW	2000 mW
Wavelength Range	635 – 644 nm	665 nm
Peak Wavelength, λ_p	639 nm	665 nm
Operation Current, I_{op}	2.25 A	2.0 – 2.2 A
Threshold Current, I_{th}	0.55 A	0.5 A
Operation Voltage, V_{op}	2.25 V	2.4 V
Forward/Reverse Voltage	2 V (Reverse)	-
Module Diameter	9.0 mm	9.0 mm TO9
Slope Efficiency, η_d	1.2 W/A	1.3 W/A
Cost	$36.50	$120.76

Table 32 - 2W Red Laser Diode Specifications

3.2.12 NEMA 17 Stepper Motor

The NEMA 17 stepper motor is a well-renown motor used for high precision CNC projects that require light motors with high torque. The BEAM's laser control system required a motor that used no more than 12V to power.

NEMA 17 Stepper Motor Selection		
Specs	STEPPERONLINE [109]	**OpenBuilds** [110]
Driving Voltage	12-24 V	12-24 V
Rated Current	2 A	1.68A
Weight	1 lbs	0.77 lbs
Price	$13.99	$17.98

Table 33 – NEMA 17 Stepper Motor Selection

3.2.13 Stepper Motor Driver

The NEMA 17 stepper motors required a driver that provided close to 2A of current without overheating. It was also important to have overvoltage and overtemperature protections in the driver module. All models reviewed for this section are sold in packs of 3 pieces and can interface with 3.3 and 5 V systems. The voltage interface was advantageous for connecting to the microcontrollers that was used to control the motor system.

Stepper Motor Driver Selection		
Specs	**DRV8825** [111]	A4988 [112]
Working Voltage	8.2–45 V	≤ 35 V

Working Current	1.5–2.2 A	1.2 A
Price	$8.99	$7.99

Table 34 – Stepper Motor Driver Selection

In Senior Design 2, we ended up changing from the DRV8825 to the DRV8411A, which are dual H-bridge motor drivers from Texas Instruments designed for driving brushed DC and stepper motors.

Chapter 4 – Design Constraints and Standard

Adhering to specific design constraints and standards was essential to ensure functionality, safety, and compliance with industry norms. This section outlines the critical limitations and guidelines that affect our design choices. Additionally, we explored relevant design standards that apply to our project for each part selected in the previous chapter, taking into consideration different sets of standards from within the US and internationally.

4.1 Design Constraints

In engineering design, addressing both design elements and constraints is fundamental to creating effective and practical solutions. The interplay of these factors determines how well a system performs, endures, and adapts to various challenges. For our project, BEAM, the careful consideration of design and constraints were crucial for achieving our objectives. The design phase involves integrating various technical and functional components to meet specific goals. For our robot, this meant optimizing the laser system for efficient water evaporation, ensuring precise targeting and control, and incorporating a robust mechanism for navigating and operating among weeds. Each design choice impacted the robot’s performance, reliability, and user experience. Constraints, on the other hand, imposed limitations that must be navigated to ensure the robot's practical viability. Environmental constraints are particularly significant, as the robot will operate outdoors and must endure diverse weather conditions. Thus, selecting weather-resistant materials and designing protective features were essential to prevent damage and maintain operational efficiency. Economic constraints also played a vital role, as the project must balance performance with cost-effectiveness. In a competitive market, delivering a robot that is both affordable and highly efficient is key to its success. Moreover, reducing pesticide use and labor costs aligns with growing demands for sustainable and environmentally friendly agricultural practices. By rigorously addressing these design and constraint considerations, our project aims to develop a robotic system that excels in performance while being durable and cost-effective. This comprehensive approach ensures that the robot not only meets the immediate needs of modern agriculture but also stands out in the market as a reliable and sustainable solution. The thoughtful integration of design elements with constraint management will ultimately drive the success and adoption of our innovative robotic technology.

4.1.1 Environmental Constraints

The efficiency and effectiveness of the laser in dehydrating weed leaves were highly dependent on factors such as humidity, temperature, and precipitation. High humidity levels, especially in Orlando's summer months, could reduce the laser's efficiency as the increased moisture content in the air and plants required more energy to achieve the desired drying effect. Similarly, extreme temperatures, whether too low or too high, could impact the robot's components, leading to potential malfunctions or reduced operational life. Cold temperatures could cause materials to contract and affect battery efficiency, while higher temperatures could lead to overheating and increased wear and tear on mechanical parts. In this regard, understanding these environmental conditions helped in planning and scheduling the robot's operation and during periods when the weather was most conductive to its function. Furthermore, operating within defined environmental parameters helped in minimizing the ecological impact, ensuring the robot's activities did not inadvertently harm non-target plants or wildlife and maintained compliance with local environmental regulations.

As we can see in Figure 13 - Orlando Humidity by Month., Orlando's monthly humidity data reveals a clear pattern of fluctuation throughout the year, reflecting the seasonal climatic changes typical of a subtropical region. The humidity levels are at their lowest during the spring months, with March and April recording 65% and 64%, respectively. This dip in humidity suggests a drier period, which might be favorable for the laser-based weed drying method as the reduced moisture in the air could enhance the efficiency of the laser in dehydrating the weeds' leaves. As summer approaches, the humidity begins to climb, peaking in the late summer months. June shows a significant increase to 75%, followed by July and August, which are the most humid months with 79% and 80%, respectively. September maintains this high humidity at 80%, indicating a prolonged period of moist conditions. These high humidity levels could pose challenges for the laser method, as the increased moisture content in the air and plant leaves may reduce the effectiveness of the drying process.

The fall months see a gradual decline in humidity, with October dropping to 73%, and November stabilizing at 71%, similar to January. This period might offer slightly better conditions than the peak summer months but still represents a relatively high moisture environment. December, at 73%, marks the beginning of the cooler, less humid winter season, transitioning into January, when the humidity starts at 71%.

Overall, the spring months of March and April, with their lower humidity levels, emerge as the optimal periods for employing high-power lasers to dry weeds in Orlando. Conversely, the summer months, particularly July through September, with their peak humidity, present the most challenging conditions for this method. The robot should operate optimally within a humidity range of 60-70% for maximum efficiency in drying

weeds. This range is typically observed during the spring months (March and April) in Orlando [67]

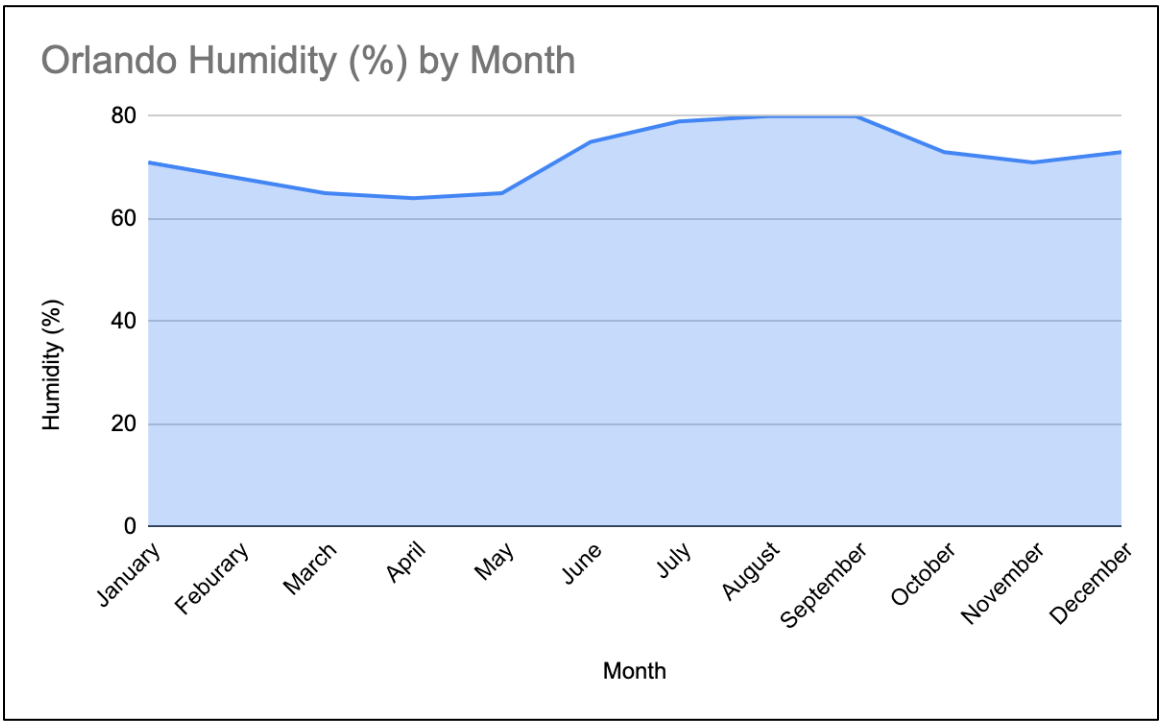

Figure 13 - Orlando Humidity by Month [67].

Other factors such as rainy days and precipitation patterns present varying conditions for operating a robot that uses lasers to dry weeds' leaves. Referencing Table 16 - Weather Factors in Orlando , the month of January experienced only 5 rain days and 58 mm of precipitation, making it a relatively good period for laser operation since the dry conditions would facilitate efficient weed drying. Similarly, February's 5 rain days and 52 mm of rainfall are conducive to this method. March maintained this favorable trend with 5 rain days and slightly higher precipitation at 64 mm, though still manageable for the laser's effectiveness. April, with 5 rain days and 55 mm of rain, continues to provide suitable conditions for the laser-based weed drying approach. May, however, introduced more challenges with an increase to 7 rain days and 70 mm of precipitation. This uptick indicated the beginning of more frequent rain, which could intermittently hinder the laser's performance. The situation worsens in June, which sees 14 rain days and 157 mm of precipitation. This significant increase in rain frequency and volume makes June a challenging month for the laser method due to the high humidity and wet conditions that are less conducive to drying. July and August are the most challenging months for laser operations. July had 16 rain days and 158 mm of precipitation, while August peaks with 17 rain days and 170 mm of rainfall. These months are marked by frequent and heavy rain,

posing substantial difficulties for the laser's effectiveness in drying weed leaves. September, with 14 rain days and 142 mm of precipitation, remains unfavorable for the laser method, though slightly less so than August. The frequent rains during these months would likely disrupt the drying process, making them the worst periods for using the laser technique. The conditions improve in October, which sees a reduction to 8 rain days and 69 mm of precipitation, marking the transition back to drier weather. This change makes October a more suitable month for laser operations compared to the preceding summer months. November and December, with only 4 rain days each and the lowest precipitation levels of 36 mm and 51 mm respectively, present the best conditions for operating the laser-based weed drying robot. The reduced rainfall and fewer rain days during these months would enhance the effectiveness of the laser in drying the weed leaves efficiently [].

4.1.2 Economic Constraints

Building an autonomous laser weeding robot for agricultural use involves several economic constraints such as research and development costs, materials and manufacturing costs, maintenance and repairs over the robot's lifespan, economic viability for farmers, and market and competition economics. For this project, we will go into detail on how BEAM would impact market and competition, and how it would reduce costs for farmers using manual labor and pesticides.

4.1.2.1 Market and Competition

There are not many consumer-level laser-weeding robots available on the market now. The laser-weeding robots that are on the market are specifically available for large-scale farmers that have several hundred acres of land to cultivate, such as Carbon Robotics Laser-weeder [9]. The Carbon Robotics laser weeders are available for over $1,000,000 and are said to return a profit after 1-3 years. They also require a trailer and hitch to operate the machinery because it needs to be towed through the fields to laser weeds. These large machines are often too expensive and hefty to prove useful for small scale farmers. There are also some large-scale machines, like the LettuceBot by Blue River Technology, [11] that use pesticides to remove weeds, but these are still quite expensive and are designed to be towed by a tractor through large fields. Many of the smaller farm and garden machines available are used for strictly mowing lawns or are too small to sufficiently cover fields of 10-50 acres. An example of the smallest robot we found designed specifically for removing weeds was the Tertill weeding robot [14]. This small solar powered robot is available at full price for $350 and kills weeds with string trimmers and specially designed wheels. There were no small-scale laser weeding robots available on the market for less than the $12,331 RBTX by ingus autonomous agriculture laser weeding robot [113]. The total cost of the BEAM robot will be less than $1,000, and it is built to be most useful for smaller farms or large gardens. The BEAM robot could be very competitive for this portion of the market and would be advertised as a lower cost environmentally friendly way for small

farmers to control weeds. With proper maintenance, the lifespan of the BEAM robot could be at least 10 years and would provide farmers higher return on investment.

4.1.2.2 Reducing Costs in Labor and Pesticides

The economic impact of laser-handled weeding agricultural robots is multifaceted. It requires a major initial investment, has the capacity to create a major shift in the agricultural technology market, and helps to move weeding methodology away from using a much higher degree of manual labor and chemical compounds. Replacing it with a much cleaner, energy-efficient, and cost-efficient alternative would save farms of all sizes a lot of unnecessary costs on labor and pesticides. Laser weeding robots, such as those made by Paul Mikesell, the CEO of Carbon Robotics, have a high initial cost, compared to a midsize tractor that would run farmers numbers in the 5-figure range. [114] This upfront initial cost can be a serious barrier to entry, especially for smaller farms. Larger farming may find it easier to budget financially for new equipment, mostly due to the long-term savings in labor and chemical costs of pesticides. These new robots introduce a competition to the agricultural technology that the market hasn't been seen before. This much cleaner and safer alternative is going to challenge the dominance of chemical herbicide corporations over industrial weeding. Carbon Robots is one of the leading players in this space; however, other startups are continuing to enter the market. This may potentially continue to drive innovation and reduce costs over time. Leading to a new cycle of increased competition in this space, and ultimately to even more accessible technology being used by a much broader range of farmers.

Laser weeding offers many advantages over traditional manual labor and pesticide use. It provides environmentally friendly and much more precise weed control; this helps to reduce soil disruption and the elimination of negative environmental and health impacts associated with chemical herbicides. Along with precision weed removal, laser weeding allows for a much more accurate solution without affecting the surrounding plants, thus reducing overall crop damage [115]. For large-scale farms, this can lead to significant cost and operation efficiency over time. This is due to the reduction in labor costs and potential issues with groundwater contamination, and other issues caused by the rampant use of these chemical pesticides. Some pests have now become more resistant to certain pesticides the more they are being used, resulting in even higher use to compensate, propagating the situation until pesticides may become ineffective entirely, similar to the situation involving anti-biotics and our overuse causing a similar effect on how we treat bacterial infections. Smaller farms would also greatly benefit from the use of this technology; if they were able to get past the initial cost barrier, they would also see great long-term savings. [116] In the future, we hope that further initiatives and potential government subsidies would support this new technological adoption in agriculture. It could play a critical role in making these robots much more accessible to smaller farms and allow farms on any scale to benefit environmentally and financially.

Laser weeding offers many advantages over traditional manual labor and pesticide use. It provides environmentally friendly and much more precise weed control; this helps to reduce soil disruption and the elimination of negative environmental and health impacts associated with chemical herbicides. Along with precision weed removal, laser weeding allows for a much more accurate solution without affecting the surrounding plants, thus reducing overall crop damage [115]. For large-scale farms, this can lead to significant cost and operation efficiency over time. This is due to the reduction in labor costs and potential issues with groundwater contamination, and other issues caused by the rampant use of these chemical pesticides. Some pests have now become more resistant to certain pesticides the more they are being used, resulting in even higher use to compensate, propagating the situation until pesticides may become ineffective entirely, similar to the situation involving anti-biotics and our overuse causing a similar effect on how we treat bacterial infections. Smaller farms would also greatly benefit from the use of this technology; if they were able to get past the initial cost barrier, they would also see great long-term savings. [116] In the future, we hope that further initiatives and potential government subsidies would support this new technological adoption in agriculture. It could play a critical role in making these robots much more accessible to smaller farms and allow farms on any scale to benefit environmentally and financially.

4.1.3 Manufacturability Constraints

The BEAM project consists of several main parts in its design, including the use of sensors to navigate and identify weeds, we are not required to build these sensors from scratch, other parts that we are allowed to purchase such as the chassis, motors and wheels, solar panels help us to reduce the amount of design needed for mechanical parts, and concentrate on the electrical aspect of the project which is building a working PCB that integrates all these different components.

One of the main constraints we have to consider is the manufacturability constraints since as students, we are limited by availability of materials and their durability, even doing proper research does not mean the design is final, some components might be changed throughout the process or they might not be as resistant as entailed in their specifications which causes problems because our intended environment is outdoors, which would add to the overall cost of the project, going over budget. In addition, we have to keep in mind a simple-enough design that can be achieved with the already available equipment at the lab. We also need to finalize a design as soon as possible to order parts since the suppliers can run out of stock, leaving us to change the design to fit a new component.

4.1.4 Health and Safety Constraints

A constraint to consider is health and safety since our project is meant to eradicate weeds, we implement the use of laser by using a 5W diode whose intensity can damage someone's

corneas, to safely test this we need to use proper equipment at the lab and consider the location for the demo environment.

A key component of our design is the use of batteries to keep the robot operating for hours, however, the improper use of them such as overheating or failure in the design can make them explode or leak. In addition, we need to test out each part of the design before integrating them together to avoid any damage to the electrical circuit.

4.2 Industrial Design Standards

Abiding by engineering standards is crucial in the development of the BEAM robot to ensure safety, reliability, and consumer protection. Industrial design standards provide a framework that ensures our robot will meet essential safety, quality, and performance criteria. Compliance with these standards not only enhances the robot's marketability, but also protects consumers by guaranteeing that the product is safe to use and performs as expected. By integrating these standards into our design process, the project aims to deliver a high-quality, trustworthy product that aligns with regulatory requirements and the industry's best practices.

4.2.1 Standards for Lithium-Based Batteries

In the United States, many standards have been developed for installation, testing, and design of lithium batteries. There are internationally recognized created by the International Electrotechnical Commission (IEC), Underwriters Laboratories (UL), and Japanese Standards Association (JSA) [117]. The IEC has several standards for li-ion batteries including performance, safety, and testing. The Li-ion performance standard IEC 61960 discusses secondary cells and batteries containing alkaline or other non-acid electrolytes, and secondary lithium cells and batteries for portable applications. This standard is important to reference for the BEAM project and goes into detail about the performance of Li-ion batteries such as charge recovery, charge retention, final voltage, nominal voltage and many more features. It goes into detail about many electrical tests that can be performed to ensure that the capabilities of a Lithium-Ion battery fall within normal levels. The IEC safety standard IEC 62133-2:2017 is also very important to reference because it discusses general safety considerations surrounding battery wiring, ventilation, temperature/voltage/current control, and appropriate charging procedures [118].

4.2.2 Standards for Charge Controllers

The IEC has also produced a performance standard IEC 62509 that normalizes functionality and performance of a photovoltaic battery charge controller. The requirements for this standard are divided into 5 categories: battery lifetime protection,

efficiency, user interface, fail safe functions, and marking and documentation. This standard will help guarantee reliable operation and essential protection functions of charge controllers. This allows charge controllers to better protect batteries and increase user awareness of the charge controller's functions. In this standard, section 4.3.3.5 describes how charge controllers should be able to compensate charging set-points based on temperature. This is very useful in a component that will be exposed to high temperatures and needs to perform accurately. This standard greatly benefits overall charge controller design and usage, and the advantages increase the value of the charge controller for BEAM [119].

4.2.3 Standards for Solar Panels

Similarly to lithium-ion batteries, solar panels have many national and international standards created by the International Electrotechnical Commission (IEC), the Institute of Electrical and Electronics Engineers (IEEE), the Underwriters Laboratories (UL), and the American Society for Testing and Materials (ASTM) [120]. IEEE offers many guides for monitoring resources connected to electric power systems using PV, and practices for testing performance of stand-alone systems. The IEC has many standards on PV characteristics, commissioning tests and inspections, PV design for stand-alone systems, installation, monitoring, safety, and performance. IEEE Std 1526-2003 is a standard that discusses the best practices for testing and monitoring the performance of stand-alone PV systems. It discusses how many PV problems occur, and recommended practices to address them. This standard discusses several tests and inspections for the entire PV and battery system that could prove useful for arranging the power system for BEAM [121].

4.2.4 Standards for Motors

The IEEE Standards Association put together a guide (IEEE std 115-1983) where it lists and explains the testing procedures for DC Machines that includes the setup, analysis, and the reporting of test results, it can be divided in two main categories; the test of the machines designed for essentially ripple-free operation and the ones designed for use with rectifier power supplies [122]. It aids manufacturers, designers, and engineers to have a consistent and reliable method for testing these machines by providing forms and instructions on the different components that should be tested, environment conditions, how to perform different measurements, and how to determine its performance level.

The general tests consist of four categories, the first is the preliminary tests which include the conditions of the location of the tests, the ideal ambient air and altitude (3300ft [122]) where the tests should be performed, the terminal markings following the manufacturer's diagrams and ANSI/NEMA, the direction of the rotation when not specified. It also contains the winding resistance measurements at 25°C to calculate the copper losses in the motor, the air gap measurements of each motor's pole should be to the nearest 0.100mm for integral-horsepower and to the nearest 0.050mm for fractional-horsepower [122] and

the diameter of the wire should be “at least 70% of the difference between the diametric distance of the main pole faces and the outside diameter of the rotor” [122] , how the polarity of each field winding should be independently determined and the impedance drop of field coils is an indication of a coil having shorted-turns, how vibration can be measured using a low ripple DC source and the mounting conditions change from small to large machines because of impracticality. In addition, it specifies the percentage a brush has to be in contact with the commutator in order to be a good fit and the different methods for test the brushes functionality, and the conditions that insulation resistance between the windings and the frame should be tested.

The second category are the performance determination tests that include the magnetic saturation curve requirements, how to achieve a successful commutation, how to calculate the regulation for motors and generators, how to calculate the efficiency for both motors and generators and different methods depending on the machine size for fractional and integral horsepower, the different I^2R losses for armature, windings, brush-contact, shunt-field, exciter, and stray-load. The third category are the temperature tests where it specifies the type of instruments that should be used, the several methods for the measurements, the test procedure with the amount of time they should last depending on whether they’re a rated machine test or a load test, the armature shut-down temperature determination. The final category consists of miscellaneous tests that consist of audio-noise test, electromagnetic inference test, voltage wave shape, etc. Lastly, it states that these tests may not be all that should be performed since a particular standard may vary depending on the machine’s type or size [122].

4.2.5 Standards for Motor Controllers

There are several standards to consider when choosing or designing a motor controller, which varies according to the current type. One of them is the IEC 61508 series called Functional Safety Standard by the International Electrotechnical Commission where it highlights the safety standards for electrical, electronic, or programmable systems [123]. These series categorize its integrity levels by their average probability of failure on demand and per hour whether it is on low mode or continuous mode, and provides risk reduction for different automated devices that may include sensors, actuators, micro-processors, etc. Another example to take into consideration is the IEC 60204-1 called the Safety of Machinery because it covers the programmable electronic equipment including different components working in a coordinated manner and it is specific for equipment not surpassing 1000V and 200Hz [124]. It also specifies the voltage range for both AC and DC supplies, the ambient temperature and altitude, and its storage, protection against electric shock and the protection of the equipment.

4.2.6 Standards for Laser Safety

When working with high-power lasers such as the 1W, 2W, and 5W red and blue laser diodes for the project, it is essential to adhere to stringent laser safety standards to ensure the safety of operators and the environment. Lasers of these power levels typically fall under Class 4, which means they can cause severe eye and skin damage and are a fire hazard.

In the context of a robot designed to use Class 4 lasers for drying weed leaves, adherence to laser safety standards is paramount to ensure both operational effectiveness and safety. These standards, such as IEC 60825-1, ANSI Z136.1, ISO 11553 series, and FDA Laser Product Safety Regulations, provide comprehensive guidelines that influence every aspect of the robot's laser usage [125].

Firstly, the robot's design incorporates engineering controls specified by these standards. It includes safety interlocks that automatically shut off the laser if protective enclosures are opened, preventing accidental exposure to high-power laser beams. This feature ensures that the robot can safely operate in environments where humans or animals may be present.

Administrative controls are equally crucial. The robot is programmed to undergo regular hazard assessments and operational checks to ensure that the laser emission remains within safe limits as defined by the standards. This involves monitoring the laser power output and ensuring that it does not exceed levels that could potentially cause eye or skin damage to operators or bystanders.

Furthermore, the robot's operation is guided by clear protocols derived from these standards. Operators are trained extensively in laser safety protocols, including how to handle emergencies involving laser exposure. This training ensures that operators understand the risks associated with Class 4 lasers and are prepared to respond appropriately in any situation.

Personal protective equipment (PPE) is another critical component. The robot provides operators with laser safety goggles specifically designed to protect against the wavelengths emitted by Class 4 lasers. This PPE is essential for safeguarding operators' eyesight during weed drying operations, where direct exposure to laser radiation is possible.

Overall, by adhering to these laser safety standards, the robot not only optimizes the efficiency and effectiveness of weed drying processes but also prioritizes the safety of operators and bystanders. It integrates robust engineering controls, meticulous administrative procedures, comprehensive operator training, and appropriate PPE to mitigate risks associated with Class 4 laser use in agricultural applications. This approach ensures that the technology contributes positively to agricultural practices while

maintaining the highest standards of safety and compliance with international laser safety regulations [125].

4.2.7 Standards for MCU

In the rapidly evolving field of robotics and MCUs, ensuring the reliable operation of these devices requires strict adherence to these engineering standards. The IEEE provides several standards and technical specifications:

IEEE 1801-2018 is a standard that provides a UPF format, specifying the power intent in the design of integrated circuits. Covering important aspects including power domain, power management strategies, and power modes, these are vital for creating low-power integrated circuits. [126]

Another useful standard to introduce would be IEEE 1620-2008, which is the standard for testability and diagnostic characteristics and metrics. Our robot will require rigorous testing and adjustment to make sure our design is working as we intend, so a set of standards and guidelines for testing and diagnosing these systems will be a boon for maintaining the overall reliability of the robot and its results. [127]

IEEE 1725-2011 is a standard focused on mobile computing devices, specifically for ensuring the safety and reliability of rechargeable battery systems. Our robot will have a rechargeable solar-powered battery, so these guidelines will serve us well when integrating these systems together. [128]

Finally, the IEEE 29119-1-2013 Standard provides a framework for testing the software of the MCU, which will be very helpful for our project as our coding knowledge could be supported by these standards. [129]

Chapter 5 – Comparison of Chat GPT and Similar Platforms

ChatGPT is a language model developed by OpenAI and has gathered significant attention for its advanced capabilities in language processing and generation. It is an AI tool that offers a multitude of applications, including generating content, providing personalized recommendations, and automating customer service. In the field of engineering, ChatGPT has proven to be an asset, helping with complex problem-solving, technical documentation, and streamlining communication among teams. However, while its benefits are substantial, it is important to consider the potential drawbacks and limitations that accompany its use. This chapter aims to explore both the advantages and disadvantages of ChatGPT, focusing on its utility in engineering and some broader applications.

5.1 Chat GPT Pros

ChatGPT is highly effective for information consolidation and has a vast knowledge base on many subjects. ChatGPT's knowledge is derived from many diverse sources including books, websites, academic and scientific research papers, Wikipedia, and other publicly available databases and information repositories. This immense availability of information allows the conversational AI to consolidate information on almost any topic and provide users with quick responses to any question. One of the best ways to use ChatGPT is for consolidating basic information about a subject.

Case Study 1: Question: "Tell me about linear motors."

> "Linear motors work by directly converting electrical energy into linear motion using electromagnetic principles. Here's a brief description of how they function:
>
> 1. **Components**: A linear motor consists of two main parts:
>   - **Forcer (Primary)**: Contains windings that generate a magnetic field when electric current passes through them.
>   - **Track (Secondary)**: Contains permanent magnets or a magnetic material that interacts with the magnetic field from the forcer.
> 2. **Operation**:
>   - **Electromagnetic Induction**: When current flows through the windings in the forcer, it creates a magnetic field.
>   - **Magnetic Interaction**: This magnetic field interacts with the magnetic field of the track.
>   - **Linear Force**: The interaction between the two magnetic fields produces a force that propels the forcer along the track, creating linear motion.

Key Points

- **Direct Drive**: The force generated is directly applied to move the load without the need for intermediate mechanical components like gears or belts.
- **Precision and Speed**: Linear motors offer high precision, rapid acceleration, and smooth motion, making them ideal for applications requiring exact positioning and high-speed operation.

Applications

Linear motors are used in a variety of fields, including:

- **Transportation**: Propelling maglev trains.
- **Manufacturing**: Moving components in CNC machines and robotic systems.
- **Medical Devices**: Precision movement in MRI machines and other diagnostic equipment.

Overall, linear motors provide an efficient and precise way to achieve linear motion in many advanced technological applications" [130].

In Case Study 1, the user asks ChatGPT to be informed about linear motors, and is then provided with components for this motor, how the motor operates, key points for the motor, and its applications. All the information was readily combined into an arranged list for the user to read. The 24/7 availability of an AI that can promptly search a large database to collect and coalesce information is an extremely beneficial tool to use when starting research or looking for answers to questions. The AI even searches across many databases to develop a well-rounded response with accurate information for the user.

Another benefit of ChatGPT is its ability to provide quick pros and cons for comparing simple components. If a user wants to compare the difference between a linear motor and a DC motor then ChatGPT will compare both on several specifications such as cost, design and control, variety of specific component types, and other motor specific parameters. The user can also use prompt customization to focus on specific areas of interest in the AI's responses. This is very efficient for focusing, comparing, and understanding the difference between well-known components but may be less helpful for specific components because ChatGPT may provide the wrong data. ChatGPT is useful for providing well known qualitative information about components, and not necessarily quantitative information about a part. It is always important to fact check specific data when using ChatGPT as a resource.

Another Pro of using a tool like ChatGPT is generating creative ideas because it is trained to discover patterns, to handle and analyze massive amount of data in a matter of seconds, making it useful to pull information from multiple sources such as reports, scholarly

articles, and websites the same time and compacting the said information. To achieve what we want, we first need to feed it a prompt or we can also feed it information in order to get a more detailed explanation of the ideas we want.

Case Study 2: Prompt: "I need ideas for a senior design project for the Electrical and Computer Engineer College"

"Certainly! Senior design projects in Electrical and Computer Engineering (ECE) can span various domains and technologies. Here are some ideas across different subfields of ECE:

Embedded Systems/Internet of Things (IoT)

1. **Smart Home System:** Design a centralized IoT-based system that controls various home appliances (lights, HVAC, security) through a mobile app or voice commands.
2. **Health Monitoring Device:** Create a wearable device that monitors vital signs (heart rate, temperature, etc.) and sends alerts to caregivers or doctors when anomalies are detected.
3. **Environmental Monitoring System:** Develop a sensor network to monitor air quality, temperature, and humidity in urban areas and display data on a web interface.

Robotics and Automation

1. **Autonomous Delivery Robot**
2. **Industrial Automation System**
3. **Robotics Arm Control**

Signal Processing and Communication

1. **Wireless Communication Network**
2. **Audio Signal Processing**
3. **Radar System**

Power Systems and Renewable Energy

1. **Solar Power Optimization**
2. **Energy Harvesting Device**
3. **Battery Management System**

Computer Vision and Image Processing

1. **Object Recognition System**
2. **Gesture Recognition Interface**
3. **Medical Imaging Analysis**

Other Ideas

1. **Blockchain-based Secure Voting System:**
2. **Augmented Reality (AR) Application**
3. **Wearable Technology for Sports**

These ideas can be tailored and expanded based on specific interests, available resources, and expertise within your team or academic institution. It's important to

consider feasibility, scope, and potential impact when choosing a senior design project" [130].

In Case study 2 we fed it a straightforward, yet a slightly more specific prompt. In the example above we condensed the information given by the AI tool because of space reasons, it generated five precise subfields of ECE accompanied by a broader category for scenarios not encompassed by the initial subfields, each one presented three ideas and it even suggested execution approaches, in some of the example it detailed the project's functionality in a real world application and the desired setting for testing. Case Study 2 demonstrated the impact that AI tools can be for generating creative ideas through the use machine learning algorithms because it reduced what would typically require hours of research across different source materials (like university websites detailing past projects) into seconds by providing concise yet detailed-enough ideas and in an organized manner. It also proves helpful for brainstorming ideas when given prompts such as "give me more examples for this" or asking it to ignore a certain part of the prompt after it is no longer useful, so it stops searching across multiple sources for obsolete information.

ChatGPT can also be used to cross language barriers and gain understanding of complex word translations in specific fields. This is especially useful for students who understand multiple languages and use this to expand their resource base. Language barriers are problematic in general because they impede effective communication and understanding in various aspects of life. In social interactions, language barriers can create misunderstandings, foster feelings of isolation, and prevent meaningful connections between individuals from different linguistic backgrounds. Especially, language barriers pose a considerable problem in healthcare because they hinder effective communication between patients and healthcare providers, leading to misunderstandings and misdiagnoses. Patients who cannot communicate their symptoms accurately may not receive the appropriate treatment, which can result in adverse health outcomes and complications. However, using ChatGPT offers patients a simple method to overcome these communication challenges as study conducted at Stanford University School of Medicine showed ChatGPT (GPT-4) can accurately and understandably translate common patient-focused otolaryngology questions into multiple languages [131].

In Case Study 3, a native Korean speaker asked ChatGPT to translate a hard medical paragraph that was generated by ChatGPT and terminologies for each medical word.

Case Study 3: Prompt: "Please translate this paragraph in Korean and provide definitions for each word: The pathophysiology of myocardial infarction involves the abrupt rupture of an atherosclerotic plaque within a coronary artery, resulting in the formation of a thrombus that obstructs blood flow. This occlusion leads to ischemia and necrosis of the myocardial tissue distal to the blockage. The resultant myocardial cell death triggers an inflammatory response, with the release of cytokines and infiltration of neutrophils and macrophages, which further exacerbates tissue damage."

심근 경색의 병리생리학은 관상동맥 내의 아테로스클러틱 돌기의 급작스러운 파열로 시작되어 혈액 흐름을 막는 혈전 형성을 초래합니다. 이 폐쇄는 막힘 지점 이후의 심근 조직에서 허혈과 괴사를 초래합니다. 이로 인해 발생하는 심근 세포의 사망은 염증 반응을 일으키며, 사이토카인의 방출과 중성 세포 및 마크로파지의 침윤을 포함하여 조직 손상을 더욱 악화시킵니다.

Definitions:

- 심근 경색 (simgeun gyeongsak): Myocardial infarction
- 병리생리학 (byeongri saengrihak): Pathophysiology
- 관상동맥 (gwansang dongmak): Coronary artery
- 아테로스클러틱 (ateroseukeulleotik): Atherosclerotic
- 돌기 (donggi): Plaque
- 혈전 (hyeoljeon): Thrombus
- 혈액 흐름 (hyeoraek heuleum): Blood flow
- 폐쇄 (pyesoe): Occlusion
- 허혈 (heohyeol): Ischemia
- 괴사 (goesa): Necrosis
- 심근 조직 (simgeun jojik): Myocardial tissue
- 사망 (samang): Death
- 염증 반응 (yeomjeung baneung): Inflammatory response
- 사이토카인 (saitokain): Cytokines
- 중성 세포 (jungseong sepo): Neutrophils
- 마크로파지 (makeuropa ji): Macrophages
- 조직 손상 (jojik sonsang): Tissue damage

Surprisingly, ChatGPT offered a Korean translation of a complex medical paragraph in Case Study 3, providing not only definitions for each term but also phonetic transcriptions. However, there was a minor mistake in the phonetic transcription for "plaque," which should be "dolggi," not "donggi." Nonetheless, the translated paragraph flowed naturally, employing appropriate translations of conjunctions, prepositions, and without any grammatical errors discernible from a native speaker's perspective.

ChatGPT also facilitates easy learning of coding for students. Learning coding can be difficult for many students due to several reasons. Firstly, it involves grasping abstract concepts like algorithms and data structures, which can be challenging to understand initially. Additionally, mastering the syntax and grammar of programming languages is crucial, as syntax errors can lead to bugs and frustration. The Faculty of Art, Computing and Creative Industry at University Pendidikan Sultan Idris conducted research subjected on Polytechnic students in the Electrical Engineering Department, who took the fundamental programming class. The results of the statistical analysis indicate that students

have a moderate level of understanding of the topic. The most challenging aspect for them involves grasping abstract concepts related to the role of variable position in computer memory, such as multi-dimensional arrays, looping statements, and functions during program execution. Students also struggled with understanding the basic programming structure and designing programs to solve specific tasks. Additionally, the majority of students found practical situations, like laboratory activities, to be very helpful in learning programming. However, it was identified that insufficient provision of examples by lecturers significantly influences students' understanding of programming [132]. In this sense, ChatGPT offers students the opportunity to learn coding by providing relevant code for systems and explanations for each script.

In Case Study 4, the user asked ChatGPT for a MATLAB code to obtain a Fourier Transform of an image that the user uploaded.

Case Study 4: Prompt: “How do I get a Fourier transform of the image through MATLAB?”

To perform a Fourier transform of an image in MATLAB, you can follow these steps:

1. **Read the Image**: Load your image into MATLAB using the imread function.

```
img = imread('your_image.png');  % Replace 'your_image.png' with your image file path
```

2. **Convert to Grayscale (if necessary)**: If your image is color and you want to perform Fourier transform on a grayscale version, convert it using rgb2gray.

```
img_gray = rgb2gray(img);  % Convert to grayscale if needed
```

3. **Perform Fourier Transform**: Use the fft2 function to compute the 2-dimensional Fast Fourier Transform (FFT) of the image.

```
fft_img = fft2(img_gray);
```

4. **Shift the FFT**: By default, MATLAB's fft2 places the zero frequency component (DC component) in the top-left corner. To view the transform with the zero frequency in the center, use fftshift.

```
fft_img_shifted = fftshift(fft_img);
```

5. **Display the Fourier Spectrum (Optional)**: To visualize the Fourier spectrum, you can plot it using imshow and abs to show the magnitude.

```
magnitude_spectrum = abs(fft_img_shifted);
```

imshow(log(1 + magnitude_spectrum), []); % Log-transform for better visualization

This process will compute and visualize the Fourier transform of your image in MATLAB. Adjustments can be made based on whether you want to work with the original or grayscale image and how you prefer to visualize the transform.

ChatGPT supplied the code for obtaining the Fourier-transformed image, we applied the codes to the following image in Figure 14 - Original Image 'a' inserted to MATLAB called ‘a’

Figure 14 - Original Image 'a' inserted to MATLAB

ABelow in Figure 15 - Code applied to MATLAB is the screenshot of MATLAB script window. We evaluated them in Command Window and checked the outcome image.

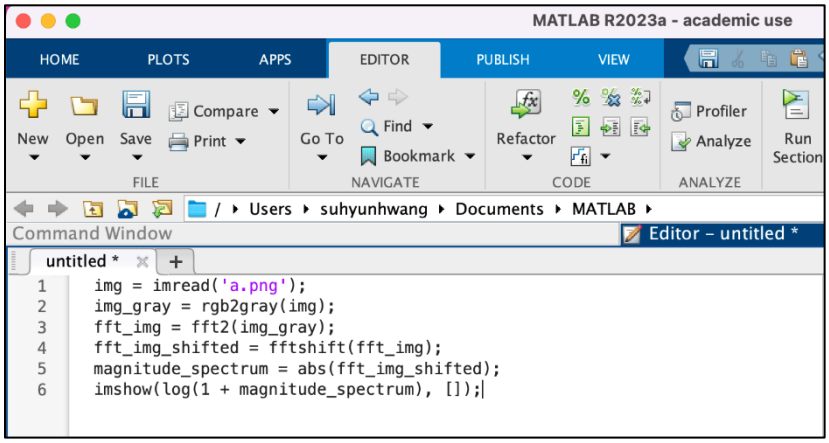

Figure 15 - Code applied to MATLAB

Figure 16 - Fourier Transformed Image is the outcome image. We can see the image was Fourier transformed in a right way, and as such, ChatGPT indeed provides useful codes and explanations that students can apply and learn.

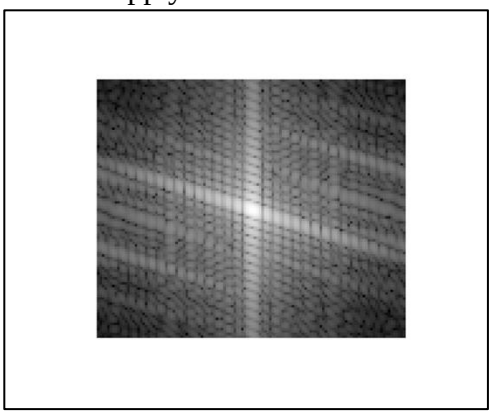

Figure 16 - Fourier Transformed Image

5.2 Chat GPT Cons

ChatGPT is a fantastic tool for generating solutions to given problems; however, it is nowhere near perfect. At times, the issue arises that chat GPT will give out either inaccuracies or just straight-up false information. This is likely due to the overall inherent limitations of the data that is given for training, as well as the specific AI models' inability to browse the web and check for verification the same way we do. This mostly comes down to one major issue with the technology that prove to be its tightest bottleneck. The first and more important issue of the two is the overall lack and nature of the training data. Chat GPT has been trained on a myriad of text data scrubbed from all reaches of the net. A very basic recap of how ChatGPT transforms text into useful information goes as follows: The AI scans and processes information from relevant sources, such as webpages. This data is then learned by the AI through a process called backpropagation, where the model adjusts its parameters to improve accuracy. Further details on backpropagation are beyond the scope of this paper and project. The point being that while the AI system can "learn" and "know" things, it is only able to draw from potentially flawed resources created by humans. The legality as well as morality of data farming and basically stealing most of the internet's text and images without proper compensation is still something that is widely debated within the AI industry as well as in all other industries that it affects. OPENAI and other AI organizations have tried to solve this issue by using AI-generated content to continue to train the AI models, but there is a very serious and glaring flaw with that solution. That being the overall increase and projection of errors. If the AI is fed bad information created by another mistaken AI, these inaccuracies can become propagated and applied in the training cycles. This can severely degrade the performance and accuracy of new models. Not to mention that there are some horrifying and sometimes comical examples of how these poorly trained AI algorithms can lose the sense of real work nuances in favor of making sure a user is given a result. Leading to potential consequences for the people who

depend on these resources for accurate information. The greatest number of examples showing AI hallucinations ironically, comes from Google's own Gemini AI model. Ironically a website famous for its accuracy and prestige is now being flooded and oversaturated by its own AI results at times directly contradicting normal google search results, and overall misleading, and confusing its users. Most of the training data comes from web documents, math, and code attached to their own Google AI page. A reference has been provided to a page that has shown plenty of examples of incorrect or dangerous responses. Some of these include the response to "What are the health benefits of taking a bath with a toaster?" Google's AI responded that it would be a "fun way to unwind and wash away stress." The AI then thankfully immediately contradicted itself by correctly stating that it may be dangerous and lethal and to not attempt it. Another example was the suggestion to mix glue into a cheese sauce to make it stickier when responding to the prompt "cheese not sticking to pizza." Thankfully, the AI does seem to be able to correct itself mid-prompt; however, a user is less likely to read the corrected portion due to the habit of internet users focusing on the first few highlighted lines, and thus having the chance to take this very dangerous and false information as the truth without proper verification [133].

As previously mentioned, AI tools operate on defined parameters and rely heavily on particular data, therefore, when presented with an ambiguous or vague prompt, they may struggle to accurately interpret the meaning, humans can often draw context of a sentence by facial expressions or tone of voice, however, AI systems solely source of context is that piece of text that when it's insufficient, it can lead to wrong or irrelevant outputs that don't address the user's needs. When given the prompt "Write a Report on Robots" it started by listing the types of robots, their applications and advancements, and impact on society, however I wanted a more detailed explanation of agriculture robots and their electronic components, meaning that AI needs a more detailed input for the desired output.

One of the biggest problems with information collection using ChatGPT is its inability to understand complex user input. If a user uses ambiguous language or wants the chat to use complex problem solving, it might struggle to follow along and forget necessary details. When a user provides too many details to keep track of, the chat's response can be full of errors or become oversimplified. ChatGPT often struggles to maintain context over long conversations, which can lead to inconsistencies in responses. These responses will often turn up as contradictory information or incorrect data. Length inputs can also overwhelm the system and cause it to miss important details. To lessen complexity issues with the system, users can ask follow up questions to clarify vague responses, break down lengthy or detail-heavy problems into smaller questions, or verify ChatGPT's information across reputable sources. Using these skills will help users mitigate limitations around complex information with the AI and allow it to provide more useful responses.

Another concern is that ChatGPT does not cite its sources, which can present challenges regarding the accuracy and reliability of the information it provides. When prompted to cite sources, ChatGPT may generate responses that include inaccurate websites or links

that lead to outdated or unmaintained sources. This lack of citation and reliance on internal data means that information generated by ChatGPT may not always reflect the most current or verified data available. This issue is particularly evident in fields where information rapidly evolves, such as current events or cutting-edge research. As a result, users should exercise caution and verify information obtained from ChatGPT through other reliable sources before relying on it for critical decisions or authoritative information. This aspect highlights the importance of using ChatGPT as a tool for generating ideas and insights rather than as a sole authoritative source of information.

Another major flaw with large language models like ChatGPT comes from the architecture issues, and vast amounts of training data make it difficult to understand what is really going on under the hood of these LLMs. These large language models are built using neural networks with billions of different parameters, each with their own weights and biases. These models operate by predicting the next word in a sequence that is based on the probabilities derived from extensive training data on diverse and massive datasets. These probabilities are so obscure and abstract that it is often too difficult for them to be fully comprehended by other humans, including the people creating the LLM. When an LLM is trained, these models are exposed to a myriad of texts; their main way of learning is based on statistical correlations rather than a true "understanding" like people would have. [134]

These models generate responses by estimating the probability of the sequence of words, which can more often than not lead to "hallucinations," the generation of plausible but completely incorrect information, or just completely made-up and non-existent information. Even the AI developers and researchers who create these models do not fully understand their inner workings. Because of the magnitude of the data required to be processed, connections and patterns cannot be explicitly programmed or easily understood. [135]

Even Stephen Wolfram has complained that AI has turned more into a "black box" than anything more interpretable. A black box is defined as "any complex piece of equipment, typically a unit in an electronic system, with contents that are mysterious to the user." If AI turns more and more into a black box and we leave more and more control in our own hands, the ethical and practical challenges of technology like this become much more readily apparent. As mentioned before, the training data itself can introduce biases, and the models can, at times, produce or recreate content that would reflect these inherent biases. [136] Efforts made to align AI outputs with ethical guidelines would and have inadvertently induced even more forms of bias. This goes without mentioning the ethical question of scraping the internet of text and using it to create a commercialized product without compensation, as these require an entirely different discussion.

In summary, these AI large language models have very impressive capabilities, and it is the depth of their operations and the scale of their training data that contribute both to the capabilities mentioned as well as the reason that they have become so complex that even their creators find it truly challenging to fully grasp. The complexity undercuts the

importance of ongoing research and careful application of the technologies in order to mitigate their risks while properly harnessing these technologies responsibly.

Chapter 6 – Hardware Design

The hardware design section focused on the base components of the BEAM robot where each element played a crucial role in the overall functionality and performance of the robot. This detailed the selection and integration of materials for durability purposes, the electrical power system and the design parameters that were taken into account, the implementation of the laser system regarding the lenses and intensity of the beam, and the testing conducted on a breadboard that later led to the finalization of the PCB.

6.1 Hardware

The hardware design of the BEAM robot determined its structural integrity, power efficiency, and operational efficiency. The selection of frame materials and hardware components was essential to ensure the robot was durable, lightweight, and capable of withstanding the harsh conditions of agricultural environments. The electrical power system and power delivery mechanisms were designed to provide reliable and efficient energy management for the robot to run all peripherals and the driving motors. By carefully considering these hardware elements, our design aimed to create a vehicle-type robot that could perform reliably in the demanding agricultural terrain.

6.1.1 Materials and Design

The frame of the BEAM robot was constructed out of lightweight v-slot aluminum. This material is corrosion-resistant and cheaper than other material options such as steel. Aluminum is also a softer metal, so it is easier to cut to length than other metals [137]. The metal's malleability made it easier to shape with common power tools when we needed to adjust the length of the framing. The v-slot aluminum was very easy to apply hardware to, we used brackets, t-nuts, and M5 screws to construct almost any shape or frame with this type of metal. The v-slot aluminum is also very widely used in hobbyist projects, so there were a lot of well-documented websites and many accessible 3D models for printing brackets or carriages for the laser control system's gantry.

6.1.2 Electrical Power System and Power Delivery

The power requirements of our system came from the Raspberry Pi 4, ESP32WROOM, and laser control system. The first section of our power system provided voltage and current for the Raspberry Pi 4, which required 5V and 3A to function. The Raspberry Pi's maximum recommended voltage is 5.25V [138]. A buck converter was used to drop the battery's voltage output from 12V to 5V to power the electronics on board. The circuit had 12V in and 5V out, along with 3A output to support the ideal voltage and current requirements for the Raspberry Pi 4. A later portion of the circuit was designed to drop from 5V/3A through another power regulator circuit to 3.3V/0.8A for the ESP32WROOM. While designing the circuit for the TPS40200-Q1 buck booster, it was important to note

several parameters such as the desired output current, output ripple voltage, over and undershoot voltage, the efficiency we wanted to see from the system, and the switching frequency. After noting these values, we followed the TPS40200-Q1's datasheet provided by Texas Instruments to find appropriate values for inductors, resistors, and capacitors.

TPS40200-Q1 Design Parameters [78]						
PARAMETER		**TEST CONDITIONS**	**MIN**	**NOM**	**MAX**	**UNIT**
V_{IN}	Input voltage	-	8	10	12	V
V_{OUT}	Output voltage	I_{OUT} at 3A	4.85	5	5.15	V
	Line regulation	0.2 % V_{OUT}	4.99	5	5.01	V
	Load regulation	0.2 % V_{OUT}	4.99	5	5.01	V
V_{OVER}	Output overshoot	For 3A load transient from 3A to 0.3A	-	45	100	mV
V_{UNDER}	Output undershoot	-	-	30	-	mV
I_{OUT}	Output current	-	1	2	3	A
Efficiency		At nominal input voltage and maximum output current	90%			
F_S	Switching Frequency	-	-	300	-	kHz

Table 35 – TPS40200-Q1 Design Parameters

The decided efficiency target for the BEAM switching regulator was 90% and with the output parameters being 5V/3A, the output power is equal to 15W. Using the power efficiency equation, we found how much power needed to be delivered to the input to achieve 90% efficiency in the system. P_{IN} was found to be 16.67W using this equation, and then using both P_{IN} and P_{OUT}, the total power loss for the system was expected to be around 1.67W.

$$Efficiency = \frac{P_{OUT}}{P_{IN}}$$

(7) – Power Efficiency

$$P_{IN} = \frac{P_{OUT}}{Efficiency} = \frac{15W}{0.90} = 16.67W$$

$$P_{loss} = P_{IN} - P_{OUT} = 16.67W - 15W = 1.67W$$

(8) – Power Loss

The buck converter circuit required a FET to control the power output during its turn-on period. This was beneficial for a system with high input voltages and was supposed to prevent extreme power dissipation [139]. The FET works in combination with a current sensing resistor that detects when the current switches and an error amplifier with a 700mV reference.

FDC654P MOSFET Information						
Parameter		**Test Conditions**	**Min**	**Typ**	**Max**	**Unit**
$R_{DS(on)}$	Static Drain-Source On-Resistance	V_{GS} = -10V, I_D = -3.6A	-	63	75	mΩ
		V_{GS} = -4.5V, I_D = -2.7A	-	100	125	
		V_{GS} = -10V, I_D = -3.6A	-	90	115	
BV_{DSS}	Drain-Source Breakdown Voltage	V_{GS} = 0V, I_D = -250µA	-30	-	-	V

Table 36 – FDC654P MOSFET Information

6.1.2.1 *FET Selection Criteria*

The TPS40200-Q1 datasheet had a section detailing FET selection criteria and parameters to look for. $R_{DS(on)}$ of the FET rises with breakdown voltage and it is important to select a FET with the lowest breakdown voltage possible to prevent $R_{DS(on)}$ from rising. Then, to select the size of the power FET, we needed to know the losses from switching and DC in the circuit. DC losses are inversely related to device size, and device size is proportional to $R_{DS(on)}$ so it is important to select an $R_{DS(on)}$ that results in a small loss of power [ref]. The total power-loss budget we found earlier was 1.67W. The total FET losses must be smaller than this number. The FDC604P p-channel MOSFET by onsemi has an $R_{DS(ON)}$ of 0.075mΩ and should result in a low voltage breakdown. Next, we found the DC conduction loss in a FET using Equation (9) – DC Conduction Loss.

$$P_{DC} = {I_{RMS}}^2 \times R_{DS(on)}$$

(9) – DC Conduction Loss

We know $R_{DS(on)}$ at V_{GS} = -10V is 75mΩ, V_{IN} = 12V, V_{OUT} = 5V, I_{OUT} = 3A, D=0.4167, L = 10µH, and the switching frequency f_{sw} = 100kHz. To accurately find the DC conduction loss in a FET, we need to know the DCR value for the output inductor. The datasheet for the TPS40200-Q1 recommended a ferrite core inductor that can deliver our maximum current of 3A and has a saturation current of I_{MAX} plus one-half the ripple current, or 3.15A. This ripple current is caused by the inductor switching during current flow changes in the

switching regulator. Using the current recommendations, we can find the inductance using the equation below.

$$L_{MIN} = \frac{V_{IN} - V_{OUT}}{I_{PEAK}} \times t_{ON} = \frac{12V - 5V}{0.3A} \times (1.388 \times 10^{-6}s) = 32.3\mu H$$

(10) – Minimum Inductance for FET

FET Selection Equation List and Definitions	
$I_{RMS}{}^2 = \left[D \times \left(I_{OUT}{}^2 + \frac{\Delta I_{PP}{}^2}{12}\right)\right]^{\frac{1}{2}}$	$\Delta Ipp = \Delta V \times D \times (t_S/L_I)$
$\Delta V = VIN - VOUT - (DCR + RDS(on)) \times IOUT$	RDS(on) = FET on-state resistance
DCR = inductor DC resistance	D = duty cycle, (Vout/Vin)
t_S = reciprocal of the switching frequency	L = inductance

Table 37 – FET Selection Equation List and Definitions

The inductor that best suits the criteria for the buck booster is the DR125-330-R by EATON Electronics. This inductor has a ferrite core, a rated inductance of 33 µH, a current rating of 3.28A, and a saturation current rating of 3.84A. The DCR of this inductor is 0.0505Ω and it was used to complete the I_{RMS} formula to find the total DC power loss in the MOSFET as 145mW.

$$I_{RMS}{}^2 = \left[\frac{5V}{12V} \times \left((3A)^2 + \frac{(0.30A)^2}{12}\right)\right]^{\frac{1}{2}} = 1.937\ A$$

$$P_{DC} = 1.937\ A\ \times\ 75\text{m}\Omega = 0.145\ \text{W}$$

Next, a low-ESR ceramic capacitors is needed on the output of the circuit can drastically reduce the ripple voltage for higher ripple currents. The ceramic capacitor CC0805JKX7R9BB105 by YAGEO is 1µF and has an ESR of about 0.007Ω, making it a great choice for an output capacitor for this circuit. For a current output of 3A, a 10% ripple current (ΔI_{PP}) is 0.30A and produces a 2.225 mV ripple voltage based on the following equation:

$$V_{ripple} = \Delta I_{PP} \times ESR + \frac{\Delta I_{PP}}{8 \times f_{SW} \times C} = 0.3A \times 0.007\Omega + \frac{0.3A}{2.4 \times 10^3} = 2.225mV$$

(11) – Voltage Ripple Equation

Where: ΔI_{PP} = 0.30A, ESR = 0.007Ω, f_{SW} = 300kHz, and C = 1µF

Following the ceramic capacitor, we needed a rectifier on the drain of our FET. When choosing a rectifier for the MOSFET output, we had to take into consideration that rectifier must have a larger breakdown voltage than the max voltage input to allow for switching transients. Because our input voltage is 12V, the rectifier needed to be able to withstand this value, so we chose the SS3003CH shottky barrier diode by onsemi. This diode is rated for up to 30V/3A, and has a forward voltage drop of 0.42V. Following the selection of the rectifier diode, several resistor and capacitor values were found by analyzing the switching frequency of 300kHz, calculating the overcurrent threshold level, and researching the function of the soft-start capacitor and how frequency compensation works in the TPS40200-Q1. Combining all these parts, the circuit schematic is shown below.

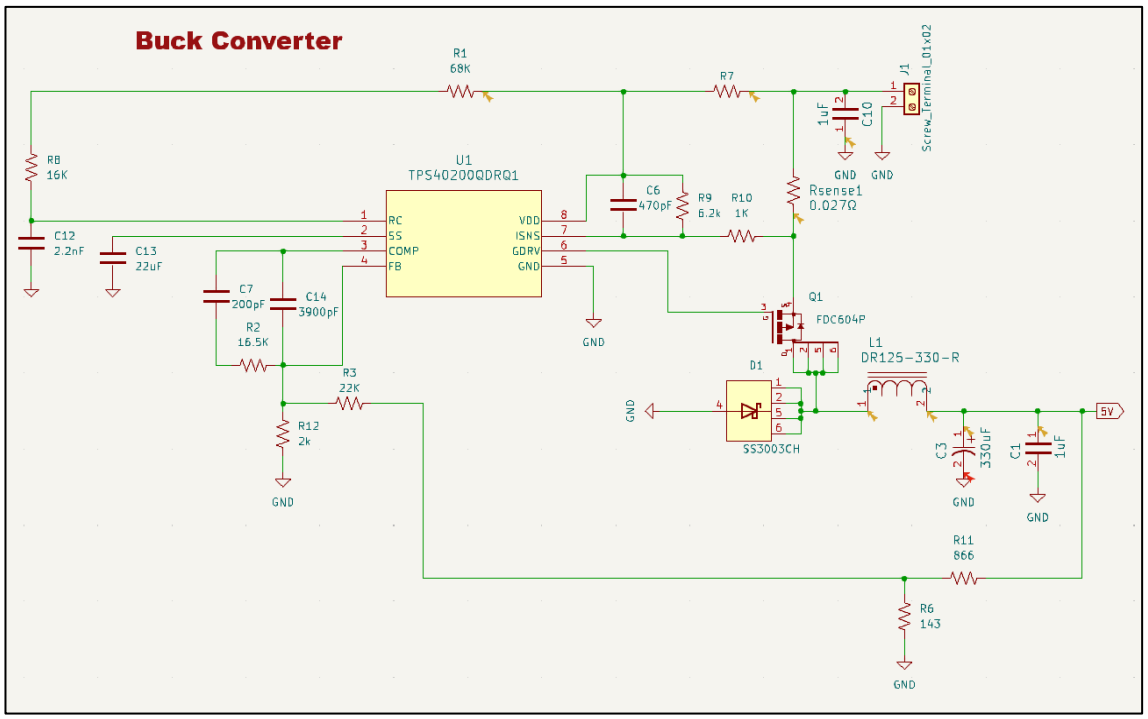

Figure 17 – Buck converter circuit diagram

Unfortunately, for the TSP40200, the datasheet given was not only difficult to follow, but included several equations that seemed to give conflicting information or assumptions on what specific values resistors and capacitors were supposed to be. This led to an imbalance in the circuit during testing that would overload the FET and burn the IC. Because the

design was so complicated, our team ended up switching to the TPS62142RGTR, a switching regulator in the same family. The design for this circuit not only had less components, but the part was also available in Texas Instruments WEBENCH tool, which allows users to customize power regulator circuits. This allowed our team to lay out both a regulator circuit for the 12V to 5V drop, but also a circuit for the 5V to 3.3V drop using the LM1117 linear regulator.

6.1.3 Motor Control

To create the schematic for the motor control system we took the datasheet for the L293D driver as reference. We chose DC motors for the navigation, however, when a motor is running it creates a magnetic field that increases the longer and faster the longer it's on until it reaches a certain point. When the motor is stopped, it will do anything possible to keep this field going meaning it will switch the voltage applied to the motor that can be x-times greater than the original voltage, causing a significant voltage spike on the terminal that when not taken into consideration it'll blow the integrated circuit. To combat the back EMF produced by the motors, the use of flyback diodes connected to each terminal of the motor is implemented so that either in forward or reverse biased direction the circuit is

protected because they allow for EMF discharge if the flyback diode chosen has a high enough voltage rating.

Figure 18 – Navigation Motor Control Schematic (SDI)

The layout diagram in the datasheet advise to use a capacitor of 0.1µF in connection to the power logic pin and one of 1µF to the power supply pin, however, to absorb some absorb some of the excess charge so not all of it goes back and acts as an energy reservoir as a final design, three capacitors were placed in parallel at each power supply pin of the drivers.

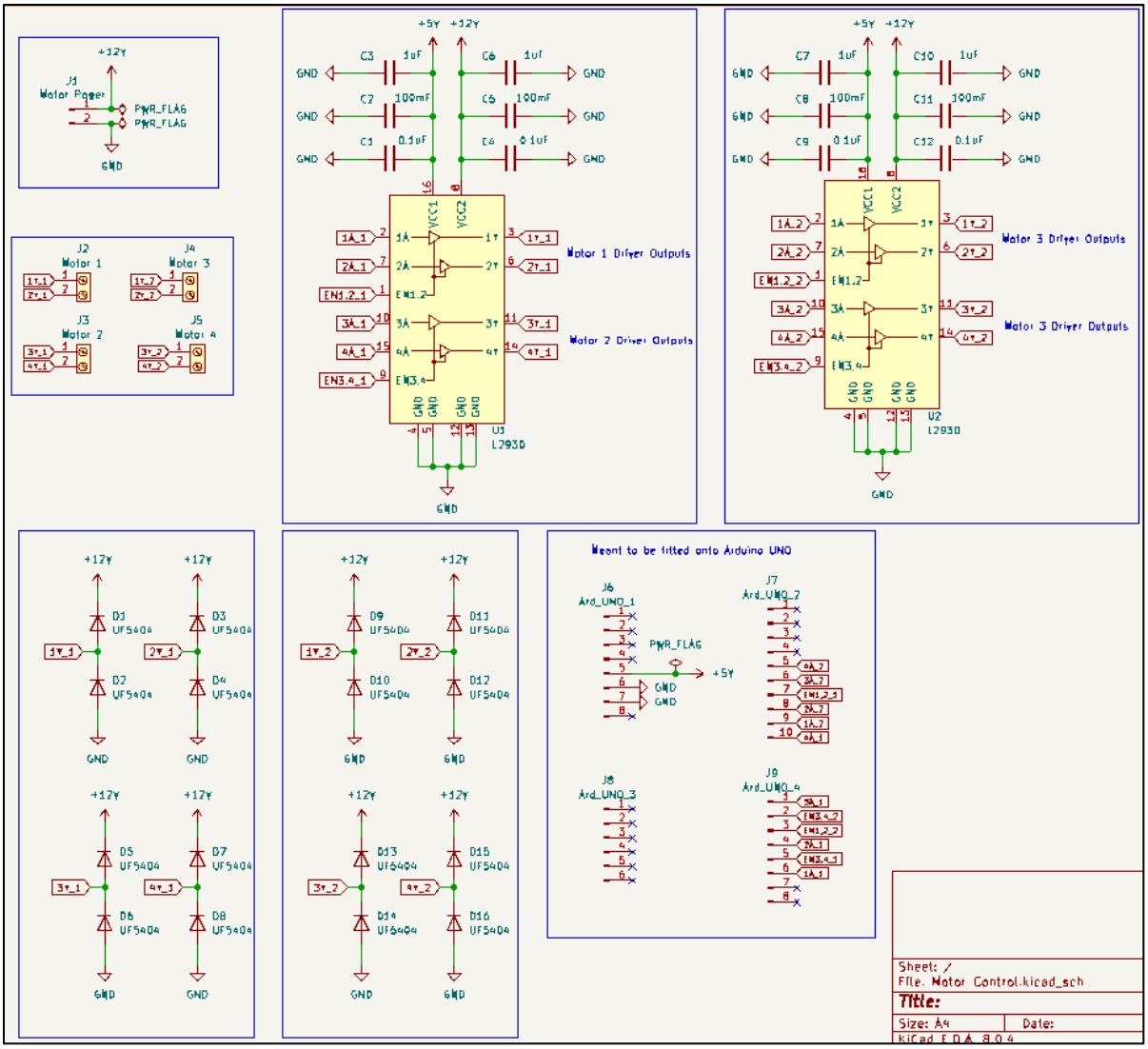

In Senior Design II we decided to change the DC motor driver to a BTS7960B because of its higher-level current limitation of 43A, its implementation of two MOSFETs, one for the low side and one for the high side, and its low path resistance of 16mΩ. This driver is

a half bridge that is why the use of two drivers are needed to achieve bidirectionality, looking at the protection functions of the datasheet [140], there is a risk of undervoltage shutdown when it goes below 4 volts which poses a problem since the ESP32 outputs 3.3V, to combat this, a level shifter was placed in between the GPIO pins and the motor drivers. The TXS0108E is an 8-bit bidirectional level shifter that has 20 pins, the desired voltage for the lower and higher side needs to be supplied while using 0.1µF capacitors. The tri-state buffer output-mode enable pin was pulled low using a 1kΩ resistor.

The driver has seven pins, three of those are for the control of the motor, one enable pin and two for direction, looking at the application example of the datasheet [140] and the layout considerations, 10kΩ resistors were connected in between the level shifter output pins and the driver pins to protect them from excess currents. The pins from the voltage supply and power output were connected with a capacitor of 470nF to reduce noise. The resistor value used for the Slew Rate pin on both drivers was 5.1kΩ according to the low and high side characteristics.

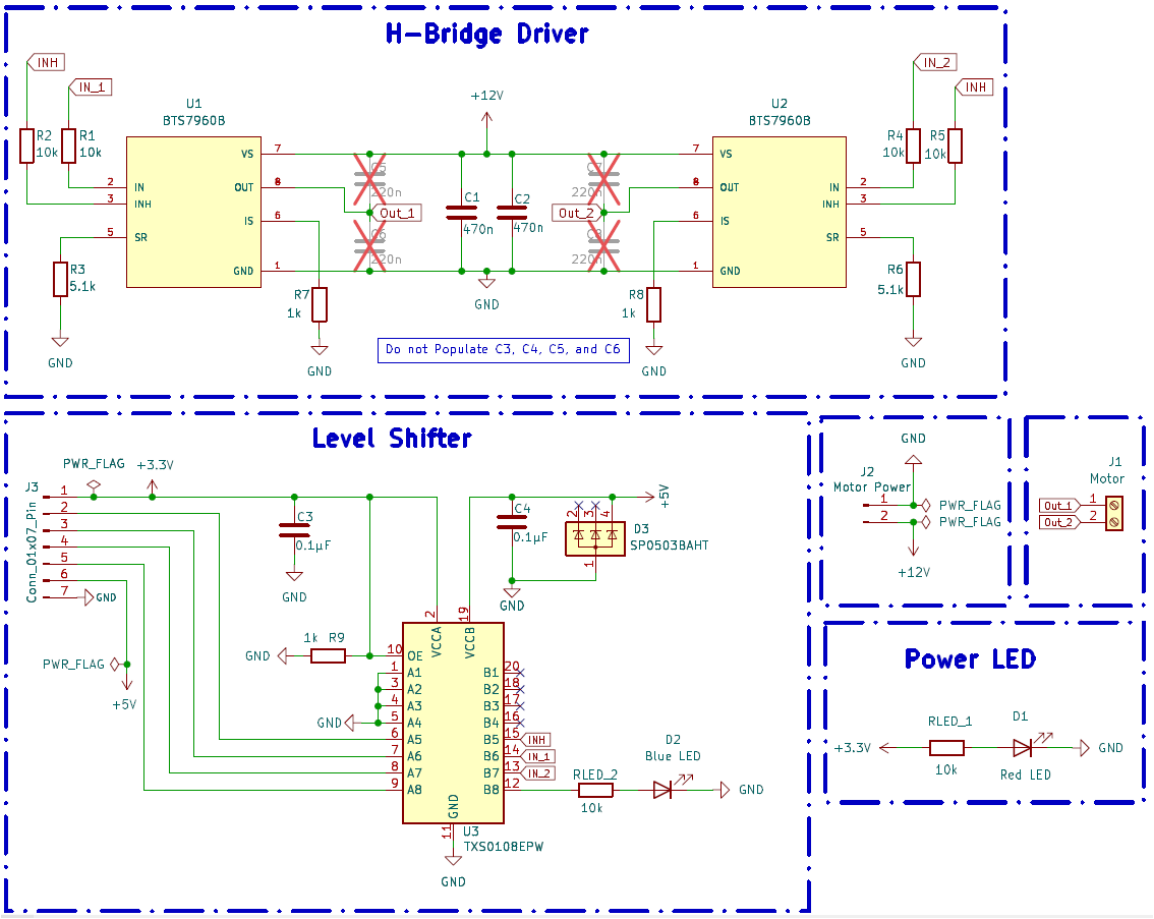

Figure 19 - DC Motor Driver PCB (SD2)

6.1.4 MCU ESP/Raspberry Pi Plugin

To create the schematic for the MCU/PCB we took the datasheet for the ESP32 and raspberry Pi 4 as reference. We connected the VCC and the GND pins for basic voltage control. The other connections are directly connected for the SPI connection framework. We connected the ESP32 SDO (GPIO 23) to the Raspberry Pi GPIO 10 (MOSI). The ESP32 SDI (GPIO 19) was connected to Raspberry Pi GPIO 9 (MISO). Additionally, the ESP32 SCK/CLK (GPIO 18) was connected to the Raspberry Pi GPIO 11 (SCLK). Finally the ESP32 SCS/CMD (GPIO 5) was connected to the Raspberry Pi GPIO 8 (CE0). At the moment the only pins necessary to connect are the relevant data pins for the SPI connection framework, as the main purpose of our PCB is to connect these two boards via hardware as well as in software.

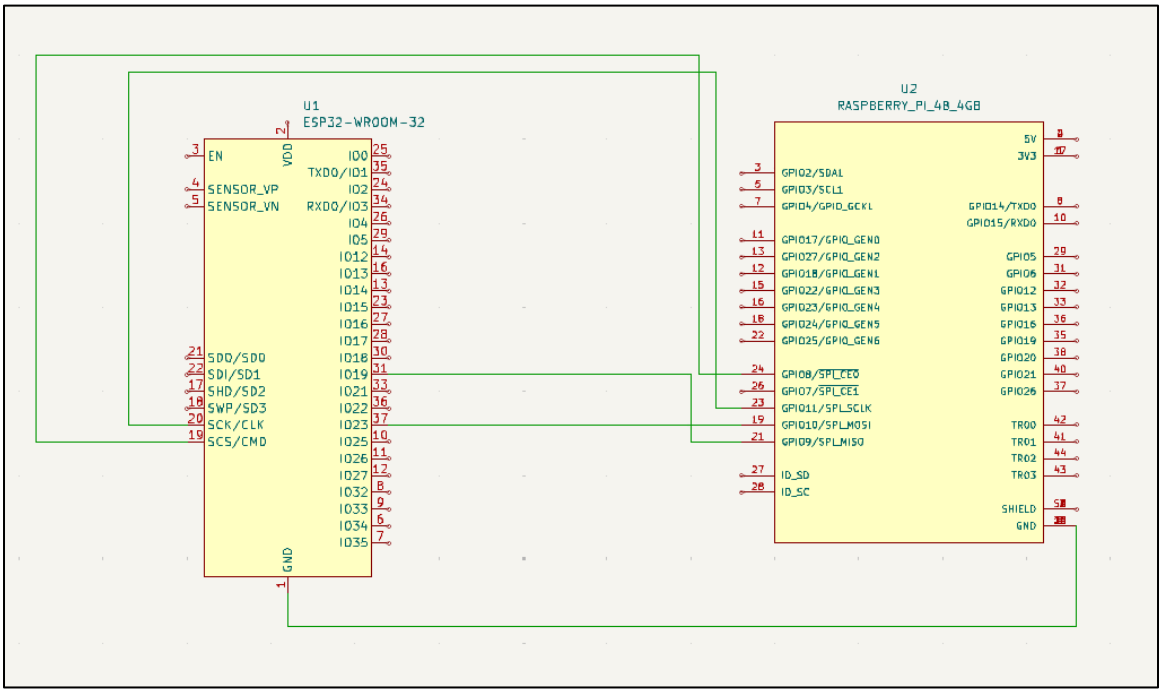

Figure 20 - MCU/PCB Connections Schematic (DATA PINS ONLY)

6.1.5 Laser System

One undesired characteristic of laser diodes is their elliptical beam shape. The beam waist of a laser diode typically has a diameter of about one micron in the vertical direction, perpendicular to the active layer, and a few microns in the horizontal direction, parallel to the active layer. This results in an elliptical ratio that usually ranges from 1:2 to 1:4. Moreover, the far-field divergence of the beam differs significantly between the vertical and horizontal directions, with a typical ratio of 2:1 to 4:1. The vertical direction, where

the divergence is greater, is referred to as the "fast axis," while the horizontal direction is known as the "slow axis." As the beam propagates, the size in the fast axis direction expands more rapidly than in the slow axis direction, leading to a vertically elliptical beam shape [59].

Another undesired characteristic of laser diodes is their large divergence angle. The full width at half maximum (FWHM) divergence angle, a critical parameter in the laser diode industry, is commonly used to specify beam divergence. For laser diodes, this angle typically ranges from 15 to 40 degrees in the fast axis direction and from 6 to 12 degrees in the slow axis direction. These FWHM values provide a standardized measure of beam divergence, which is essential for understanding and controlling the behavior of laser diode beams in various applications. This pronounced divergence is particularly evident in the fast axis direction, necessitating specialized lenses for effective collimation or focusing of the beam. To address this challenge, lenses must incorporate at least one aspheric surface to correct spherical aberration and maintain a numerical aperture (NA) of at least 0.3. This specification helps to prevent severe beam clipping. However, even with a lens featuring an NA of 0.6, some degree of beam clipping is unavoidable. The market offers a variety of aspheric lenses specifically designed for collimating laser diode beams. These lenses typically have numerical apertures ranging from 0.3 to 0.6. Despite their advanced design, these lenses cannot completely eliminate beam clipping in the fast axis direction. This unavoidable clipping results in several undesirable effects, including the formation of side lobes, shifts in the focal point, and an overall increase in beam divergence. The impact of these issues on the performance of laser diodes underscores the importance of careful lens selection and design in applications requiring precise beam control. The presence of side lobes, for instance, can interfere with the beam's intended path and reduce its effectiveness in applications requiring high precision. Similarly, focal shifts can alter the beam's focus, compromising accuracy and efficiency. Increased divergence further exacerbates these problems by spreading the beam over a larger area, reducing its intensity and precision [59].

6.1.5.1 Lens

To optimize light collection during the process of laser collimation, it is essential to consider the divergence angle in the calculations. By employing a larger divergence angle, one can ensure that a significant portion of the laser light is captured. The divergence angle is a critical factor because it directly influences the amount of light that can be collimated, thereby impacting the overall efficiency and effectiveness of the laser system.

An important aspect of this process is the numerical aperture (NA) of the collimating lens. The NA is a dimensionless number that characterizes the range of angles over which the lens can accept or emit light. For successful collimation, the NA of the collimating lens must be greater than the NA of the laser diode. This requirement ensures that the lens can accommodate the full divergence of the laser beam, allowing for maximum light collection. By carefully selecting a collimating lens with an appropriate NA, one can achieve optimal collimation, resulting in a well-defined and focused laser beam [141].

To calculate the numerical aperture of the diode, NA, the equation below is used. Here, θ is a beam divergence angle.

$$NA = \sin\left(\frac{\theta}{2}\right)$$

(12) Numerical Aperture of Laser Diode [141]

Table 38 represent the specification of beam divergence angles for both laser diodes selected. For 2W blue laser diode, the maximum divergence angle is 50°. Calculating the numerical aperture, using the equation, the numerical aperture is 0.423.

$$NA_{2W\ Blue} = \sin\left(\frac{50°}{2}\right) = \sin 25° = 0.423$$

For blue laser diode that has 5W of output power, the maximum divergence angle is 53°. The numerical aperture 0.446 after calculating with the equation.

$$NA_{5W\ Blue} = \sin\left(\frac{53°}{2}\right) = \sin 26.5° = 0.446$$

The maximum divergence angle of 2W red laser diode is 65°. Putting this into equation, we get 0.537 for the numerical aperture.

$$NA_{2W\ Red} = \sin\left(\frac{65°}{2}\right) = \sin 32.5° = 0.537$$

Beam Divergence (°) of Selected Laser Diodes			
2W Blue Laser Diode			
	Min	Typical	Max
Parallel	5	14	25
Perpendicular	30	44	50
5W Blue Laser Diode			
	Min	Typical	Max
Parallel	4	10	16
Perpendicular	35	43	53
2W Red Laser Diode			
	Min	Typical	Max
Parallel		9	
Perpendicular		65	

Table 38 - Beam Divergence Angle

Once we figured out the minimum numerical aperture of the collimating lens, it is easier to select which lens would interact with the laser beam. First of all, we know that the numerical aperture of the collimating lens should be not be less than 0.537, which is the maximum value out of all the laser diodes that will be used for testing. In consideration of the ideal value of numerical aperture and something easy to equip with the laser module, we selected a collimation lens that is 6.5mm length and works best for 405, 445, 520, and 638 nm of wavelength. The numerical aperture is 0.6, which is larger than all three laser diodes selected for the experiment.

Collimation Lens Specification	
Size	M9 X P0.5 X 6.5 mm
Material	D-ZK3
Wavelength	445, 450, 638, 650 nm
Focal Length	4.05 mm
Numerical Aperture	0.6
Clear Aperture	5.3 mm
Coating	400 – 700 nm

Table 39 - Collimating Lens Specification

To select a lens to focus the collimated laser beam, we used software called 3DOptix to simulate the laser beam's path. Since the exact laser diode we planned to use was not available in the software, we customized a light source with parameters matching the

diode's specifications. For a 2W blue laser diode, we specified a Gaussian beam shape with a divergence angle of 7° parallel and 22° perpendicular. We designed the lens with parameters based on these specifications and observed the beam's behavior. (simulated lens spec) Although the lens's radius of curvature was not specified, making it challenging to achieve the exact focal length of the actual lens, we aimed to get as close as possible. The simulated beam was highly divergent, with a significant difference between the x-axis and y-axis radii. The beam passing through the collimation lens was not perfectly parallel, but the lens did reduce the divergence compared to the beam before it passed through the lens.

For the focusing lens, we used a double convex lens that has 25.4 mm of diameter, 10 mm thickness, and 24.9437 mm of effective focal length. After placing the lens 24.9437 mm far away from the collimation lens, we were able to find the focal point. However, due to some laser diode's unique characteristics such as divergence angle, and astigmatism, it was difficult to fully focus the entire beam. The focal point was significantly distant from the laser diode's position, resulting in the lens not effectively converging all the rays.

Focus Lens Specification	
Diameter	25.4 mm
Material	Optical glass, BK7, Fused Silica, Schott, OHARA, CaF2, Germanium etc.
Radius of Curvature	24.72 mm
Focal Length	24.9437 mm
Clear Aperture	25.4 mm

Table 40- Focus Lens Specification [142]

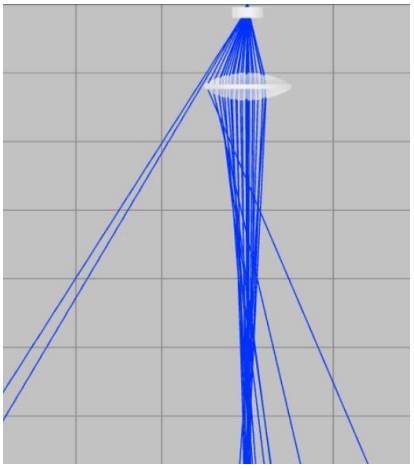

Figure 21 - 3DOptix Simulation with One Focus Lens

To address this issue, we placed a second lens identical to the first one 24.9437 mm after the initial focal lens and observed the ray behavior. Given the high divergence of this specific laser diode and the discrepancy between horizontal and vertical divergence, the rays were still not perfectly focused. However, the new setup managed to focus over 80% of the rays, showing a significant improvement over the previous configuration.

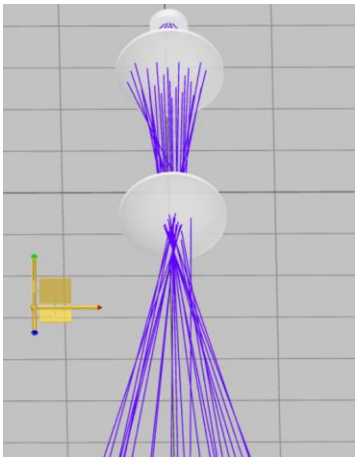

Figure 23 - 3DOptix Simulation with Two Focus Lenses

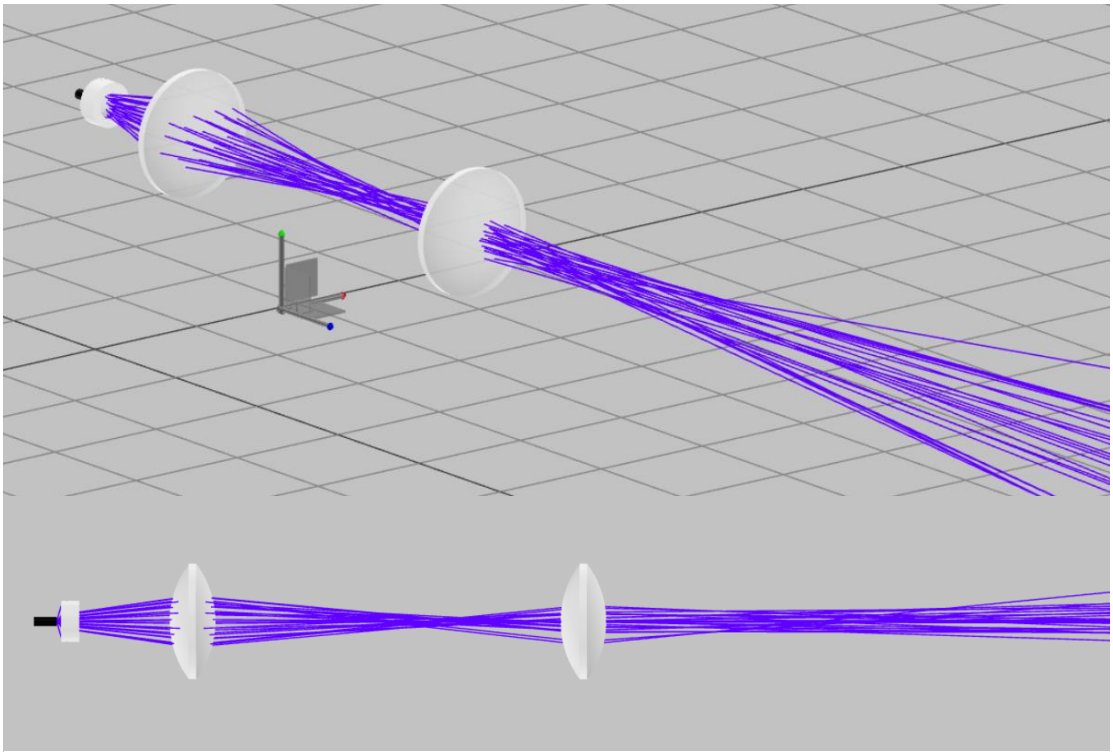

Figure 22 – Laser Beam Alignment Diagram

After experimenting with two focusing lenses, we realized the beam spot was too small to effectively treat the leaf. To address this, we decided to increase the beam spot size to cover more of the leaf area. To achieve this, we designed a Galilean beam expander—a compact two-lens system with no focal point between the lenses. This design offers a smaller footprint compared to other beam expansion methods, enabling a streamlined system for wider beam coverage.

For the beam expander, we selected Newport lenses KBC013 and KPX076. The input lens, KBC013, is a bi-concave lens with a focal length of -6.3 mm and a diameter of 6.35 mm. The exit lens, KPX076, is a plano-convex lens with a focal length of 25.4 mm and a diameter of 25.4 mm.

Lens	Shape	Diameter	Focal Length	Coating
KBC013	Bi-Concave	6.35 mm	-6.3 mm	430 – 700 nm
KPX076	Plano-Convex	25.4 mm	25.4 mm	400 – 700 nm

Table 41 - Beam Expander Lenses

The distance between the lenses, ddd, is calculated by summing their focal lengths:

$$d = f_2 + f_1$$

(13) Distance between Two Lenses

Where f_1 is the focal length of the input lens, f_2 is the focal length of the exit lens, and d is the distance between the two lenses. Substituting the values:

$$d = 25.4 + (-6.3) = 19.1\, mm$$

According to the equation, the distance between the two lenses is calculated to be 19.1 mm. This means the center of the input lens will be separated from the center of the exit lens by 19.1 mm to achieve effective expansion of the beam spot size.

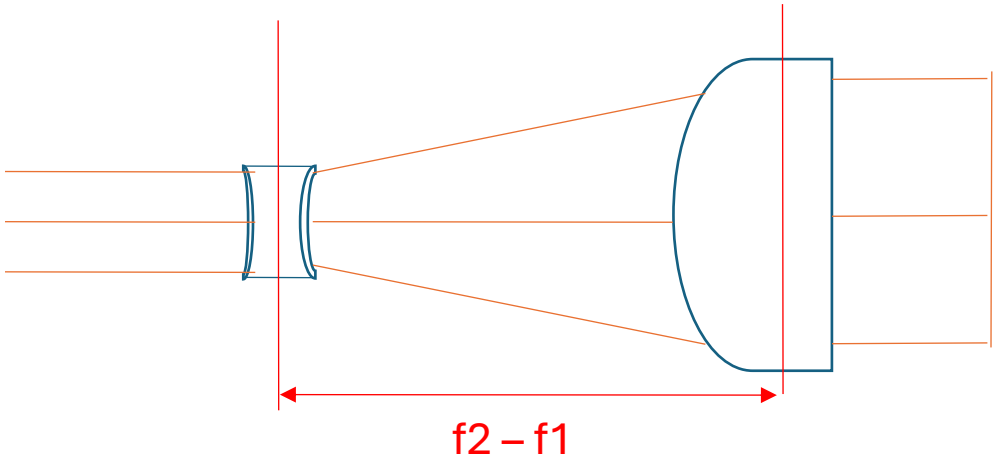

Figure 24 - Schematic of Two Lenses

The magnification factor, M, is determined using the following equation:

$$M = -\frac{f_2}{f_1}$$

(14) Magnification Factor

Substituting the focal lengths of the lenses:

$$M = -\frac{25.4}{(-6.3)} = 4.03$$

With a magnification factor of 4.03, the beam size will be approximately four times its original size after passing through the beam expander.

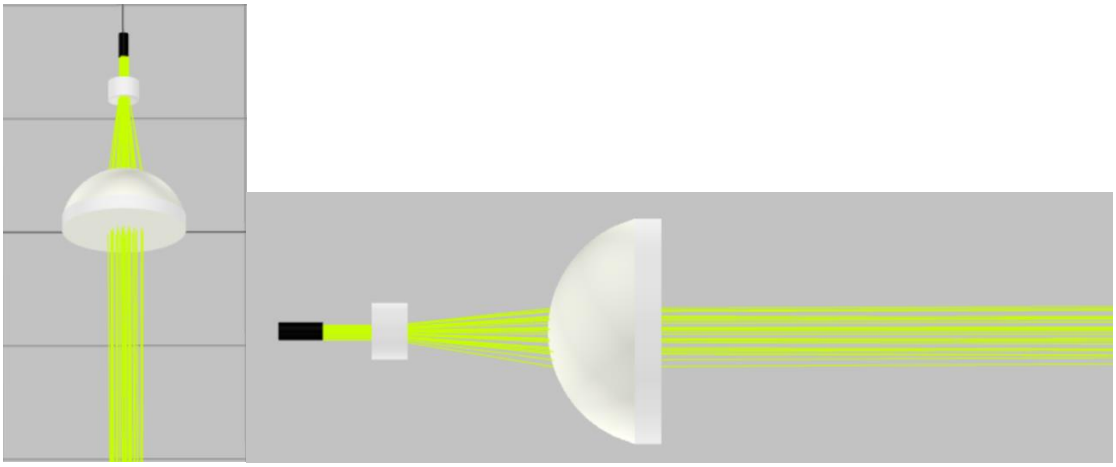

Figure 25 – 3D Scchematic of Beam Expander Lenses

6.1.5.2 Intensity of Laser Beam

Light intensity is a fundamental concept in understanding the behavior and impact of light on various systems, including plant growth. Light intensity refers to the amount of energy delivered by light per unit area, and it is a scalar quantity, meaning it has magnitude but no direction. The calculation of light intensity is expressed by the equation:

$$I = \frac{P}{A}\ (W/m^2)$$

(15) Light Intensity

where I represents the intensity, P is the power of the light, and A is the area over which the light is distributed [143].

In the context of plant growth, light intensity plays a crucial role as it directly influences the process of photosynthesis. However, when the light intensity exceeds a certain threshold—known as the saturation point—plants can experience a phenomenon called photoinhibition. Photoinhibition occurs when the light intensity is so high that it overwhelms the plant's photosynthetic machinery, particularly the photosystem II (PSII) complex. This leads to a reduction in photosynthetic efficiency and a temporary decrease in the plant's capacity to produce energy. While photoinhibition serves as a protective mechanism to prevent more severe damage to the photosynthetic apparatus, it also limits the plant's ability to harness light energy effectively. Too little light can limit photosynthesis, while too much can cause photoinhibition, making it crucial to manage light exposure to ensure optimal plant performance [144].

In optical physics, the intensity of a laser beam at a given location is typically defined as the optical power per unit area transmitted through an imaginary surface perpendicular to the direction of propagation. The units of optical intensity (or light intensity) are typically expressed in W/m² or, more commonly, W/cm². Intensity is the product of photon energy and photon flux, and it is sometimes referred to as optical energy flux [145].

The intensity profile of a laser beam usually follows a Gaussian distribution. The intensity can be calculated using the equation below. I_0 denotes the peak intensity, r represents the radial distance from the center of the beam, and w is the characteristic radius of the beam [146].

$$I(r) = I_0 \exp\left(-\frac{2r^2}{w^2}\right)$$

(16) Intensity of Laser Beam

6.1.5.3 Beam Waist

Laser beams, particularly Gaussian beams, do not distribute their power uniformly. Instead, they have a peak intensity at the center, which gradually decreases towards the edges. This non-uniform distribution makes the calculation of the beam's effective area, and consequently its intensity, more complex and necessitates an accurate determination of the beam's radius. The radius of a laser beam, often referred to as the beam waist or spot size, is the distance from the beam's center to the point where the intensity falls to $1/e^2$of its maximum value.

The radius of a Gaussian beam at a distance z from the waist is given by:

$$w^2(z) = w_o^2\left(1 + \left(\frac{\lambda_o z}{\pi n w_o^2}\right)^2\right) = \omega_o^2\left(1 + \left(\frac{z}{z_R}\right)^2\right)$$

(17) Radius of a Gaussian Beam

Here, w_o is a parameter that denotes the location along the laser beam where the radius is at its minimum, and the beam is most tightly focused. This point is critical because it represents the highest intensity region of the beam, where the power density is at its peak. The size of the beam waist influences the precision and efficiency of laser applications. The Rayleigh range (z_R) is the distance from the beam waist to the point where the beam's cross-sectional area has doubled. It is a measure of the distance over which the beam remains relatively collimated and maintains a small divergence. The Rayleigh range is given by:

$$z_R = \frac{\pi n w_o^2}{\lambda_o}$$

(18) Rayleigh Range

The beam divergence angle (θ) describes the angle at which the laser beam expands as it propagates away from the beam waist. For Gaussian beams, the far-field divergence angle can be approximated by:

$$\theta = \frac{\lambda_o}{\pi n w_o}$$

(19) Beam Divergence Angle

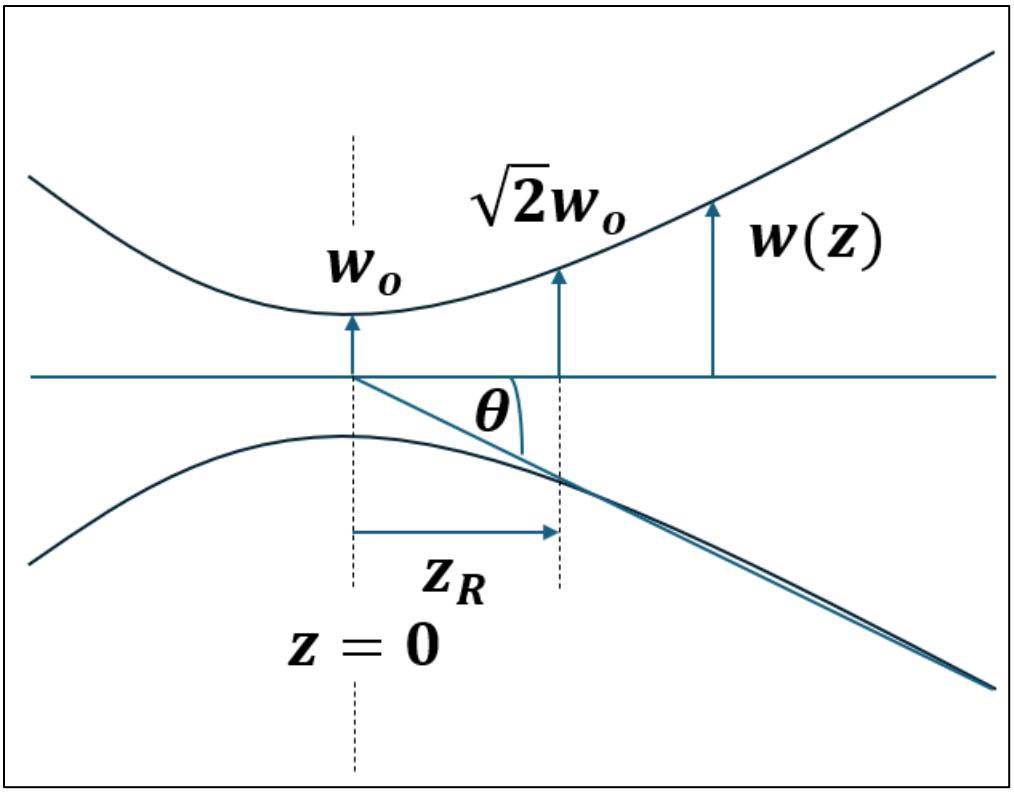

Figure 26 Characteristics of Gaussian Beam Waist w(z)

To measure the beam radius $w(z)$ at two different points along the propagation direction, ensuring these points are equidistant from the beam waist. Providing that these distances from the beam waist were denoted as z_1 and z_2, the beam waist at two points can be calculated by following:

$$w(z_1) = w_o\sqrt{1+\left(\frac{z_1}{z_R}\right)^2}$$

$$w(z_2) = w_o\sqrt{1+\left(\frac{z_2}{z_R}\right)^2}$$

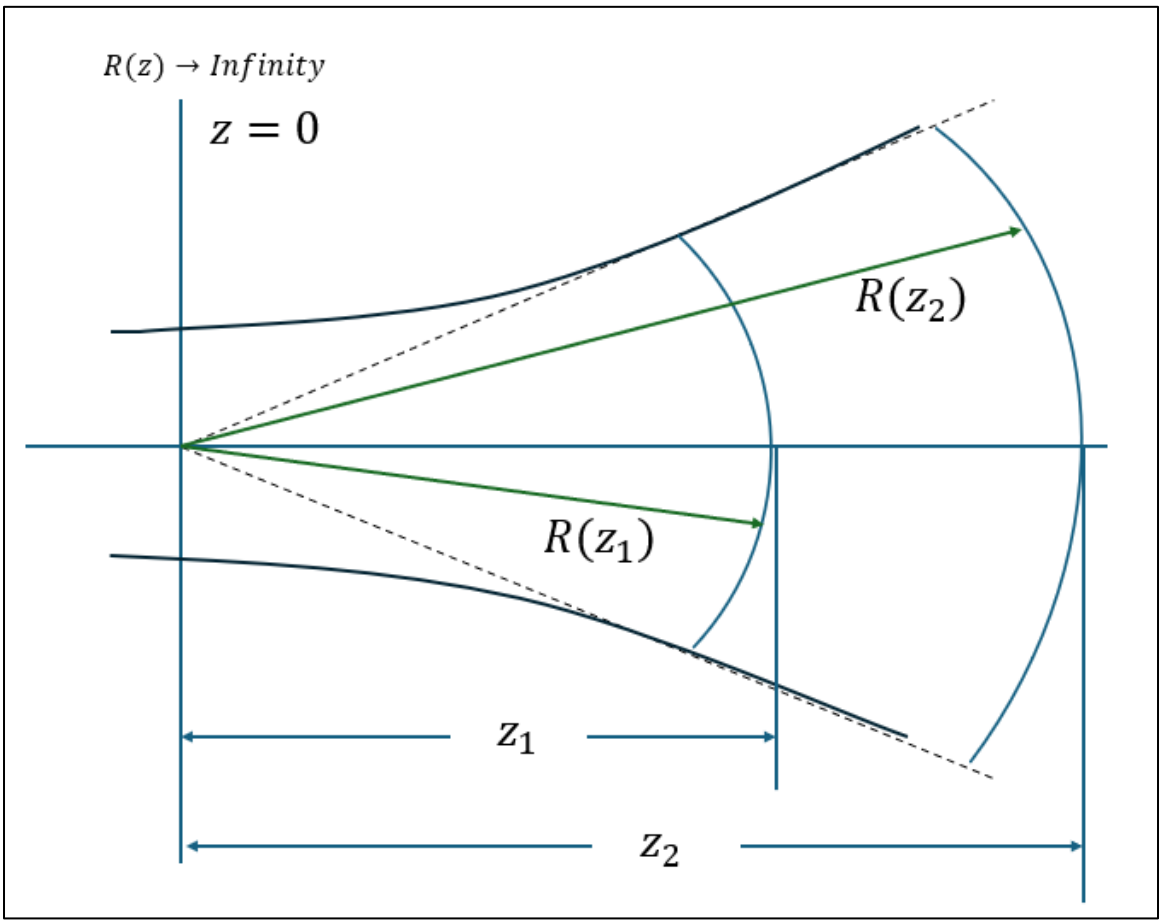

Figure 27 - Characteristics of the Gaussian Beam Radius of Curvature

Since we know the divergence angle for our laser diodes, we can calculate their minimum beam waist. The beam waist can be calculated by the equation below. We will utilize the maximum divergence angles to observe the potential beam waist.

$$\tan\theta = \frac{\lambda}{\pi w_o}$$

$$w_o = \frac{\lambda_o}{\pi \tan \theta}$$

For a 2W blue laser diode, which has peak wavelength of 445 nm, using maximum parallel and vertical half divergence angles of 12.5° and 25°, respectively, the beam waists in x and y directions are $0.639\ \mu m$ and $0.304\ \mu m$, respectively.

$$w_{o,\backslash\backslash} = \frac{445 * 10^{-9}}{\pi \tan 12.5\,^\circ} = 0.639\ \mu m$$

$$w_{o,|} = \frac{445 * 10^{-9}}{\pi \tan 25\,^\circ} = 0.304\ \mu m$$

For a 5W blue laser diode, which has 440 nm of wavelength at its peak, the parallel and vertical half divergence angles are 8° and 26.5° . Calculating these, the beam waists in x and y directions are $0.997\ \mu m$ and $0.28\ \mu m$.

$$w_{o,\backslash\backslash} = \frac{440 * 10^{-9}}{\pi \tan 8\,^\circ} = 0.997\ \mu m$$

$$w_{o,|} = \frac{440 * 10^{-9}}{\pi \tan 26.5\,^\circ} = 0.28\ \mu m$$

For a 2W red laser diode that has a peak wavelength of 638 nm, the parallel and vertical half divergence angles are 4.5° and 32.5°. Calculation of the beam waists give $2.58\ \mu m$ and $0.31\ \mu m$.

$$w_{o,\backslash\backslash} = \frac{638 * 10^{-9}}{\pi \tan 4.5\,^\circ} = 2.58\ \mu m$$

$$w_{o,|} = \frac{638 * 10^{-9}}{\pi \tan 32.5\,^\circ} = 0.31\ \mu m$$

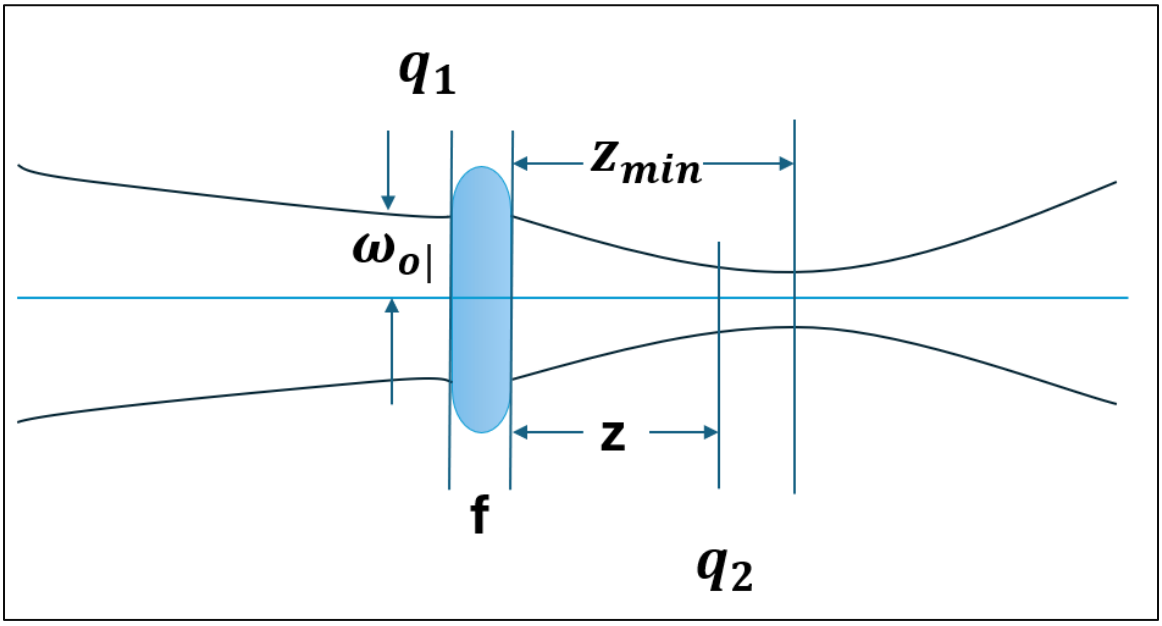

Figure 28 – Lens System with a Single Thin Lens

After implementing the beam expander, the beam size expanded to approximately four times its original size, and the changes in beam diameter over distance were measured.

The graph below depicts the horizontal and vertical beam diameters at various distances from the beam expander to the leaf treatment spot. As the treatment distance increased, the horizontal beam diameter experienced a significant expansion, whereas the vertical beam diameter showed only a slight increase.

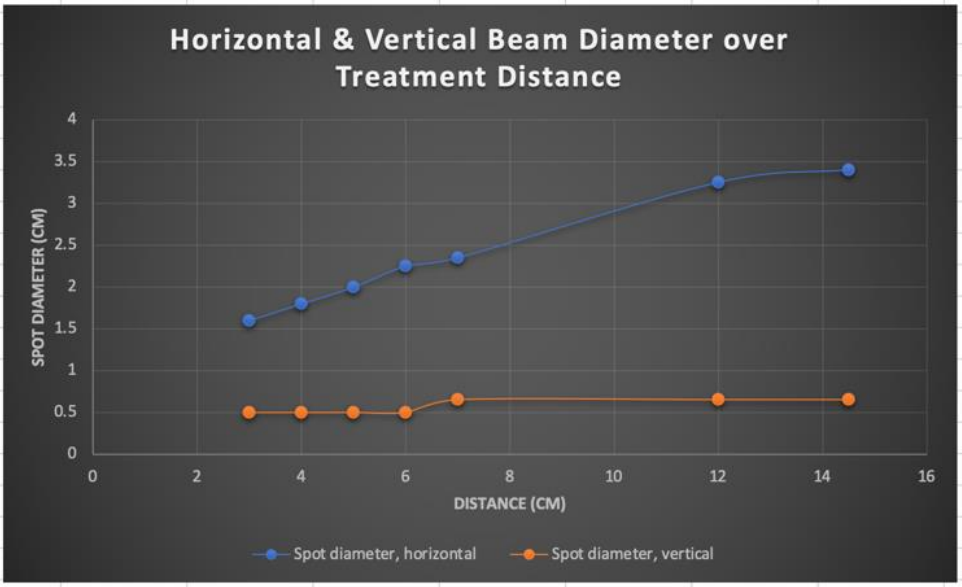

Figure 29 - Horizontal & Vertical Beam Diameter over Treatment Distance

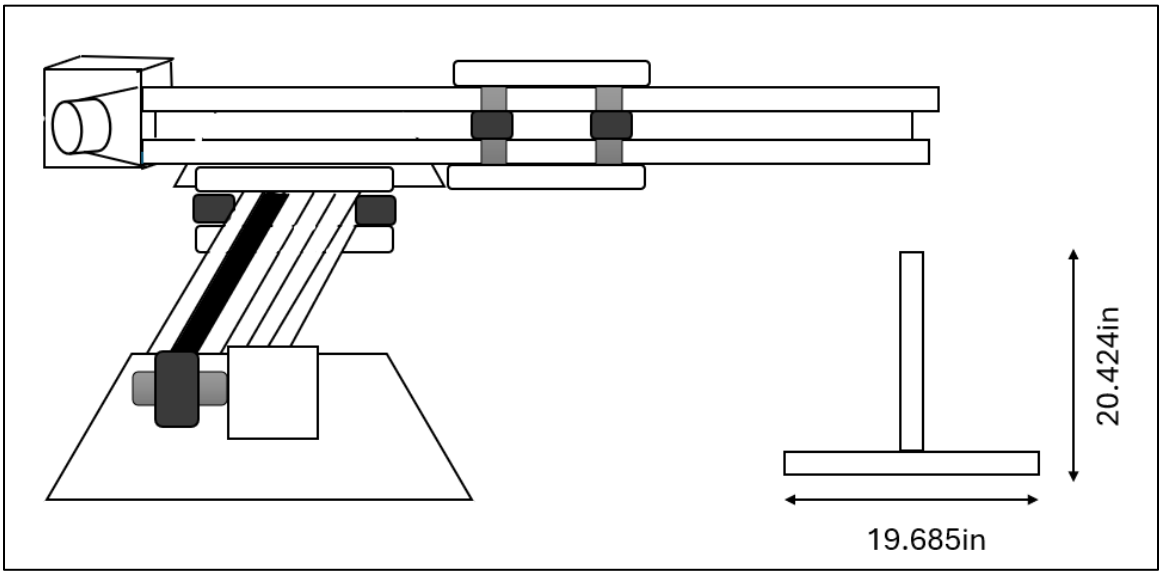

Figure 30 – Laser Control System Schematic Diagram

The laser control system will be constructed from v-slot aluminum frame and will operate in an area that is 19.685 inches by 20.424 inches. It consists of two gantry-type pulleys perpendicular to each other that are operated by stepper motors. They will function in an XY cartesian system as described earlier in the paper, where one carriage moves the Y axis in the +X or -X direction, and the other carriage moves the laser diode system along the +Y or -Y direction. The Y axis carriage will position the laser diode at a degree that is normal to the surface of the ground in order to perform weeding treatments.

6.2 Breadboard Testing

Breadboard testing was a fundamental step in the design and development of electronic circuits for the BEAM project, providing a versatile and cost-effective platform for experimenting and validating circuit designs before committing to a more permanent solution such as a PCB. When working with components like stepper motors and laser diodes, breadboard testing becomes particularly useful. This method allowed our team to prototype and troubleshoot our circuits, ensuring that all components function correctly and interact as expected. By using a breadboard, we easily modified and optimized our circuit configurations, identified and fixed errors early in the development process, and gathered valuable insights into the behavior of our system. This chapter delves into the

significance of breadboard testing, highlighting its role in our testing process for the stepper motor and laser diode driver circuits, and allowing our team to achieve reliable and efficient performance.

6.2.1 DRV8255 and NEMA 17 Stepper Motor Testing

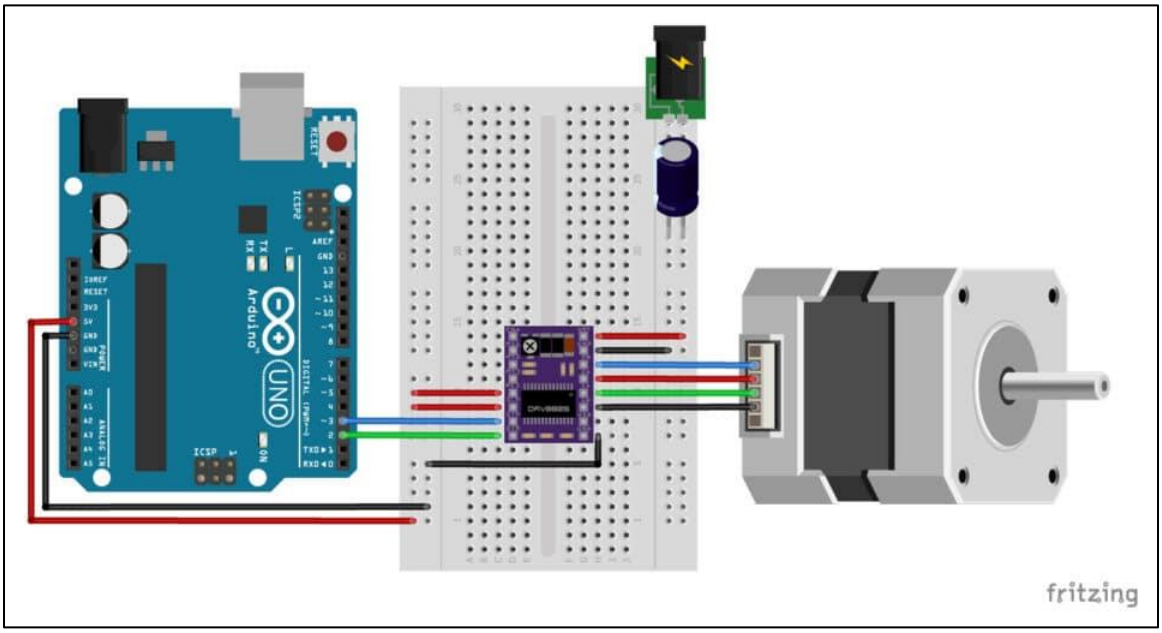

Figure 31– DRV8255, Arduino Uno, and Stepper Motor Connections [147]

The breadboard wire connections for Arduino Uno to DRV8255 to stepper motor are shown in Figure 31. The DRV8255 has an onboard potentiometer that was used to limit the current through the motor's windings. For testing small motors, 1A is a good value to power most NEMA 17 motors. The NEMA 17 stepper motor that we used was conducted in full step mode, so we needed to account for the current through each coil in the motor being limited to 70% power and use 1.4A to power the test system. We used Equation (20) to calculate the desired current limit value for the system, and probed the system with a multimeter to monitor the voltage change so we could adjust the potentiometer appropriately [147]. To accurately set the current limit to 1.4A, we needed a voltage reference of around 0.750V.

$$I_{Limit} = V_{REF} \times 2$$

(20) - Current limit for stepper motor

When we tested the stepper motor setup in full-step mode at I_{Limit} = 1.4A, the motor would skip steps and vibrate in place without turning. To resolve this issue, we attempted to increase the I_{Limit} which resulted in a smoother, but still erratic rotation. Another attempt to resolve this issue involved setting the driver to rotate the motor in half steps. This greatly

improved the performance of the motor and allowed it to rotate much smoother. The motor would still skip steps every few seconds, so we increased the speed from 0.02% of the max speed to 0.075% and that allowed the motor to rotate smoothly without skipping any steps. The AccelStepper Library by Mike McCauley is an open-source software used to control stepper motors and was used to complete the stepper motor test code located in Appendix C – Software Code [148]. While we planned on integrating this library into our final code on the ESP32, we moved to the Stepper.h library by Tom Igoe, which is also an open-source library. This library had more controls over h-bridge stepper motor controllers than the AccelStepper library did, so it proved more useful during software development.

6.2.2 Laser Diode Testing

To test the laser diode, our team used a DC power supply set at 1.7V and 2.5A. These are the typical settings for the M140 blue 2W laser diode. We powered the diode through the anode and cathode pins, wiring the positive voltage to the anode and the negative to the cathode. We then positioned the laser diode 1cm above the leaf of a weed without focusing lenses and activated the diode for testing. The 2W blue diode at 1cm was very immediately burning a spot in the leaf. After 30 seconds the intensity of the laser diode was decreasing, but the effect on the leaf was still evolving. Even after the lasing stopped, the leaf continued to shrivel and dry out. After testing the blue diode, the IR laser diode was set up for lasing. After setting the DC voltage and current to the rated values for this diode, it did not produce a beam, but instead a small amount of light. This leads our team to believe that the diode obtained for testing was either faulty, or there was user error involved in the process.

Overall, the anticipated results of both diodes were for the leaf to dry out, but instead the blue laser started to burn the plant material. Further testing needs to be completed to successfully find a viable range for drying plant material without burning. Testing will continue with the 2W laser diodes, but if plant material continues to burn instead of drying out, a laser diode with less power may need to be acquired. Another item noted during the experiment was that the blue diode was receiving a large wattage and released a lot of heat during its trial. For future testing, a temperature regulator or heat safe connector should be implemented to protect the laser diode and supporting equipment. More testing also needs to be conducted on the IR laser diodes to see if they will successfully burn plant material.

6.2.3 DC Motors

For testing the DC motors with the driver chosen, a development kit of the ESP32 was used along with a BTS7960B driver board. The logic supply of 3.3V was connected, the INH pin from the driver was connected to a regular GPIO pin while the right and left input pins were connected to PWM pins. The last thing was to supply the motor with 12V and a minimum current of 2A. Once the bidirectionality of the driver was confirmed, the same test was performed except a level shifter was used, for the risk of undervoltage, in between

the connections of the ESP dev kit and the driver, the level shifter used was the TXS0108E module that needs a supply of 5V.

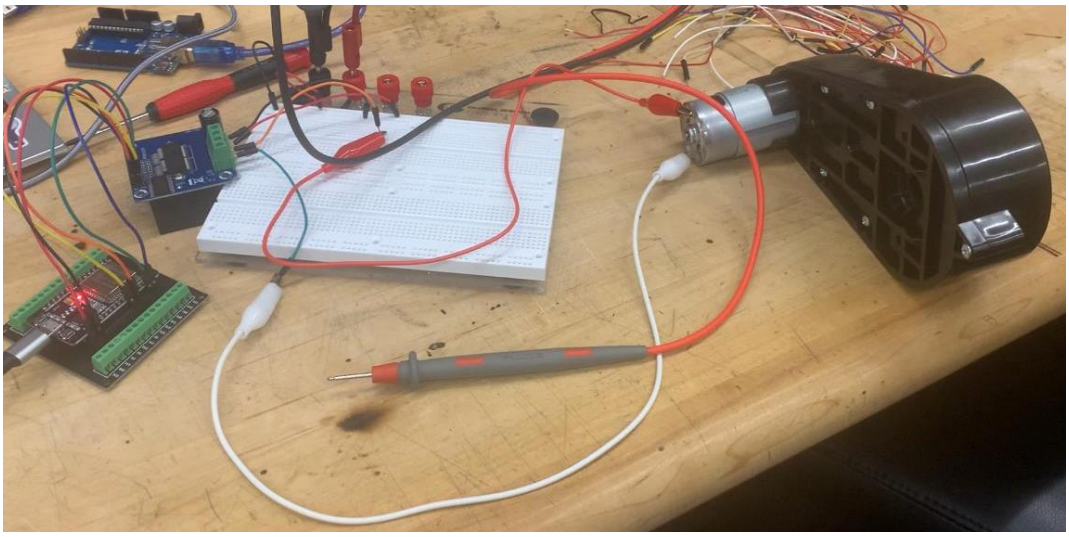

Figure 32 – DC Motor Driver Breadboard Test

Chapter 7 – Software Design

This section features various flowcharts that detail the processes for different systems, offering a clear visual representation of the interactions and workflows involved in the robot's operations which will translate into programming. We also delve into the object detection system and how a customized dataset that meets our project's goals is created, highlighting its importance in accurately identifying and targeting weeds for elimination. It includes an analysis of ROS and Micro-ROS discussing their respective advantages and suitability for our project. Finally, we discuss the use of SLAM which enables the robot to navigate its environment effectively while building a map in real-time.

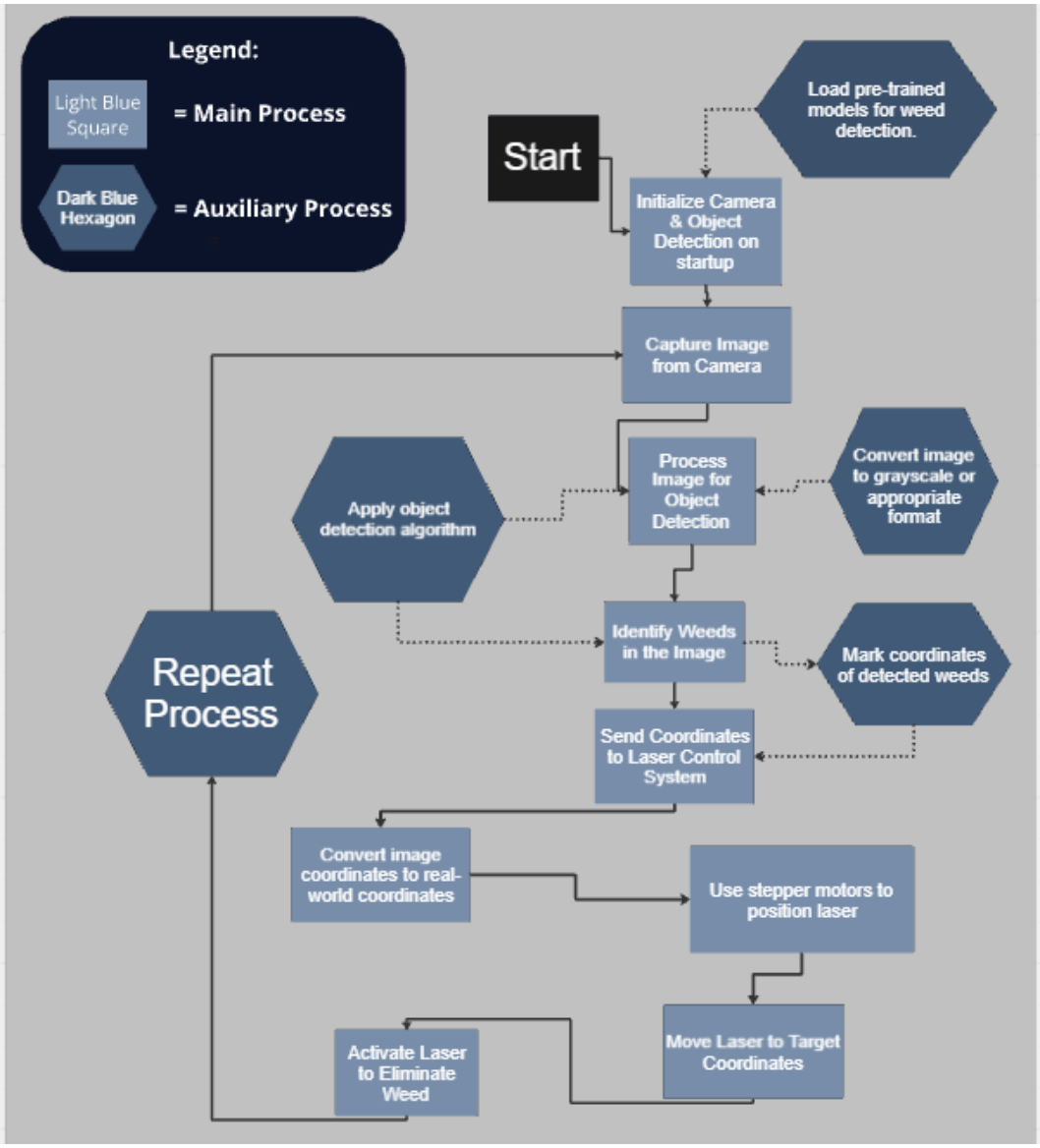

Figure 33 - Raspberry Pi Object Detection Workflow

The process for using the Raspberry Pi 4 and its use of object detection to scan an area and find weeds and/or other unwanted plant material The Raspberry Pi then loads the data into a pre-trained model for weed detection. The image is turned to grayscale, or another suitable format needed to properly process and tag the individual weed. Once the object is detected, the system will find the coordinates of the detected weeds, which are sent to the laser control system. Turning the coordinates into the proper motion for the stepper motors to position the laser above the weed targeted. The weed would then be promptly eliminated. The robot would then repeat the process until it was no longer required.

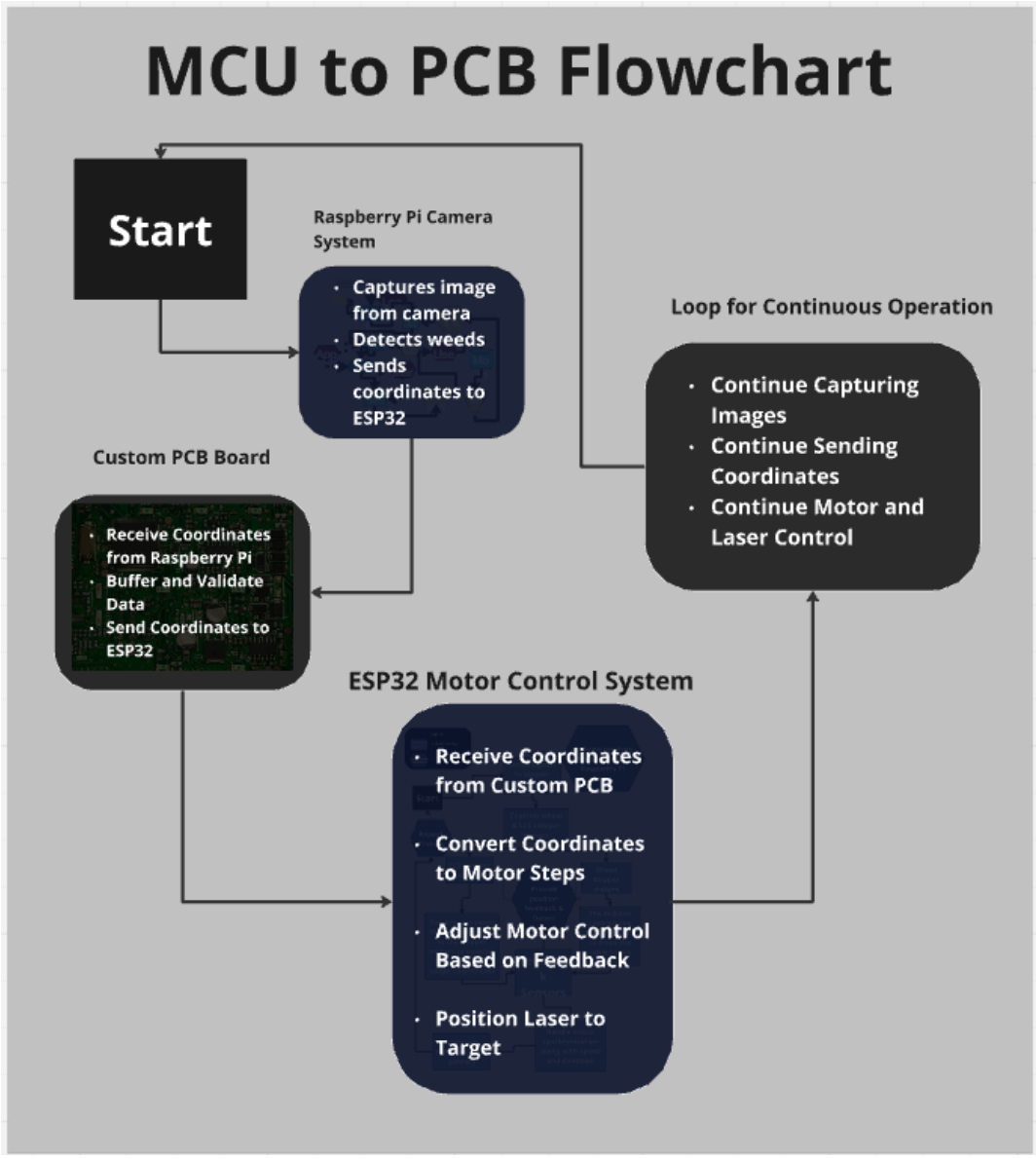

Figure 34 - MCU to PBC Flowchart

This process begins when the Raspberry Pi camera captured an image, detecting one or multiple weeds in the image. These coordinates are then sent to a custom PCB board, which receives and validates this data, forwarding the coordinates to the ESP32. The system receives these coordinates, converts them into motor steps, adjusts the motor controller based on feedback, positions the laser at the target, and eliminates the weed(s). This process continues in a loop; units are no longer required.

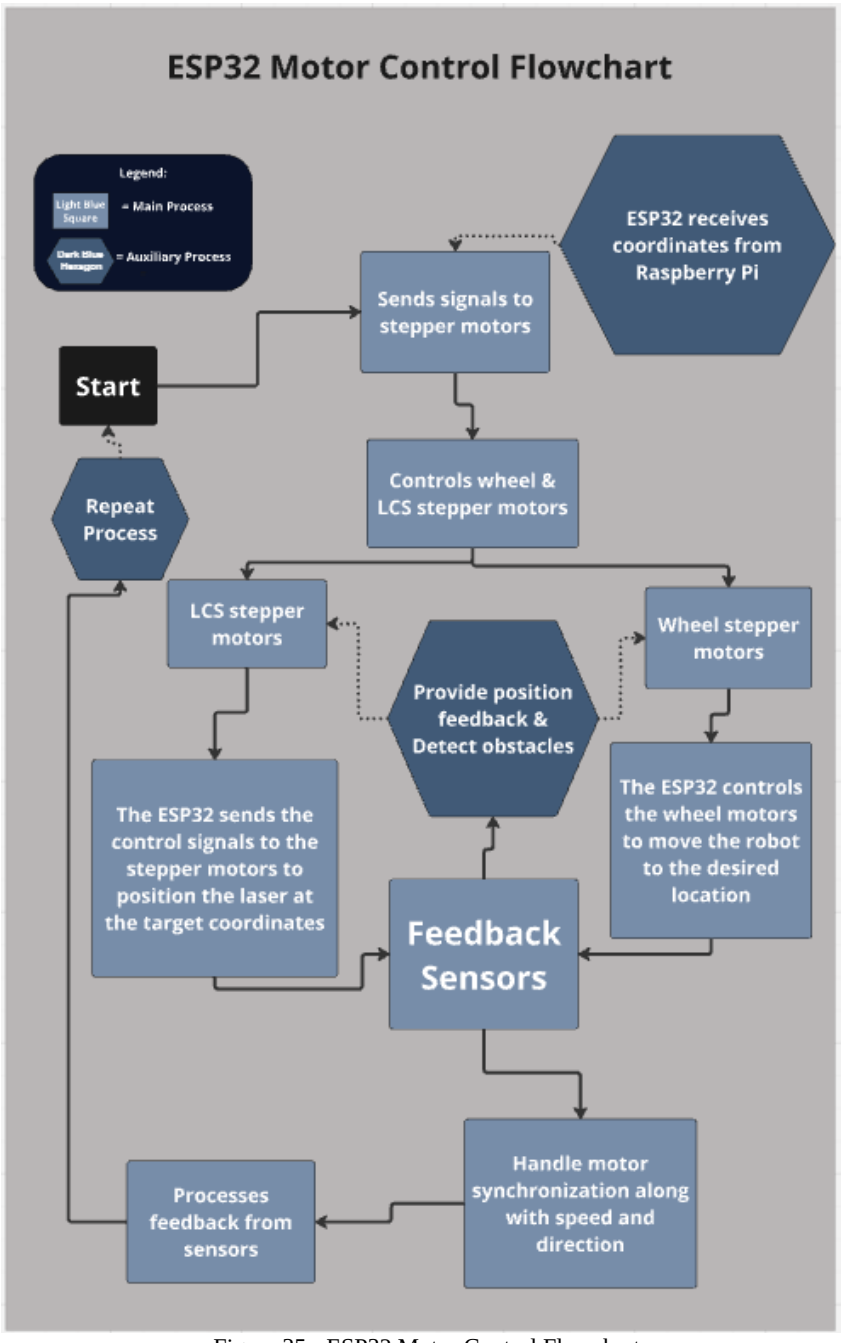

Figure 35 - ESP32 Motor Control Flowchart

This process starts with the ESP32 receiving coordinates from the Raspberry Pi. These coordinates are used to control the movement of stepper motors with the motor driver. The ESP32 will send signals to control both the wheel and laser control system stepper motors for proper adjustment. Feedback sensors play an important role by providing position feedback as well as detecting obstacles. The entire process repeats continuously, ensuring effective weed elimination.

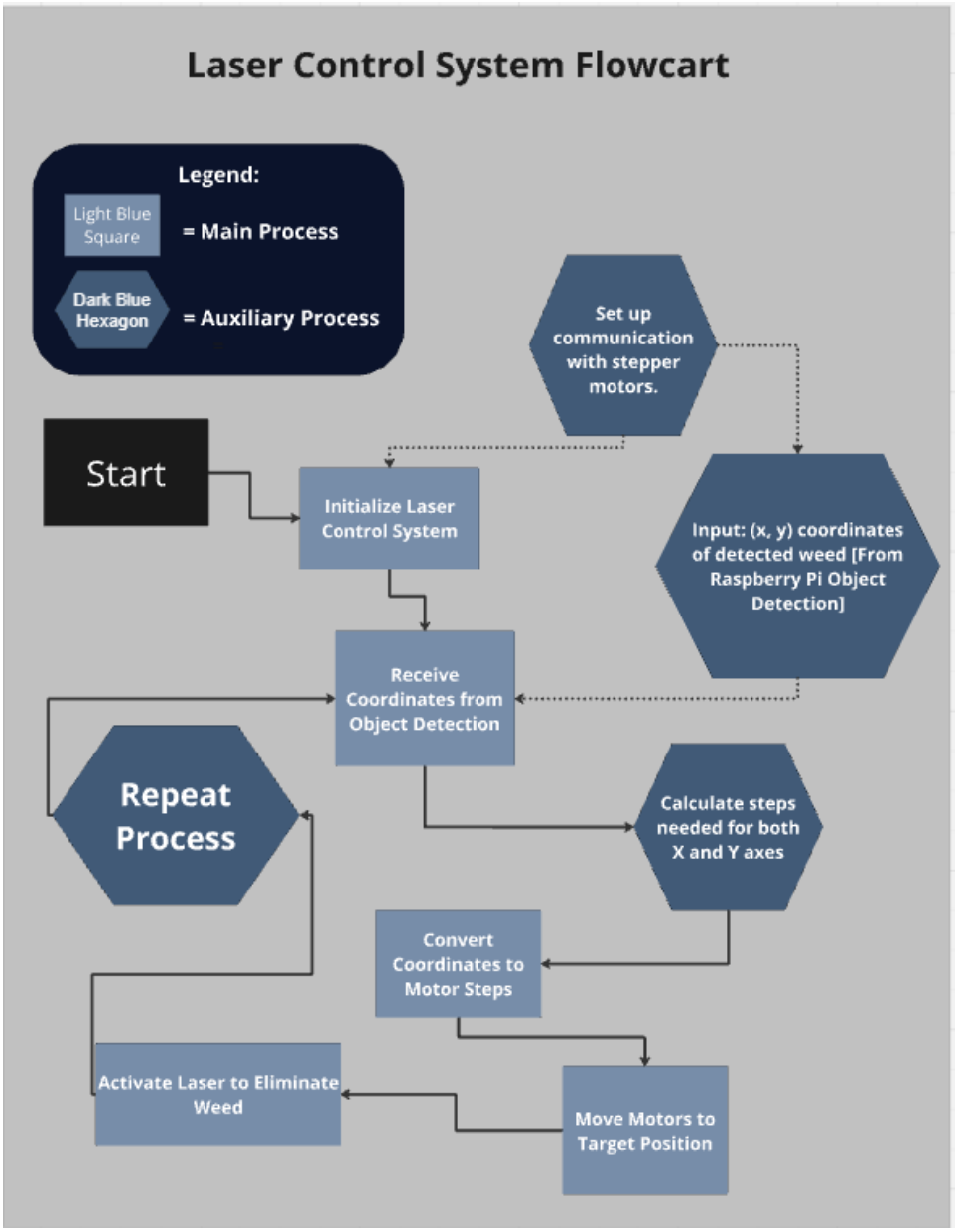

Figure 36 - LCS Flowchart

This process begins with the initialization of the laser control system. Once initialized, the system will set up communication with the stepper motors. Using a cartesian X/Y coordinate plane, it will receive the X/Y coordinates of the detected weeds, receiving them from the Raspberry Pi object detection software. Once this is completed, the coordinates are used to calculate the necessary steps for the X and Y axes, which are then converted into motor steps. Once the motors are in position, the laser activates to eliminate the weeds. This process will repeat itself continuously to ensure all of the detected weeds are targeted and eliminated.

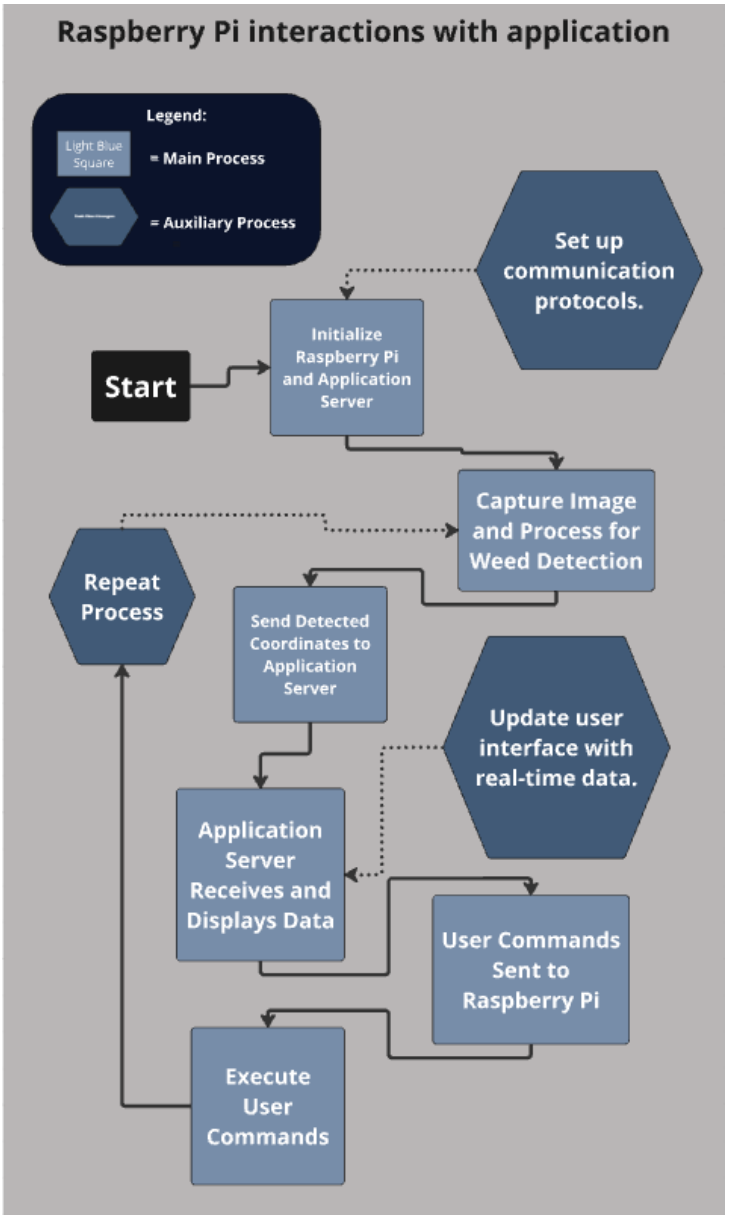

Figure 37 - Raspberry Pi Application Interaction Flowchart

This process will begin with the initialization of the Raspberry Pi and the application server. This is then followed by the setting up of the communication protocols. The Raspberry Pi captures images and processes them for weed detection. The detected coordinates are sent to the application server, which will then receive and display the data; the user interface will be updated with real-time data; and the user commands are sent back to the Raspberry Pi, which then executes these commands. The process will repeat itself continuously to maintain a real-time weed detection and user interaction application.

7.1 Object Detection

The goal of the BEAM project is to laser weeds off for farming purposes to not use harmful pesticides, to achieve this first we needed to train a model set by feeding it different images of the plants we wanted to detect, both crops and weeds, test this model to obtain the most accurate version and adjust it if necessary, and the transfer the model set to the RGB camera so it could communicate with the MCU to inform the laser when to activate for the elimination of the weeds. One of the struggles to obtain an accurate model for object detection was that different angles can make the RGB camera misinterpret an object as something entirely different. Even though the camera is design to interpret different colors, another common struggle was lighting since a this too can make an object look different, to combat this, the set of data taken to build the model needs to include photos taken in different angles and lighting. We also incorporated a light on the interior of the robot to provide adequate lighting for capturing images.

Figure 38 – Labels for Object Detection

There are several platforms that are designed for easy object detection training of model sets, to create a simple model for testing we used Edge Impulse, where after creating a new project, we imported the photos of grass and one type of weed, created the labels for both options in each picture, highlighting which part corresponds to grass and which part to weeds.

After creating all the labels, we split the pictures for training and testing equivalent to 80%/20% for the dataset, designated the desired outputs, and specifies the settings for training such as the number of cycles, learning rate, training processor, and validation size, all of these were monitored and adjusted a number of times to obtain the most accurate version possible. This model served as a base for the final one in Senior Design 2 where more objects and a more thorough data set were fed into the training set.

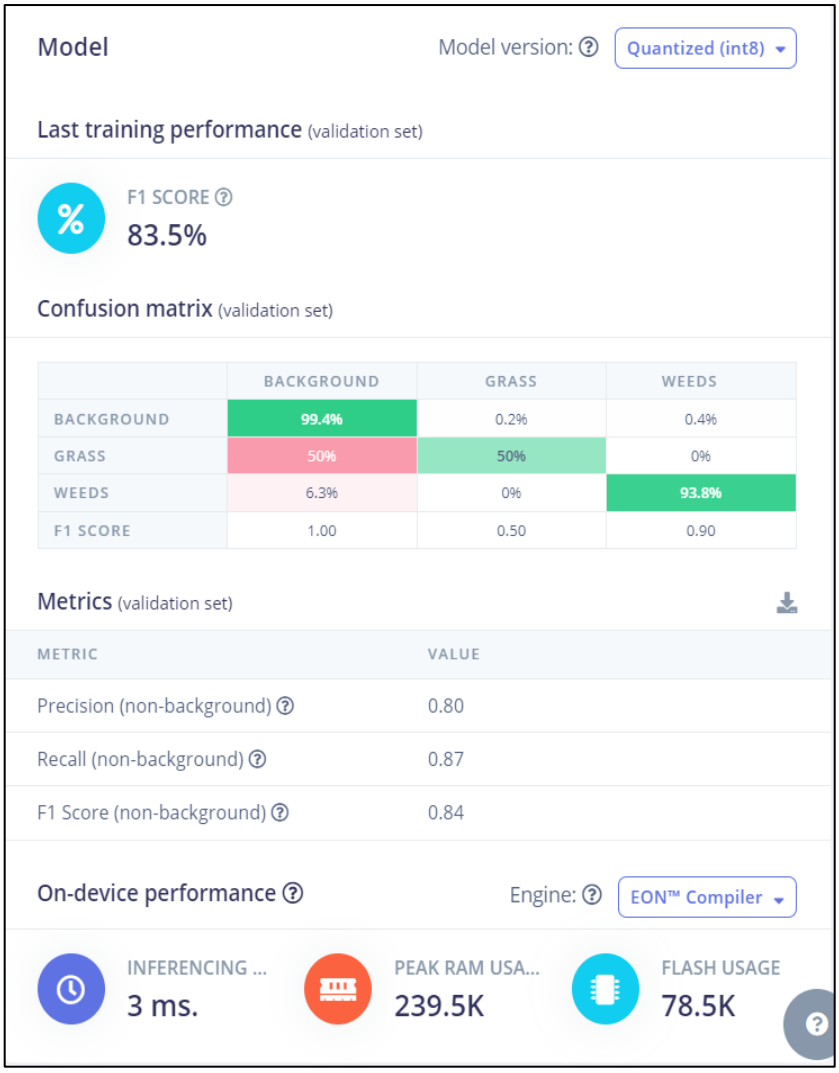

Figure 39 – Object Detection Model Set

Creating a data set for the BEAM project not only required a great number of pictures for normal crops and weeds, it also required us to program the laser to act out in accordance to the results from the RGB Camera. As you can see from Figure 39 – Object Detection Model Set, the accuracy level is not that high because of the similarity between grass and weeds in terms of size and most importantly color, it misidentified grass by a great percentage making it not ideal. As previously stated, to improve accuracy for the object detection software, we needed to have at least 30 pictures per plant for one angle with great lighting and since we want the best chances for the RGB camera to correctly identify each weed and crop we need to include different angles into the set.

Later in Senior Design 2, we realized that Edge Impulse would not provide the best results for developing our object detection model. We moved to a different website called Roboflow that allowed users to upload data and train models based on the datasets. They also provided several different platforms for which to upload your model to, such as tensorflow lite and several editions of yolo like yolov4 and yolov5. We created our model using 176 images split between training and testing the model. Our final version of the model was extremely accurate (85-90% success in identifications) and had a high recall rate for objects that seemed to "move" between different image frames. Overall, we had more success with Roboflow and succeeded in uploading our model to the Raspberry Pi 4 for continued testing and software development.

7.2 ROS and Micro-ROS

ROS, or Robot Operating System, is an open-source framework for developing robotic systems and applications. Providing a collection of tools, libraries, and conventions aimed at simplifying the task of creating complex robot behavior across a wide variety of robotic systems. Some of the key features of ROS include modularity, which allows developers to build software in modular pieces named "nodes," which can be reused in different applications. ROS provides communication tools for nodes to exchange crucial information to help process the complicated tasks required by robotic systems. ROS also includes a wide array of tools for things such as visualization, simulation, data logging, and debugging. Another great benefit of using ROS is the large community and vast repository of already-existing packages to help support errors and problem solving [149]. Micro-Ros is an extension of the ROS framework that brings the benefits of the ROS 2 system to microcontrollers. It is specially designed to enable small, resource-constrained devices, such as the ESP32, to communicate and work within a ROS 2 network. Some key differences that help enable this extension are its lightweight framework, which allows it to be optimized for the microcontrollers required with limited computational resources and memory. Additionally, Micro-ROS is designed to operate with real-time operating systems, enabling real-time control and communication. [150]

Micro-ROS enables the ESP32, among other boards, to participate in the ROS ecosystem, this allowed us to leverage the powerful features of ROS while being adapted to the more

resource-constricting nature of using a microcontroller. This integration allowed us to build the robotic system required with high-performance computers and resource-constrained devices working together seamlessly.

7.3 SLAM Mapping, Lidar, and Gazebo

SLAM, or simultaneous localization and mapping, is a process where a device creates a map of an unknown environment while keeping track of its own location within that environment. Using a LiDAR, or Light Detection and Ranging, device in SLAM is ideal for its high precision and ability to work in various lighting conditions. Some advantages of using LiDAR for outdoor SLAM are its accuracy, as LiDAR can provide high-precision measurements, which are necessary for creating accurate maps using SLAM. Lidars are also capable of long-range detection as well as high-speed data acquisition to enable real-time mapping and localization of large outdoor environments. Some challenges we faced were, firstly, the high cost of a quality LiDAR. We also needed to consider that SLAM localization requires a significant amount of computation to process large volumes of LiDAR data in real-time. Overall, using LiDAR for outdoor SLAM mapping provides a high-accuracy solution, making it suitable for various applications, including the purposes of our project. [151]

Our team working on the BEAM project wants to include a 3D mapping software/simulator to provide more information about the robot's surroundings and include more features and data for the user. Gazebo is a powerful 3D robotics simulator often used alongside ROS. It provides a powerful and accurate physics engine, high-quality graphics, and a convenient programming interface, making it suitable for robotics research and development. Some of the features of Gazebo include the physics engine, allowing developers to simulate the dynamics of robots and their interactions with the environment. It incorporates the modeling of forces, torques, and potential collisions. The high-quality graphics also offer realistic rendering of environments and models of your robot. It uses technologies like OpenGL to visualize how the robot navigates and interacts with its surroundings, modeling potential paths and goals for the user to watch the robot navigate in real time. A sensor simulator can also be incorporated into Gazebo and can simulate a large range of sensors used in robotics, including cameras, LIDARs, GPS, and more. The virtual sensors in the simulation produce realistic data streams that mimic what actual sensors would generate. Users working on Gazebo also created complex environments for the simulation, adding in objects, terrains, and structures. This allowed for the testing of robots in diverse and challenging scenarios. Finally, this software is closely integrated with ROS, allowing for seamless communication between the simulation and ROS nodes. This integration was crucial for development, testing, and debugging ROS-based applications in a controlled and safe environment.

Chapter 8 – System Fabrication/Prototype Construction

This section outlines the critical steps taken to bring the BEAM robot from conceptual design to a functional prototype with the different levels our project has and the dimensions. In addition, we have the PCB design for the different systems while keeping in mind the schematic previously created, layout considerations, and the selection of appropriate materials to ensure reliability and performance.

8.1 Beam Dimensions and Levels

The dimensions for the BEAM robot were estimated to be 30x30x15 inches for the frame, not include height from the wheels. This was accurate for the construction of the frame during Senior Design 2. The robot had four levels. Level one was the top of the robot; this includes the solar panel and lidar mounted to the roof of the robot for better access to the sun and for a higher observation point. Level two contained the raspberry pi 4 camera system, PCB mounts, and the linear actuator shield system; this level looks down through the open area in level three to see weeds located on level four. Level three houses the laser control system, consisting of the stepper motors and cartesian-based movement system. Finally, level four is the ground plane where the weeds are located. A diagram for the four-level setup is shown in Figure 40 – BEAM Level Diagram .

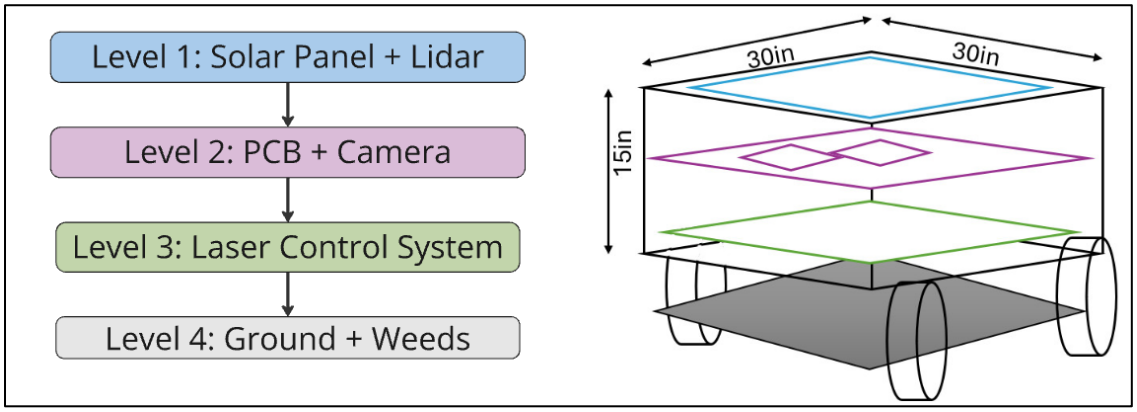

Figure 40 – BEAM Level Diagram

8.2 PCB

Printed Circuit Boards (PCBs) were very important components in the development of the BEAM project, as well as in any project. Serving as the backbone for electrical connections and communications between various subsystems, the design and implementation of the PCB were essential for integrating the sensors, microcontrollers, power management systems, and laser control units into a cohesive and efficient system. The PCBs were designed to ensure robust performance, reliability, as well as safety, facilitating seamless communication and power distribution across the system.

The TPS40200-Q1 voltage regulator's datasheet provided adequate documentation for how to arrange components on the PCB for maximum efficiency of the system. These guidelines included placing the input power supply close to the TPS40200-Q1, maintaining the power supply so it is well-regulated, and keeping the AC current loops and output loop very short. The datasheet also recommended keeping the switching node small to reduce parasitic capacitance, and far away from the TPS40200-Q1 to reduce noise influence over the regulator [78]. In Senior Design 2, the main PCB housed the regulator and included its connections to the Raspberry Pi 4 and the ESP32, while a separate PCB was constructed to hold the laser driver system and its laser diode. This laser driver PCB was attached to the laser control system for positioning and was connected to the main PCB by a secured

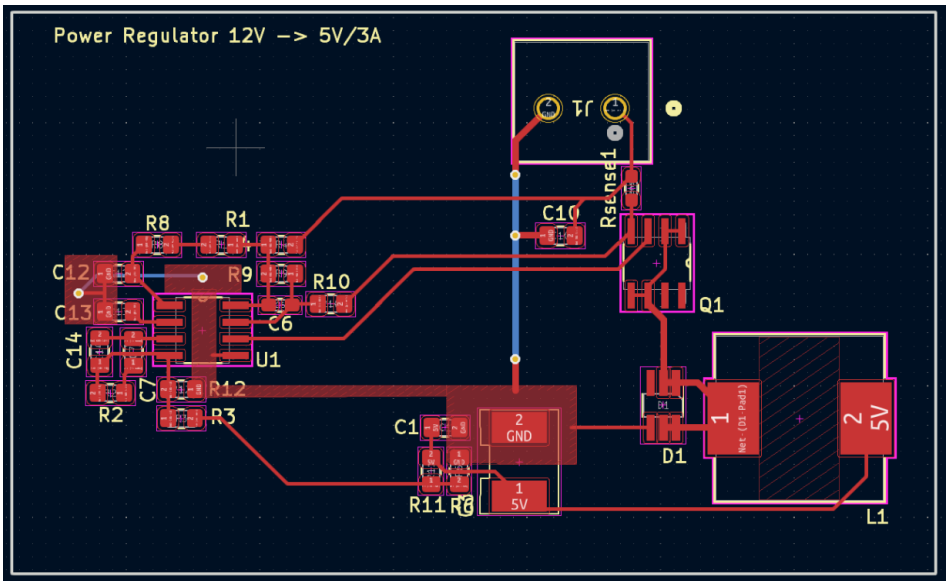

Figure 41– Power Regulator PCB

wire. This allowed the laser driver circuit to move freely, but still be controlled by the ESP32 located on the main PCB

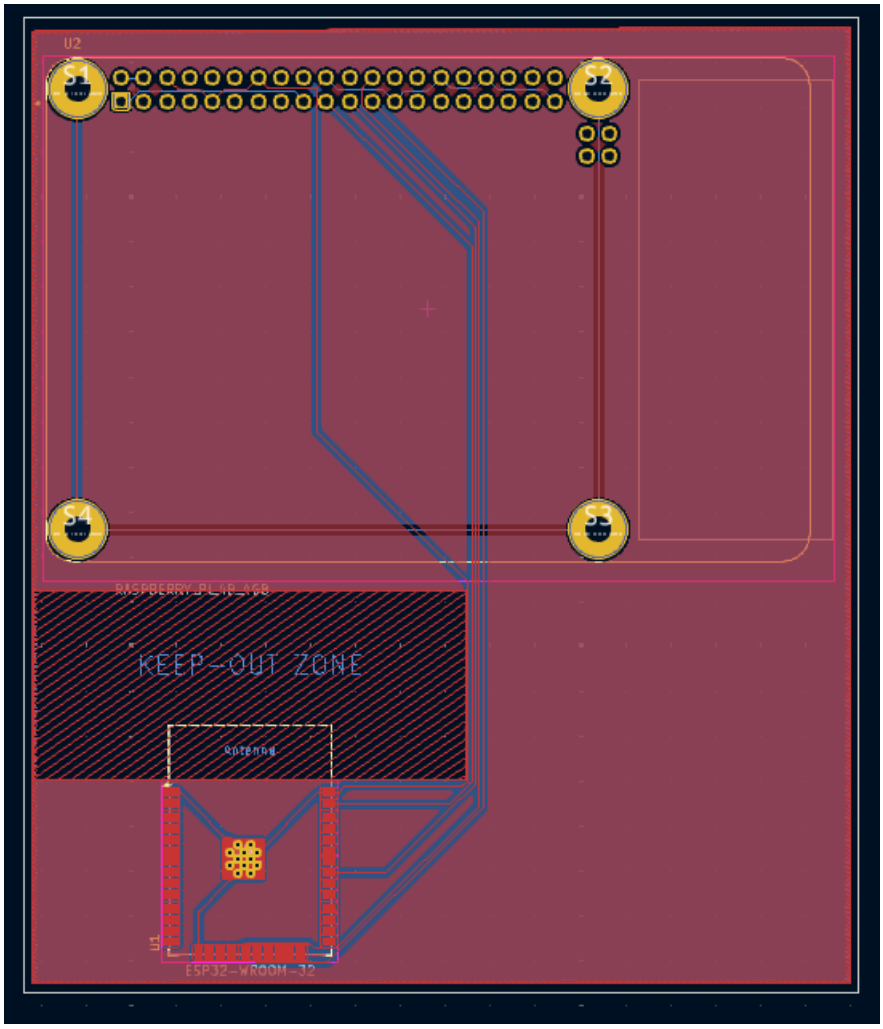

Figure 42 - MCU PCB

For the navigation motor control PCB, the three parallel capacitors were placed as close to the power supply and logic power terminals, all of their package size are 0805 for easier soldering. Choosing the layers was really important since the datasheet specifies that proper heatsink is required for high current applications, this can be done by soldering the H-bridge to a copper area or by using an external heatsink of 38 x 17 x 11.9 mm. The pin layout was chosen so the motor control can be mounted onto the driving board.

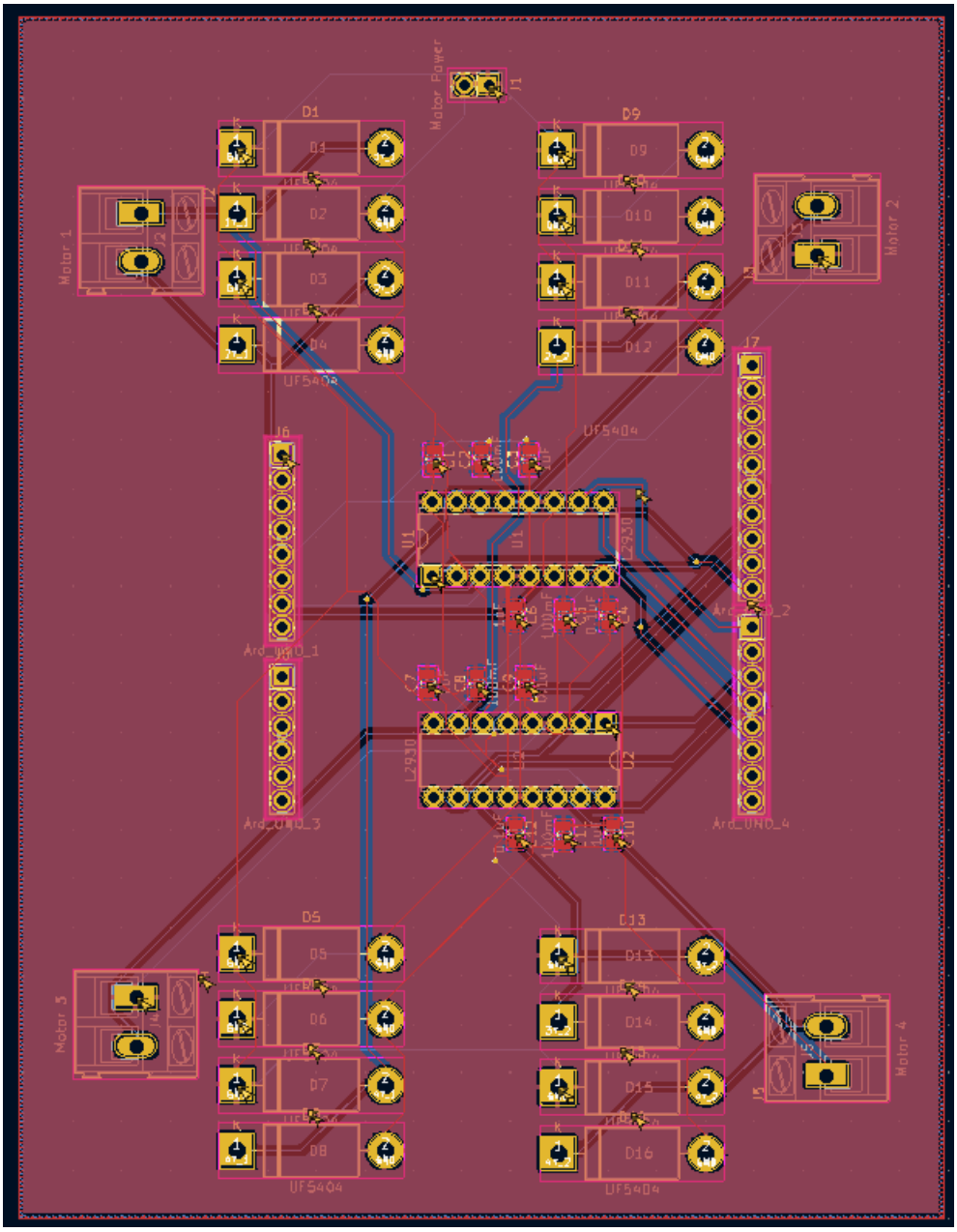

Figure 43 – Navigation Motor Control PCB

The datasheet for the BTS7960 motor driver did not provide information on how to position the components for the PCB, thus, the 0.1µF capacitors were placed close to their logic power pin and the remaining six were placed close to the moto driver ICs to minimize excessive noise since they become less effective the farther away they are. They TVS diode was also placed close to the TXS0108E level shifter to prevent damage to the chip. Two main trace widths were used in the layout of this PCB, for the digital pin connections 20

mils traces were used, since they have a lower current load and lower frequency signals; for the power supply, ground, and motor connections the trace width used was 40 mils because of the higher current needed.

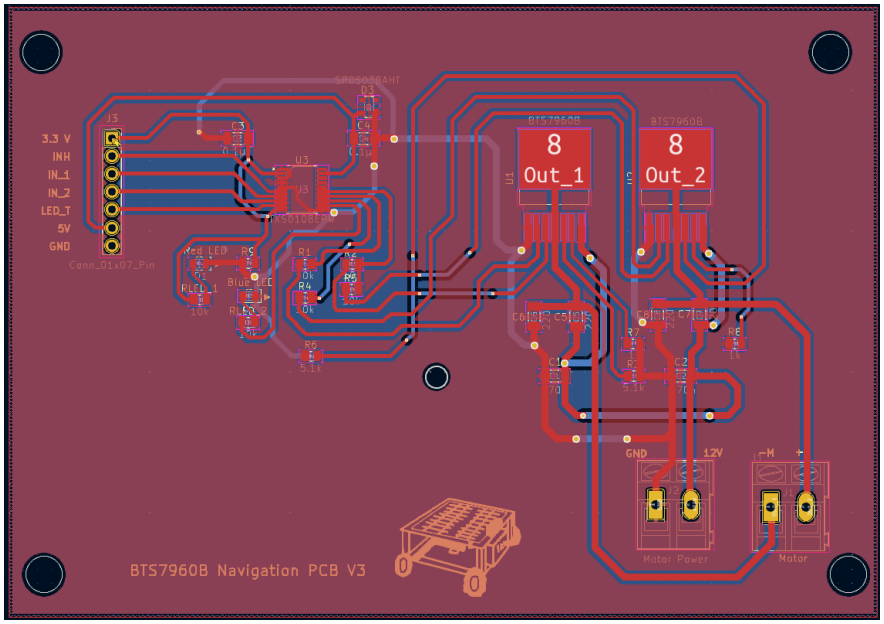

Figure 44- DC Motor Driver PCB (SD2)

The schematic connecting the motor control system, the ESP32/Raspberry Pi connections, and the power regulator are shown below. These three blocks are connected by global

power labels showing the voltage feed between the blocks. The global connections simplify the schematic and declutter wires.

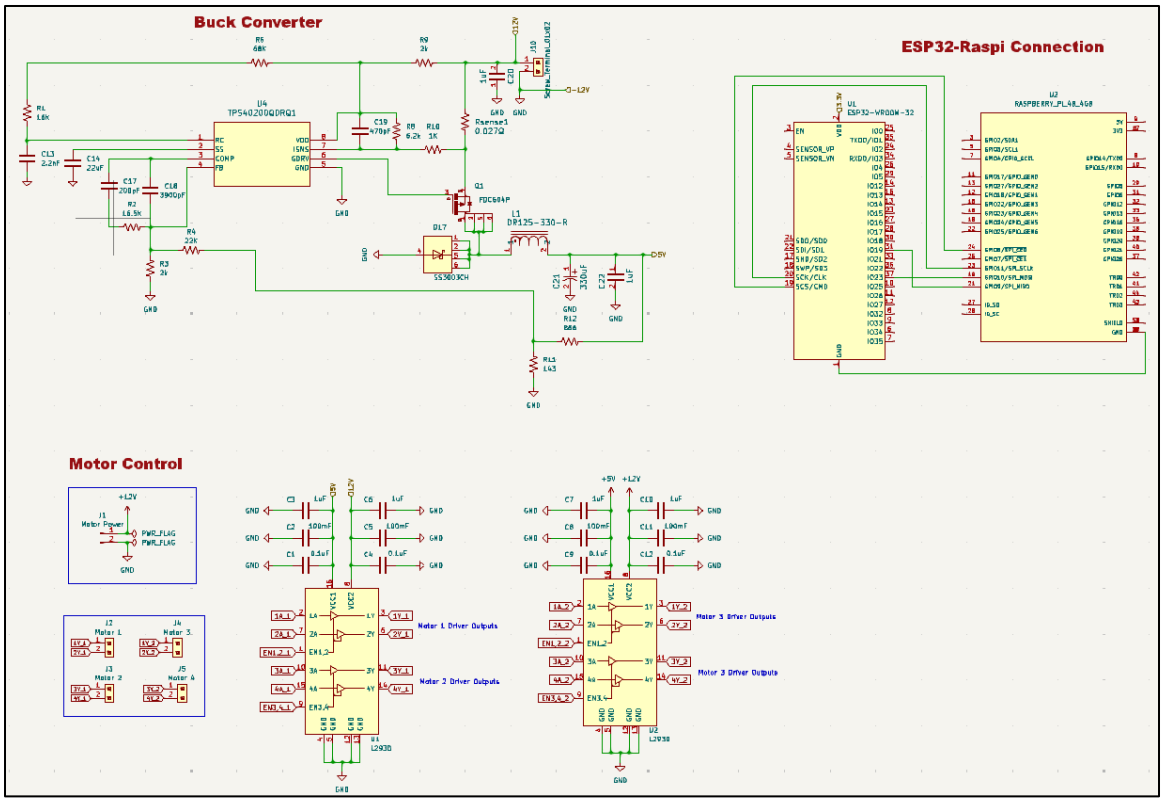

Figure 45 – Overall Schematics for BEAM

Chapter 9 – System Testing and Evaluation

Because our project had several systems that were constantly interacting with each other, a proper procedure was needed for testing to ensure optimal performance and reliability. The testing consisted of two phases, the first was with breadboard and development boards since it allowed for quick prototyping and easy evaluation of individual components. The second phase was with the designed PCBs that lead to a more efficient final product.

9.1 Navigation Motor Control Testing

To test for the motor control, we used the Arduino Uno Development Board and two L293D H-bridge motor drivers where each end of the motors were connected to a output and each driver input was connected to a digital pin of the Arduino board, the logic power from the H-Bridge was connected to the 5V pin from the Board. To run it, we have load up code from the Arduino that sends the signal to the H-bridges, where we can control the speed of each motor and for the robot to move, we have to pay attention to what each motor is going to do since bidirectionality is enabled.

Another way our team plans on testing the navigation system is to simulate it using Gazebo 3D simulation software. Gazebo is useful for providing a safe testing environment that uses realistic sensor data to navigate complex scenarios that would be provided by our collected field data. Developing and testing 3D mapping algorithms on our finished model can be risky, and expensive if collisions, or other unexpected environmental factors occur. Gazebo not only provided a safe way to test our completed robot, but also allow for quick repeatability in testing to ensure consistent conditions. This saved our team time and allowed us to quickly reset testing scenarios without having to physically move our robot, manually reset the testing environment, and reset the robot's hardware and software protocols. Gazebo can also be used for testing in different conditions such as urban areas or rough terrains. This was not only be very useful for testing out real field work on a small-scale farm vs a large home garden, but it also reduced physical wear and tear on our robot. This software is also widely used in the robotics community and contains extensive documentation, tutorials, and community support. The information provided made development easier and allowed us to more rapidly find answers to problems that arised.

9.2 Object Detection Testing

To test for the RGB camera for the Object Detection System using the Raspberry Pi 4 the programming software Thonny was used which is a python IDE included with the operating system. Object detection systems are incredibly important and outright critical in various applications, such as robotics, surveillance, and autonomous driving. Testing these systems, specifically for their accuracy and speed, is absolutely essential. Because we used a Raspberry Pi model 4 for our object detection hardware, it was important to make sure that all of the latest versions of the Raspberry Pi OS, as well as the Python,

OpenCV, and yolov5 libraries, were updated to allow our object detection model to function properly [152]. We needed to create our own library of images that could be labeled as either "plant" or "weed" with various other parameters when necessary. Labeling tools provided through RoboFlow helped us label large amounts of data in shorter times than would be possible if done manually. After the data was captured and properly labeled, we needed to begin training the model with two sets of data. These two sets were split into annotated image training and validation sets in order to ensure the model could learn effectively and have its performance accurately evaluated. Then we chose a pre-trained object detection model and adapted it to the dataset we mentioned before. Configuring the training pipeline using a training framework of our choice, we trained the model on the dataset, adjusting the parameters in order to optimize performance the best way we could. After we finished and were satisfied with the results, we evaluated the model by giving it new data to label. There are various methods for accurately quantifying the model's accuracy, such as precision, recall, or an F1 score. Ideally, we decided to use an F1 metric as it creates the best mean between precision and recall scores. Additionally, we used a confusion matrix to visualize the performance of the object detection model. This allowed us to find out the number of true or false positives or negatives. These combinations of strategies allowed us to best test our object detection model for speed and accuracy. [153] [154]

9.3 Power System Testing

Testing the power regulation system began with circuit simulation models to check the voltage and current flow through a designed circuit. Simulation software such as LTSpice was used to create component models, test the range of specific component values, and monitor voltage, current, frequency, and many more parameters through out the circuit design. One of the most important values that LTSpice brings to circuit board testing is the ability to create custom models of almost any component available. It is also renowned among electronics manufacturers like Texas Instruments, so much so that they include LTSpice files of their components for free for circuit designers to use. Testing sections of the power regulator circuit was be completed on LTSpice for simulation results and added further confidence in the quality of a design before purchasing SMD components for the main PCB.

Another form of testing that was extremely important, especially for the power regulator circuits, is thermal testing. This stage of testing was be very valuable to the development of the PCB because it pointed out problem locations on the board. If a certain section of the PCB was becoming too warm, it could damage surrounding onboard components, change signal values, and allow electrical damage to external peripherals. It was essential to design the PCB in a way that provided acceptable thermal relief to all components, and if the thermal relief was not enough to keep onboard components functioning, then the system would have been redesigned or a cooling system would have been installed to maintain a suitable board temperature.

The final form of testing that was be conducted on our main PCB was multimeter and oscilloscope testing. Before any external peripherals or important components are attached to the board, a multimeter will be used to measure the current and voltage allowed through essential nodes in the circuit. This is vital to maintaining the condition of necessary components and will allow us to potentially avoid replacing components that were damaged due to circuit malfunctions. After the multimeter test was conducted and power was connected, we connected an oscilloscope to the switching nodes of our switching regulator to ensure that the inductor was switching properly to allow the circuit to function.

9.4 Laser System Testing

There are many variables to take into consideration while testing the laser system when it is on board the BEAM robot. Weather greatly impacts laser performance because humidity can influence the beam's scattering and affect the IV characteristics of the laser diode. Condensation can also form on electronics and lenses, potentially contaminating the lens and shortening the lasers lifetime. Temperature can also influence the beam's characteristics. The laser diode performs at a specific temperature rating, and if it starts to approach extreme temperature ranges this will negatively affect the electronics performance and change the behavior of the diode. With these impacts being considered, it will significantly benefit the BEAM project to conduct testing outdoors in different weather conditions to accurately adjust for possible impacts on the efficiency of the system. Over the course of Senior Design 2, several test runs will need to be conducted in good and poor weather conditions so the results of successful weed treatments over time can be compared.

For future purposes of laser system testing, we need to include safety features to protect viewers near the robot. The BEAM robot includes a Class 4 laser, and it is extremely dangerous to unprotected eyes and harmful to exposed skin. To evaluate our system, preventative measures need to be taken to prevent observers from viewing the laser directly or rays that may scatter from the beam. In Senior Design 2, our team plans to implement a barrier system that lowers shutters to contain the active lasing area and obstruct viewing of the beam or laser scattering.

9.5 DC Motor Testing

After the PCB design for the DC motor driver was checked off, it arrived a couple of weeks later to begin the testing phase, after assembling, I connected each pin to the ESP322 dev kit similarly to the breadboard example, each board had an enable pin in a regular GPIO pin and two direction pins to PWM pins. The logic and power supply were the same as before, after assembling five boards all of them were tested successfully with a LED that was placed after the level shifter to verify the data transfer.

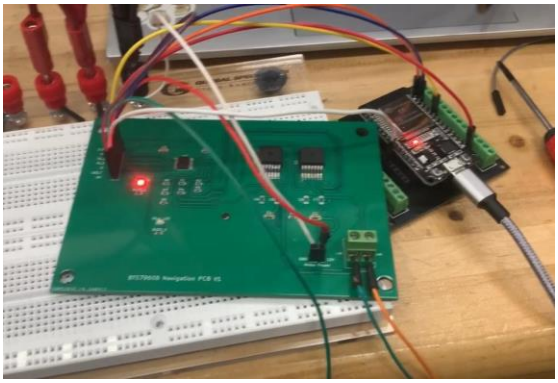

Figure 46 – DC Motor PCB Test

However, once the process of integrating two or more PCBs at a time with the battery, we ran into a problem with the back EMF. When simulating the PWM signal that the ESP sends with a power supply, the peaks of the motors reached up to 100V which was going back to the system once the motor was stopped and it kept taking out the ICs. 16V Zener diodes were used as flyback diodes across both ends of the motors to bring down and limit these peaks, which they did but not completely, because of the back EMF the integration of this PCB was not possible. Instead, two relays for direction and a PWM controller to step down the speed were used for each motor. The relays used were 5V and 10A, and since they were a one channel module, the normally open (NO) terminals were connected together, the same was done for the normally closed (NC) and logic power terminals, the NO and NC were connected to the output of the PWM speed controller, the IN terminals were used to choose the direction of the motors, if one relay is kept as HIGH while the second one is kept LOW the motor will go in a clockwise direction, while if the positions are reversed so is the direction.

Figure 47 – PWM signal from ESP for four motors.

One thing we would've done differently is to electrically isolate the system, for example, using an optocoupler to prevent the back EMF affecting the ICs.

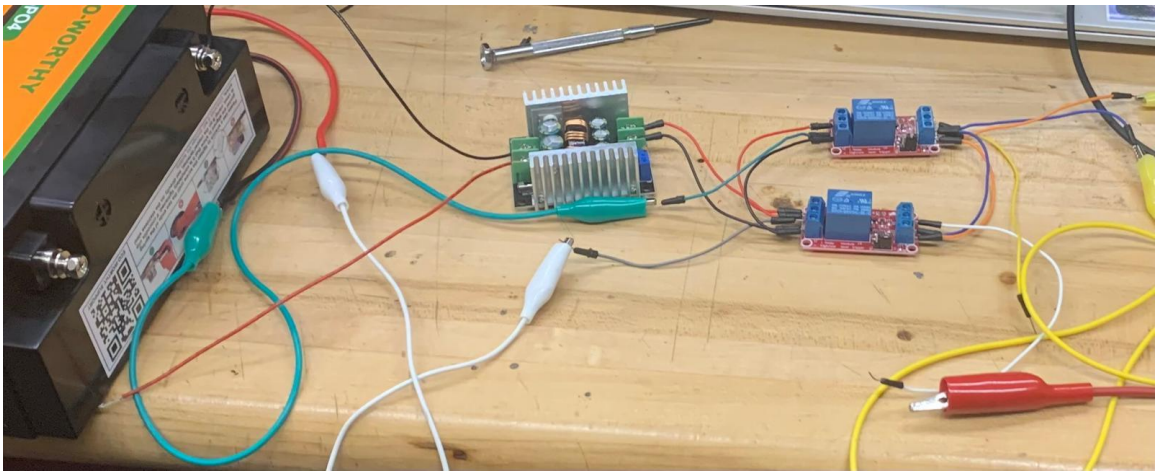

Figure 48 - DC motor setup

The same setup was used to control the linear actuator that raises and lowers the laser shield box. A step-down module provided lower voltage and current to prevent the actuator from damaging the box. During testing, it worked perfectly. However, when integrated into the laser control circuit, the system kept shutting down and required a complete restart. Even when plugged into a separate power supply, the issue persisted. This led us to identify electromagnetic interference (EMI) as the cause. To resolve this, we added ferrite cores to reduce noise in the circuit, successfully integrating it into the laser control system.

9.6 Laser Testing

Initially, we used a 1-2W blue laser diode to conduct experiments on weed treatment. However, the beam had minimal effect on the leaf spots, and it took over a minute to observe any noticeable changes. To address this, we switched to a 5W laser diode, which produced more effective results. The actual optical output power of the new diode was measured at 4.3 W.

After implementing the beam expander, the beam size expanded to approximately four times its original size, and the changes in beam diameter over distance were measured.

The graph below depicts the horizontal and vertical beam diameters at various distances from the beam expander to the leaf treatment spot. As the treatment distance increased, the horizontal beam diameter experienced a significant expansion, whereas the vertical beam diameter showed only a slight increase.

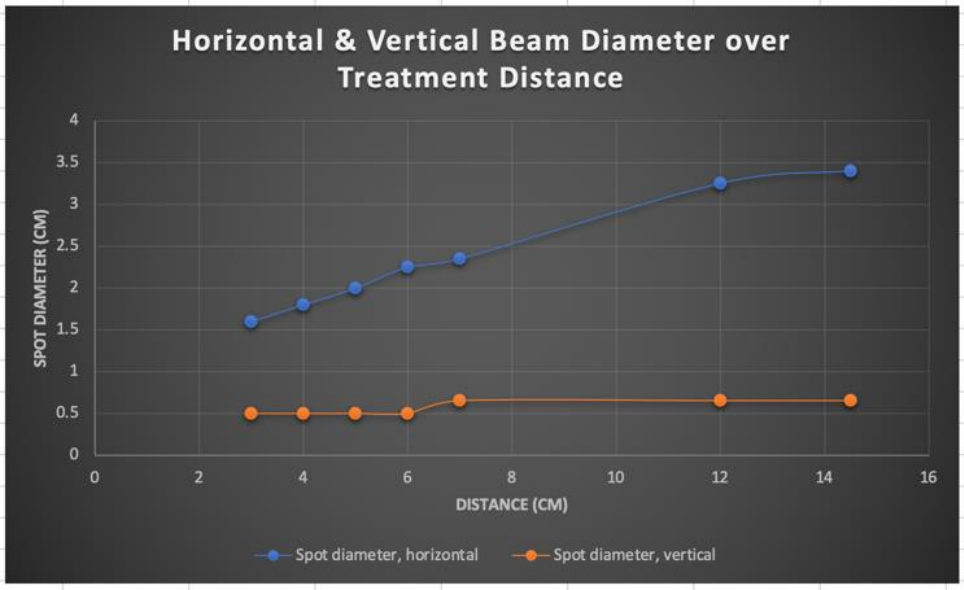

Figure 49 - Horizontal & Vertical Beam Diameter over Treatment Distance

Let a represent the horizontal beam spot radius and b represent the vertical beam spot radius. The area of the beam spot can be calculated using the following formula:

$$A = \pi ab$$

(21) Area of an Ellipse

We investigated the relationship between laser intensity and treatment time by determining the minimum intensity required to affect a treatment spot on the leaf at various distances. To prevent burning or smoke generation, we ensured the treatment time remained below the threshold at which damage could occur.

To achieve an effective treatment duration of 20 to 30 seconds without burning the leaf, we conducted experiments at distances ranging from 1 to 4.5 cm (Figure 50). The minimum intensity for each distance is plotted on the y-axis, with the corresponding time to burn the weeds labeled above each intensity point. This data was instrumental in establishing a safe upper limit for treatment duration, ensuring the process remained non-destructive.

By identifying the intensity at which burning begins, we can fine-tune both laser intensity and distance to achieve a controlled effect. This allows for effective drying of the leaf within the target timeframe while preserving the surrounding vegetation.

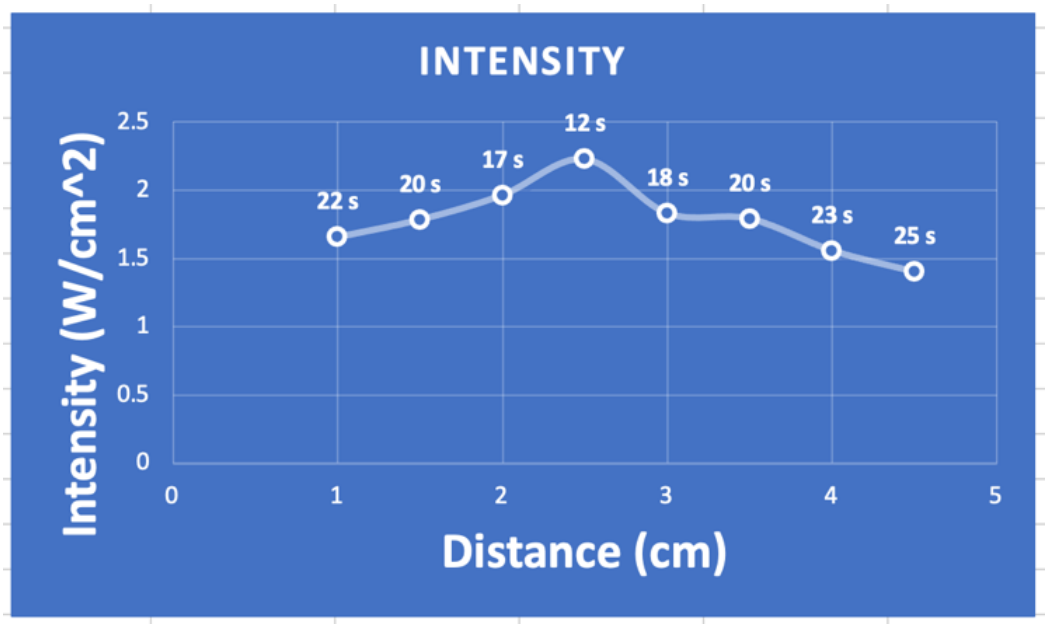

Figure 50 - *Relationship Between Laser Intensity and Distance for Weed Burning*

Figure 50 demonstrates a treatment scenario where the laser beam is nearly perpendicular to the leaf spot. Results may vary if the leaf is angled differently.

At treatment distances shorter than 2 cm, the beam was out of focus, resulting in a narrower beam size. Despite the proximity of the laser to the target, it required more time to achieve effective treatment, making distances under 2 cm inefficient and not recommended. The shortest treatment time was observed at approximately 2.5 cm. At distances greater than 3 cm, the larger beam spot size covered more area, leading to more effective treatment. However, since our laser system does not automatically adjust for height, targeting spots farther away would result in reduced treatment efficiency. Based on these findings, the optimal treatment range was determined to be between 3 and 4 cm.

During the treatment process, the laser was focused on the central part of the leaf, which occasionally left the edges untreated. However, by concentrating on the main area, we observed that the leaf wilted effectively. The treated dollarweed had a total of seven leaves—five larger leaves and two smaller ones connected. After treating all the leaves, we monitored changes over a period of two days.

Figure 51- Laser Setup

Figure 52 - *Weed Treatment Before & After*

After treatment, we continued to water the weed and maintained normal growing conditions, ensuring it received sunlight to assess its potential for recovery. The day after treatment, we observed that the leaves had dried out further. While one leaf retained some freshness at the edges, the central part had dried, indicating damage to its photosynthesis process.

By the second day post-treatment, the leaves exhibited increased wilting, and their color had shifted to a more pronounced yellow. These changes were consistent with symptoms of dehydration and overall plant drying.

Figure 53 - Appearance of Treated Weeds After 1 Day (Left) & 2 Day (Right)

Chapter 10 – Administrative Content

One of the key factors influencing the project is the financial budget, as insufficient funding can hinder our progress. To address this, we have included a table detailing the estimated total costs, which will help set clear expectations for the next phase of the project. Additionally, we have outlined the project milestones for both semesters to ensure we remain on track and effectively manage our timeline.

10.1 Budget and Financing

The budget included for the project serves as a base of what the overall cost was going to be, it was subject to change when it comes to component replacements or design changes. It was finalized in Senior Design II, once the design was approved and we tested out the PCB with the parts that we needed to order.

Item	Description	Quantity of item	Estimated Cost	Total Cost
LiDAR System [155]	LiDAR System	1	$93	$93
Blue Laser Diode [156]	Wavelength: 455 nm Optical Power: 5000 mW	1	$42	$42
Red Laser Diode [157]	Wavelength: 639 nm Optical Power: 2100 mW	1	$90	$90
Green Laser Diode [158]	Wavelength: 530 nm Optical Power: 1650 mW	1	$150	$150

Chassis and Motors: DIY and Pre-Assembled [159] [160]	DIY and Pre-Assembled Chassis and Motors	2 + 1	$70 + $80	$150
Microcontroller and Sensors [161]	Raspberry Pi and ESP with sensors	2	$80	$160
Battery and Power Management [162]	Battery and power management components	1	$37	$37
Miscellaneous Components [163]	Electronic components kit	1	$30	$30
Solar Panel [164]	Solar panel + charge controller	2	$25	$50
Total Overall Cost				$802

Table 42 – Budget

Overall our team ended up spending more than our original budget because we underestimated the costs for hardware and replacing broken electronics. Our battery and power management section was almost double what we expected it to be, along with the increased expenses for replacing laser diodes and lenses. We believe that the initial budget assumption was so much lower than the total final cost for the project was because we underestimated how much we would spend on hardware like bolts, screws, aluminum framing, and more.

10.2 Project Milestones

Below there are two tables that entail the project milestones that we need to keep track of to finish the BEAM project on time, they include the design, research, quizzes, and testing of the different components.

10.2.1 Senior Design I

For Senior Design I we had a better idea for the milestone because of the syllabus provided, we detailed a week-by-week schedule that helped us keep track of our goals.

Week	Date	Milestone Description
1	5/13/24 – 5/19/24	Form group project and storm ideas.
2	5/20/24 – 5/26/24	Choose a project idea and start the D&C Report.
3	5/27/24 – 6/2/24	Finish the first draft of D&C 10-page Report.
		Submit Bootcamp Assignment.
		Work on the group website.
4	6/3/24 – 6/9/24	Attend the D&C Group meeting.
		Start the updated version of D&C Report after meeting with professors.
5	6/10/24 – 6/16/24	Submit updated version of D&C Report to the website (20-page minimum).
6	6/17/24 – 6/23/24	Start the 60-page Report.
		Assignment on Standards
7	6/24/24 – 6/30/24	Finalize the 60-page Report
		Finish Quiz A to G.
8	7/1/24 – 7/7/24	Upload the 60-page Report. (Preferably more than 60 pages).
9	7/8/24 – 7/14/24	Attend the 60-page Report Group Meeting
		Start working on the updated version of the 60-page Report.
		Submit the updated 60-page Report onto group website
10	7/15/24 – 7/21/24	Order parts
		Work the Final draft of the Project Report.
11	7/22/24 – 7/23/24	Submit the SD I Final Report

10.2.2 Senior Design II

Setting weekly milestones for Senior Design II proved to be a little bit more difficult without a syllabus that could include project writing and/or quizzes so we decided to set overall goals to keep us on track.

Week	Date	Project Milestone
1	8/19/24 – 8/25/24	Order remaining parts
2	8/26/24 – 9/1/24	Start testing individual components functionalities.
3	9/2/24 – 9/8/24	Start the design of the App.
4	9/9/24 – 9/15/24	Finish Power functionalities
5	9/16/24 – 9/22/24	Finish Motor control
6	9/23/24 – 9/29/24	Finish Sensor functionalities
7	9/30/24 – 10/6/24	Finish connecting all code in MCU
8	10/7/24 – 10/13/24	Assemble hardware
9	10/14/24 – 10/20/24	Meet with professors
10	10/21/24 – 10/27/24	Redesign if needed
11	10/28/24 – 11/3/24	Finish App
12	11/4/24 – 11/10/24	Test app functionality
13	11/11/24 – 11/17/24	Finish final prototype
14	11/18/24 – 11/24/24	Test final prototype
		Record Demo
15	11/25/24 – 12/1/24	Finalize and submit Final Report
16	12/2/24 – 12/7/24	Live Demo

10.3 Distribution of Workload

Below there's a table that details the responsibilities that each member of the BEAM project had, even though each student was responsible for their own main sections the rest

of the members also aided whenever needed. The cooperation of all members made this project more manageable, and everybody being involved in different section ensured that the different segments could blend in more seamlessly.

10.3.1 Senior Design I

Each role assigned to the members was mostly concerned with drafting the corresponding section of the report.

Responsibility	Role
TJ Jones	
Battery Research and selection	Main Student
Charge Controller Research and selection	Main Student
Solar Panel Research and selection	Main Student
Laser Control System Research, Selection, Design, and Implementation	Main Student
Switching Regulator Circuit and PCB	Main Student
Laser Circuit Driver	Main Student
Suhyung Hwang	
Laser Diode Research and Selection	Main Student
Lens Research, Selection, and Design	Main Student
Laser System Design and Implementation	Main Student
Laser Control System Research, selection, and Design	Main Student
Laser Circuit Driver	Secondary Student
Ryan Takiff	
Executive Summary	Main Student
Lidar and RGB sensors Selection	Main Student
MCU Research and Selection	Main Student
RGB camera testing and implementation	Main Student

Past and Existing Projects Research	Main Student
MCU Design and PCB	Main Student
Object Detection Data Set	Secondary Student
Daemy Luzardo	
House of Quality	Main Student
Motor Research and Selection	Main Student
Wheels Research and Selection	Main Student
Navigation Motor Controller Research and Selection	Main Student
Lidar and RGB Camera Research	Main Student
Object Detection Data Set	Main Student
RGB camera testing and implementation	Main Student
Motor Control Design and PCB	Main Student

10.3.2 Senior Design II

In the second phase of the project, each responsibility was primarily focused on the development of the system and its integration with the others.

Responsibility	**Role**
TJ Jones	
Object detection model training and software implementation	Main Student
Robot's frame and wheel assembly	Main Student
Laser control system software, testing, and implementation	Main Student
Laser safety system software design and implementation	Main Student
Suhyun Hwang	
Laser System Design	Main Student
Laser System Testing and Implementation	Main Student
Laser System Software	Secondary Student

Ryan Takiff	
ESP32-WROOM-32 MCU PCB Testing and Implementation	Main Student
Navigation System Testing and Implementation	Main Student
ROS Software Testing and Integration	Main Student
Lidar Object Detection and Obstacle Avoidance Testing and Integration	Main Student
Shield Box	Secondary Student
Robot's Framework Wheels and Accessories	Secondary Student
Daemy Luzardo	
DC Motor Driver Testing and Implementation	Main Student
Navigation System Testing and Implementation	Main Student
Solar Panel Testing and integration	Main Student
Robot's Framework and wheels	Secondary Student
Shield Box	Secondary Student
Battery Testing and Integration	Main Student
MCU Testing and Implementation	Secondary Student

Chapter 11 – Conclusion

In conclusion, the BEAM project was created as a solution for the elimination of weeds in the farming industry to avoid the use of harmful pesticides and chemicals for field maintenance. Even though there are similar projects on the market, the BEAM robot offers small scale farmers technological advances in field management that have previously only been available for large scale industrial farms.

The BEAM project is composed of five main parts: the power systems, laser control system, navigational system, weed identification, and the laser system. The laser control system and the RGB camera work together to successfully identify weeds and prepares the system for their removal. The object detection software utilizes a vast database of weed images to make accurate identifications and protect vital crops. The implementation of lidar in the navigational system is crucial for the mapping of target areas that require weed treatment, and it also allows the robot to avoid objects and traverse uneven terrain.

The design of BEAM allows for future growth and sustainability in agriculture by allowing farmers to better locate problem areas and reduce the need for labor. By using advanced technologies, farmers will have more control over their fields and be more informed about their crop's health and growing conditions. This level of control can lead to improved crop yield and operational cost over time. With real-time data and field analysis, farmers can make informed decisions, optimize supply management, and implement sustainable farming practices more effectively.

This document serves as a record of the design and development process of the BEAM project, it is on track to be fully developed, tested, and functional by the end of Fall 2024. We intend for BEAM to promote the growth of new technologies in the industry and for future engineers to take inspiration to further research in robotics for agriculture.

Appendix A - References

[1] USDA, "usda.gov," [Online]. Available: https://www.ers.usda.gov/data-products/ag-and-food-statistics-charting-the-essentials/ag-and-food-sectors-and-the-economy/#:~:text=Agriculture%2C%20food%2C%20and%20related%20industries%20contributed%20roughly%20%241.530%20trillion%20to,0.7%20percent%20of%.

[2] U.S. Department of Agriculture, "Climate Hubs - Climate and Agriculture," 28 May 2024. [Online]. Available: https://www.climatehubs.usda.gov/hubs/midwest/drought-map#:~:text=Midwestern%20agriculture%20is%20dominated%20by,to%20hold%20water%20and%20nutrients.. [Accessed 30 May 2024].

[3] J. S. A. Krohn, "The Importance of Off-Farm Income to the Agricultural Economy," 17 May 2023. [Online]. Available: https://www2.census.gov/about/training-workshops/2023/2023-05-17-agriculture-presentation.pdf.

[4] U.S. Department of Agriculture, "NIFA Supported Research Tackles Weedy Problem," 28 March 2023. [Online]. Available: https://www.nifa.usda.gov/about-nifa/blogs/nifa-supported-research-tackles-weedy-problem#:~:text=Weeds%20reproduce%20and%20spread%20quickly,significantly%20to%20farming%20production%20costs.. [Accessed 13 June 2024].

[5] GeoPard Agriculture, "Why is weed control important in agriculture?," [Online]. Available: https://geopard.tech/blog/why-is-weed-management-important-in-agriculture/#:~:text=Weeding%20can%20be%20done%20in,Chemical%20Weeding. [Accessed 13 June 2024].

[6] A. e. a. Mustafa, "ResearchGate," June 2019. [Online]. Available: https://www.researchgate.net/figure/Disadvantages-of-herbicides-to-all-life-forms-Modified-and-redrawn-from-1_fig1_333662293. [Accessed 13 June 2024].

[7] S. K. Mathiassen, T. Bak, S. Christensen and P. Kudsk, "The Effect of Laser Treatment as a Weed Control Method," *Elsevier*, vol. 95, 2006.

[8] M. V. Bauer, C. Marx, F. V. Bauer, D. M. Flury, T. Ripken and B. Streit, "Thermal weed control technologies for conservation agriculture—a review," *Wiley*, vol. 60, no. 4, 2020.

[9] P. Mikesell, "Carbon Robotics - Autonomous Weeder," 2024. [Online]. Available: https://carbonrobotics.com/. [Accessed 13 6 2024].

[10] C. Juriens, "Ecorobotix : Smart spraying for ultra-localised treatments," [Online]. Available: https://ecorobotix.com/en/. [Accessed 13 6 2024].

[11] Successful Farming, "Blue River Technology Uses Robots, Artificial Intelligence to Kill Weeds," 5 12 2016. [Online]. Available: https://www.agriculture.com/technology/robotics/blue-river-technology-uses-robots-artificial-intelligence-to-kill-weeds. [Accessed 13 6 2024].

[12] J. Jasko, "WeedBot - Laser-Weeding Technology," [Online]. Available: https://weedbot.eu/. [Accessed 13 6 2024].

[13] E. Buchanan, "“A Robot from the Future: The Weed Terminator | West Central Research and Outreach Center," [Online]. Available: https://wcroc.cfans.umn.edu/about-us/wcroc-news/weed-terminator-2023. [Accessed 13 6 2024].

[14] Tertill, "Tertill Weeding Robot," Tertill, [Online]. Available: https://tertill.com/products/tertill. [Accessed 7 July 2024].

[15] STMicroelectronics, "STM32 Ultra Low Power MCUs," [Online]. Available: https://www.st.com/en/microcontrollers-microprocessors/stm32-ultra-low-power-mcus.html. [Accessed 8 7 2024].

[16] STMicroelectronics, "STM32 32-bit Arm Cortex MCUs," [Online]. Available: https://www.st.com/en/microcontrollers-microprocessors/stm32-32-bit-arm-cortex-mcus.html. [Accessed 8 7 2024].

[17] E. S. E. Systems, "ESP SoCs: Espressif Systems," [Online]. Available: https://www.espressif.com/en/products/socs/esp32.. [Accessed 8 7 2024].

[18] AMD, "AMD FPGAs," [Online]. Available: https://www.amd.com/en/products/adaptive-socs-and-fpgas/fpga.html. [Accessed 8 7 2024].

[19] Intel, "Altera® FPGAs and Programmable Devices," [Online]. Available: https://www.intel.com/content/www/us/en/products/programmable.html#tab-blade-1-1. [Accessed 8 7 2024].

[20] A. Ayodele, "FPGA vs. Microcontroller: Understanding the Key Differences," [Online]. Available: https://www.wevolver.com/article/fpga-vs-microcontroller. [Accessed 8 7 2024].

[21] Mclpcb, "FPGA vs. Microcontroller | What is the Difference?," [Online]. Available: https://www.mclpcb.com/blog/fpga-vs-microcontroller/#:~:text=The%20main%20difference%20is%20in,of%20code%20at%20a%20time.. [Accessed 8 7 2024].

[22] J. S. a. J. Schneider, "Field programmable gate arrays (FPGAs) vs. microcontrollers: What’s the difference?," 4 6 2024. [Online]. Available: https://www.ibm.com/blog/fpga-vs-microcontroller/. [Accessed 8 7 2024].

[23] robotshopmascot, "RobotShop Community," 03 July 2018. [Online]. Available: https://community.robotshop.com/blog/show/drive-motor-sizing-tool. [Accessed 24 June 2024].

[24] U. D. o. Energy, "Determining Electric Motor Load and Efficiency," pp. 1, https://www.energy.gov/eere/amo/articles/determining-electric-motor-load-and-efficiency#:~:text=Most%20electric%20motors%20are%20designed,dramatically%20below%20about%2050%25%20load..

[25] ZIEHL, "Alternating Current Motor: AC Motors Function and Advantages," [Online]. Available: https://www.ziehl-abegg.com/en-us/glossary/alternating-current-motor-ac-motor. [Accessed 6 July 2024].

[26] Fictiv, "The Engineer's Guide to Small Scale AC vs. DC Motors," [Online]. Available: https://www.fictiv.com/articles/the-engineers-guide-to-small-scale-ac-vs-dc-motors. [Accessed 6 July 2024].

[27] "Monolithic Power Systems," [Online]. Available: https://www.monolithicpower.com/stepper-motors-basics-types-uses. [Accessed July 2024].

[28] BYJU'S Learning, "Pulse Width Modulation," [Online]. Available: https://byjus.com/physics/pulse-width-modulation/#:~:text=Width%20Modulation%20technique%3F-,Pulse%20width%20modulation%20or%20PWM%20is%20a%20commonly%20used%20control,continuously%20varying%20(analog)%20signal.. [Accessed 19 July 2024].

[29] K. Franz, "What is an H-Bridge?," Digilent Blog, 18 April 2023. [Online]. Available: https://digilent.com/blog/what-is-an-h-bridge/. [Accessed 19 July 2024].

[30] Studica, "Robot Wheels: A Guide for Mobile Robotics," 9 October 2023. [Online]. Available: https://www.studica.com/blog/robot-wheels/. [Accessed 16 July 2024].

[31] P. Yavari, "Introduction to Types of Robot Wheels," [Online]. Available: https://gtfrobots.com/introduction-to-types-of-robot-wheels/. [Accessed 16 July 2024].

[32] Robot Platform, "Introduction to Types of Robot Wheels," [Online]. Available: https://www.robotplatform.com/knowledge/Classification_of_Robots/Types_of_robot_wheels.html. [Accessed 16 July 2024].

[33] L. David, "Guide to Solar Batteries: Are They Worth It?," MarketWatch Guides, 13 June 2024. [Online]. Available: https://www.marketwatch.com/guides/solar/solar-batteries-guide/#:~:text=Lithium%2Dion%20batteries%20are%20recommended,of%20an%20off%2Dgrid%20system.. [Accessed 14 June 2024].

[34] Power Sonic, "Glossary of Battery Terms," [Online]. Available: https://www.power-sonic.com/blog/glossary-of-battery-terms/. [Accessed 14 June 2024].

[35] Battery University, "BU-107: Comparison Table of Secondary Batteries," Cadex, 21 October 2021. [Online]. Available: https://batteryuniversity.com/article/bu-107-comparison-table-of-secondary-batteries. [Accessed 14 June 2024].

[36] University of Washington, "Clean Energy Institute: Lithium-Ion Battery," [Online]. Available: https://www.cei.washington.edu/research/energy-storage/lithium-ion-battery/. [Accessed 14 June 2024].

[37] Battery University, "BU-304a: Safety Concerns with Li-ion," Cadex, 22 February 2022. [Online]. Available: https://batteryuniversity.com/article/bu-304a-safety-concerns-with-li-ion. [Accessed 15 June 2024].

[38] Battery University, "BU-201: How does the Lead Acid Battery Work?," Cadex, 21 October 2021. [Online]. Available: https://batteryuniversity.com/article/bu-201-how-does-the-lead-acid-battery-work. [Accessed 14 June 2024].

[39] L. David and S. Lopez, "Solar Charge Controllers: What They Are, Why You Need One and What They Cost," Market Watch, 13 June 2024. [Online]. Available: https://www.marketwatch.com/guides/solar/solar-charge-controllers/. [Accessed 13 June 2024].

[40] Solar Square, "Everything You Should Know About a PWM Solar Charge Controller," 25 August 2022. [Online]. Available: https://www.solarsquare.in/blog/pwm-solar-charge-controller/. [Accessed 15 June 2024].

[41] Morningstar, "What are the Solar Battery Charging Stages?," [Online]. Available: https://www.morningstarcorp.com/faq/what-are-the-solar-controller-battery-charging-stages/. [Accessed 15 June 2024].

[42] R. H. e. a. Byrne, "Energy Management and Optimization Methods for Grid Energy Storage Systems," *IEEE Access*, vol. 6, no. http://dx.doi.org/10.1109/ACCESS.2017.2741578, p. 13237, 2018.

[43] J. Weber, "How Do Lithium Ion Chargers Work?," BatteriesPlus, 16 September 2022. [Online]. Available: https://www.batteriesplus.com/blog/power/lithium-battery-chargers. [Accessed 15 June 2024].

[44] Redway Battery, "Can a PWM controller charge a lithium battery?," 13 December 2023. [Online]. Available: https://www.redway-tech.com/can-a-pwm-controller-charge-a-lithium-battery/. [Accessed 15 June 2024].

[45] A. Jay, "What Solar Charge Controller Do I Need for Lithium Batteries?," Dakota Lithium, 28 August 2023. [Online]. Available: https://dakotalithium.com/dakota-

lithium/what-solar-charge-controller-do-i-need-for-lithium-batteries/. [Accessed 15 June 2024].

[46] MathWorks, "What Is MPPT Algorithm?," MathWorks Inc., [Online]. Available: https://www.mathworks.com/discovery/mppt-algorithm.html#:~:text=Maximum%20power%20point%20tracking%20(MPPT,changing%20solar%20irradiance%2C%20temperature%2C%20and. [Accessed 30 6 2024].

[47] NAZ Solar Electric, "What is Maximum Power Point Tracking (MPPT)," NAZ Solar Electric, [Online]. Available: https://www.solar-electric.com/learning-center/mppt-solar-charge-controllers.html/. [Accessed 30 6 2024].

[48] Sunforge, "Buck vs. Boost," Sunforge LLC, 2024. [Online]. Available: https://sunforgellc.com/buck-vs-boost/. [Accessed 30 6 2024].

[49] R. Nowakowski and R. Taylor, "Linear versus switching regulators in industrial applications with a 24-V bus," Texas Instruments Inc, 2013. [Online]. Available: https://www.ti.com/lit/an/slyt527/slyt527.pdf?ts=1719774930872. [Accessed 1 July 2024].

[50] Texas Instruments, "Linear and Switching Voltage Regulator Fundamental Part 1," Texas Instruments Inc, 2011. [Online]. Available: https://www.ti.com/lit/pdf/snva558. [Accessed 1 July 2024].

[51] Monolithic Power, "Buck Converters (Step-Down Converter)," Monolithic Power Inc, 2024. [Online]. Available: https://www.monolithicpower.com/en/learning/mpscholar/power-electronics/dc-dc-converters/buck-converters#:~:text=Buck%20converters%20employ%20a%20simple,the%20rest%20of%20the%20circuit.. [Accessed 7 July 2024].

[52] S. Liddar, "3 Ways to Reduce Power-supply Noise with Power Modules," Texas Instruments Inc, 2023. [Online]. Available: https://www.ti.com/document-viewer/lit/html/SSZT209. [Accessed 2 July 2024].

[53] A. Oggletree, N. Cellucci and R. Akinwonmi, "How Much Do Solar Panels Cost? A Full-Breakdown of Associated Costs and Factors in 2024," Forbes Media LLC., 2 July 2024. [Online]. Available: https://www.forbes.com/home-improvement/solar/cost-of-solar-panels/#average_cost_of_solar_panels_section. [Accessed 5 July 2024].

[54] Freedom Solar, "SOLAR PANEL TEMPERATURE COEFFICIENT: WHAT TO KNOW," Freedom Solar LLC, 30 August 2023. [Online]. Available: https://freedomsolarpower.com/blog/solar-panel-temperature-coefficient-what-to-know. [Accessed 12 July 2024].

[55] American Solar Energy Society, "Thin-Film Solar Panels," American Solar Energy Society, 27 February 2021. [Online]. Available: https://ases.org/thin-film-solar-panels/. [Accessed 5 July 2024].

[56] J. Marsh, "Monocrystalline vs. Polycrystalline solar panels," EnergySage Inc., 9 January 2023. [Online]. Available: https://www.energysage.com/solar/monocrystalline-vs-polycrystalline-solar/. [Accessed 5 July 2024].

[57] D. Collins, "What is microstepping?," WTWH Media LLC, [Online]. Available: https://www.linearmotiontips.com/microstepping-basics/. [Accessed 19 July 2024].

[58] C. Mwitta, G. C. Rains and E. Prostko, "Evaluation of Diode Laser Treatments to Manage Weeds in Row Crops," *MDPI*, 2022.

[59] H. Sun, "Sun, Haiyin. Laser diode beam basics, manipulations and characterizations," *Springer Science & Business Media*, 2012.

[60] M. Ott, "Capabilities and reliability of LEDs and laser diodes," *Internal NASA Parts and Packaging Publication*, 1996.

[61] I. Rakhmatulin and C. Andreasen, "A Concept of a Compact and Inexpensive Device for Controlling Weeds with Laser Beams," *MDPI*, 2000.

[62] G. Coleman, C. Betters, C. Squires, S. Leon-Saval and M. Walsh, "Low Energy Laser Treatments Control Annual Ryegrass (Lolium rigidum)," *frontiers*, vol. 2, 2021.

[63] E. Janeeshma, R. Johnson, M. S. Amritha and N. Louis, "Modulations in Chlorophyll a Fluorescence Based on Intensity and Spectral Variations of Light," *ResearchGate*, vol. 23, no. 10, p. 5599, 2022.

[64] L. Panawala, "Difference Between Chlorophyll A and B," *ResearchGate*, 2017.

[65] A. Wahid, S. Gelani, M. Ashraf and M. R. Foolad, "Heat tolerance in plants: An overview," *Elsevier*, vol. 61, no. 3, pp. 199-223, 2007.

[66] M. M. Ludlow and O. Bjorkman, "Paraheliotropic leaf movement in Siratro as a protective mechanism against drought-induced damage to primary photosynthetic reactions: damage by excessive light and heat," *Springer Link*, vol. 161, pp. 505-518, 1984.

[67] Climate Data, "Climate Data," DATA AND GRAPHS FOR WEATHER & CLIMATE IN ORLANDO, [Online]. Available: https://en.climate-data.org/north-america/united-states-of-america/florida/orlando-1262/. [Accessed 8 July 2024].

[68] E. Janeeshma, R. Johnson and N. Louis, "Modulations in Chlorophyll a Fluorescence Based on Intensity and Spectral Variations of Light," *ResearchGate*, 2022.

[69] U.S Fleet Forces Command, "Science of Sound," [Online]. Available: https://www.usff.navy.mil/Community-Outreach/US-Navy-Stewards-of-the-Sea/Science-of-Sound/. [Accessed 18 July 2024].

[70] Amazon, "LiFePO4 12V 10Ah 20Ah 30Ah Lithium Iron Phosphate Battery," Eco-Worthy, [Online]. Available: https://www.amazon.com/ECO-WORTHY-Phosphate-Rechargeable-Trolling-Fishfinder/dp/B09V79ZKVM/ref=asc_df_B09V79ZKVM/?tag=hyprod-20&linkCode=df0&hvadid=692875362841&hvpos=&hvnetw=g&hvrand=4214550561948383885&hvpone=&hvptwo=&hvqmt=&hvdev=c&hvdvcmdl=&hvlocint=&. [Accessed 8 July 2024].

[71] Amazon, "12V 10Ah Lithium LiFePO4 Deep Cycle Battery, 2000+ Cycles Rechargeable Battery for Solar/Wind Power, Small UPS, Lighting, Power Wheels, Fish Finder and More, Built-in 10A BMS," NERMAK, [Online]. Available: https://www.amazon.com/Lithium-LiFePO4-Rechargeable-Maintenance-Free-Lighting/dp/B097BRKCQP/ref=sr_1_2_sspa?dib=eyJ2IjoiMSJ9.oEc6ULEKu0fEZa7C_bHsOdc3VB5aZAmql1z_VZT9RVuxVHFPgVTcmSa8Ipp5KRVTuzni5OY3GRQ8POptUOJm9S8pGnUNw2i5M34Y_wzu6bUJq1FEBuviGmW35b2YAtz37T. [Accessed 8 July 2024].

[72] Amazon, "12V 10Ah LiFePO4 Battery, 4000+ Cycles 12 Volt 10Ah Lithium Battery Built-in 10A BMS, 12V Battery Perfect for UPS Battery Backup, Replacement SLA, Ham Radio, Deer Feeder, Lighting, Solar Projects," XZNY, [Online]. Available: https://www.amazon.com/XZNY-LiFePO4-Rechargeable-Suitable-Emergency/dp/B09Q8B8MLR/ref=sr_1_9?dib=eyJ2IjoiMSJ9.oEc6ULEKu0fEZa7C_bHsOdc3VB5aZAmql1z_VZT9RVuxVHFPgVTcmSa8Ipp5KRVTuzni5OY3GRQ8POptUOJm9S8pGnUNw2i5M34Y_wzu6bUJq1FEBuviGmW35b2YAtz37T07DLU-OgWxkfkt0. [Accessed 8 July 2024].

[73] Powerwerx, "Powerwerx MPPT-150-14.6, DC-to-DC Solar Charger Controller for Bioenno 12V LiFePO4 Batteries," Powerwerx, [Online]. Available: https://powerwerx.com/mppt-150w-solar-charge-controller. [Accessed 8 July 2024].

[74] Amazon, "10Amp 12 Volt MPPT Solar Charge Controller, Bateria Power Intelligent Portable Solar Panel Controller, Max PV 150W 30Voc Solar Regulator for Gel AGM Lead-Acid, Lithium LiFePO4 Battery (SunRock 10)," Bateria Power, [Online]. Available: https://www.amazon.com/Controller-Bateria-Power-Intelligent-Regulator/dp/B0BNKGC5SM/ref=asc_df_B0BNKGC5SM/?tag=hyprod-20&linkCode=df0&hvadid=692875362841&hvpos=&hvnetw=g&hvrand=788248

9533898190329&hvpone=&hvptwo=&hvqmt=&hvdev=c&hvdvcmdl=&hvlocint=&hvlocph. [Accessed 8 July 2024].

[75] Amazon, "10A MPPT Solar Panels Charge Controller, Portable 12V Intelligent Solar Regulator with LCD Display and LED Indicate for AGM, Gel, LiFePO4, 12 Volt Solar Battery Charger," Voltset, [Online]. Available: https://www.amazon.com/Voltset-Controller-Portable-Intelligent-Regulator/dp/B0C6M17N8H/ref=asc_df_B0C6M17N8H/?tag=hyprod-20&linkCode=df0&hvadid=692875362841&hvpos=&hvnetw=g&hvrand=4467324146172508744&hvpone=&hvptwo=&hvqmt=&hvdev=c&hvdvcmdl=&hvlocint=&hvlo. [Accessed 8 July 2024].

[76] Digikey, "TPS40200QDRQ1," Texas Instruments, [Online]. Available: https://www.digikey.com/en/products/detail/texas-instruments/TPS40200QDRQ1/1777698?utm_adgroup=&utm_source=google&utm_medium=cpc&utm_campaign=PMax%20Shopping_Product_Medium%20ROAS%20Categories&utm_term=&utm_content=&utm_id=go_cmp-20223376311_adg-_ad-__dev. [Accessed 18 July 2024].

[77] Digikey, "MC34063ADR," Texas Instruments, [Online]. Available: https://www.digikey.com/en/products/detail/texas-instruments/MC34063ADR/717456?utm_adgroup=&utm_source=google&utm_medium=cpc&utm_campaign=PMax%20Shopping_Product_Medium%20ROAS%20Categories&utm_term=&utm_content=&utm_id=go_cmp-20223376311_adg-_ad-__dev-c_e. [Accessed 18 July 2024].

[78] Texas Instruments, "TPS40200-Q1 Wide-Input-Range Nonsynchronous Voltage-Mode Controller," Texas Instruments, January 2016. [Online]. Available: https://www.ti.com/product/TPS40200-Q1?qgpn=tps40200-q1&bm-verify=AAQAAAAJ_____7x84Y59tMoguCBNh0lMUcGUKHvf3zwPbR045h_iPSAff7felx5779aVbn8KkwkSk99-YJxpV8Rism5il7GQ3gQ502VnZq6izqJWOT0HBvFrrWd8QC6Zw2nfwdxf8ekGs49WV5nAEWGFXktrcYWCMS2g2GQHzN8w6r5kQqjTcALW0Sp2R. [Accessed 18 July 2024].

[79] Texas Instruments, "MC3x063A 1.5-A Peak Boost/Buck/Inverting Switching Regulators," Texas Instruments, January 2015. [Online]. Available: https://www.ti.com/product/MC34063A?qgpn=mc34063a&bm-verify=AAQAAAAJ_____5D6sw0GuabYMkfl-UilSkzFn6_fiNXgMGl08XjklYhBRkUikK5Nm_RkZZI7KWHd1DdGx45OhqPo79UOJQ1tbEW8ZflE2fbzjSthsF7Q7N1gM9hyyVC8vuMaD4avgiudJZncgxDQkTOKEe17_zVuTyezxCYEd2AjXNJu9KZMP5xD7R_zSM0Iw45. [Accessed 18 July 2024].

[80] Amazon, "OYMSAE 20W 12V Solar Panel Car Battery Charger Portable Waterproof Power Trickle Battery Charger & Maintainer for Car Boat Automotive RV with Cigarette Lighter Plug & Alligator Clip," OYMSAE, [Online]. Available: https://www.amazon.com/POWISER-Waterproof-Maintainer-Automotive-Cigarette/dp/B08CHC1J78/ref=sr_1_2_sspa?crid=L3PRRXRR344I&dib=eyJ2IjoiMSJ9.FBNVIzGtkL4nGFOhv37zyVAqFQuh3hvJedRnPAaK6DDhI7JLTp6cV7oLxke_4bTabObfXngs8WEIANEhRFrcOZ2yK-oWJRfLDE_69ertUsfW0p3EVtuL. [Accessed 19 July 2024].

[81] Amazon, "ECO-WORTHY Solar Panel 25W 12V Monocrystalline Waterproof Panel for Charging 12V Battery of RV Boat Trailer ATV Car or Powering 12V Light, Charing 12V Battery Pack and Other Off-Grid Applications," Eco-Worthy, [Online]. Available: https://www.amazon.com/ECO-WORTHY-Monocrystalline-Waterproof-Charging-Applications/dp/B01IFJ73X4/ref=sr_1_5?crid=L3PRRXRR344I&dib=eyJ2IjoiMSJ9.FBNVIzGtkL4nGFOhv37zyVAqFQuh3hvJedRnPAaK6DDhI7JLTp6cV7oLxke_4bTabObfXngs8WEIANEhRFrcOZ2yK-oWJRfLDE_69ertUsfW0p3E. [Accessed 19 July 2024].

[82] Amazon, "SOLPERK 25W 12V Solar Battery Charger, Waterpoof Solar Panel Kit with Energy Saving Controller for Car RV Trailer Marine Boat Motorcycle Truck Tractor Etc," SOLPERK, [Online]. Available: https://www.amazon.com/SOLPERK-Solar-Battery-Charger-Maintainer-12V-Waterproof-Trickle-Motorcycle/dp/B0CJLR1ZN3/ref=sr_1_26?crid=L3PRRXRR344I&dib=eyJ2IjoiMSJ9.FBNVIzGtkL4nGFOhv37zyVAqFQuh3hvJedRnPAaK6DDhI7JLTp6cV7oLxke_4bTabObfXngs8WEIANEhRFrcOZ2yK-oWJRfL. [Accessed 19 July 2024].

[83] RobotShop, "555 Size DC Motor with Encoder, 12V - 8000 RPM," E-S MOTOR, [Online]. Available: https://www.robotshop.com/products/e-s-motor-555-size-dc-motor-with-encoder-12v-8000-rpm. [Accessed 8 July 2024].

[84] Parts Express, "Mabuchi Type Motor RS-555SH 12V DC Motor (9-15V) 57mm x 36mm," Mabuchi Motor, [Online]. Available: https://www.parts-express.com/Mabuchi-Type-Motor-RS-555SH-12V-DC-Motor-9-15V-57mm-x-36mm-125-566?quantity=1. [Accessed 8 July 2024].

[85] RobotShop, "12V 775 DC Motor w/ High Speed & Big Torque - 4000 RPM," E-S Motor, [Online]. Available: https://www.robotshop.com/products/e-s-motor-12v-775-dc-motor-w-high-speed-big-torque-4000-rpm. [Accessed 8 July 2024].

[86] RobotShop, "R540 6-12V 15000 RPM Brushed DC Motor," OSEPP ELECTRONICS, [Online]. Available: https://www.robotshop.com/products/r540-6-12v-15000-rpm-brushed-dc-motor. [Accessed 8 July 2024].

[87] Texas Instrumens, "L293x Quadruple Half-H Drivers," Texas Instrumens, [Online]. Available: https://www.ti.com/lit/ds/symlink/l293d.pdf?ts=1721481239646&ref_url=https%253A%252F%252Fwww.ti.com%252Fproduct%252FL293D%253Fbm-verify%253DAAQAAAAJ_____96V7uUWmXIdC--z8jILqiZqVxipUwsR-bvFy9ggxbExd9I5YxnPut2Jq0Jn3PxxTnw3HUfSBjbeR2DWMPJD9Jsp1UNQyEtO38kxLkF. [Accessed 20 July 2024].

[88] Texas Instrumens, "DRV88703.6-A Brushed DC Motor Driver (PWM Control)," Texas Instrumens, [Online]. Available: ti.com/lit/ds/symlink/drv8870.pdf?ts=1721517898896&ref_url=https%253A%252F%252Fwww.ti.com%252Fproduct%252FDRV8870%253Fbm-verify%253DAAQAAAAJ_____6-csE8siSOrxBW6EkWzBkkiD9IpFtGjDElhdBJyM5VNmo2jaTLVJru_nza25u5_MUpbnlc7KmQavOd84jtx_hu2evxvaL98-oIYAcZGEfgv52V. [Accessed 20 July 2024].

[89] Toshiba, "TB6612FNG Driver IC for Dual DC motor," Toshiba, 2014. [Online]. Available: https://toshiba.semicon-storage.com/info/TB6612FNG_datasheet_en_20141001.pdf?did=10660&prodName=TB6612FNG. [Accessed 20 July 2024].

[90] Texas Instrumens, "A5950GLPTR-T," DigiKey, [Online]. Available: https://www.digikey.com/en/products/detail/allegro-microsystems/A5950GLPTR-T/6707421?utm_adgroup=&utm_source=google&utm_medium=cpc&utm_campaign=PMax%20Shopping_Product_Medium%20ROAS%20Categories&utm_term=&utm_content=&utm_id=go_cmp-20223376311_adg-_ad-__d. [Accessed 20 July 2024].

[91] T Tulead, "T Tulead Toy Tire Wheels Plastic Wheels Robot Parts 2.6-Inch Diameter Gear Wheel Pack of 12," T Tulead, [Online]. Available: https://www.amazon.com/Tulead-Wheels-Plastic-2-6-Inch-Diameter/dp/B08D3BWW1Z/ref=asc_df_B08D3BWW1Z/?tag=hyprod-20&linkCode=df0&hvadid=692875362841&hvpos=&hvnetw=g&hvrand=15147132910735569835&hvpone=&hvptwo=&hvqmt=&hvdev=c&hvdvcmdl=&hvlocint=&hvlocphy=9198. [Accessed 2024 July 2024].

[92] RobotShop, "All Terrain Robot Wheel 130 x 59 mm (Pair)," JSUMO ULTIMATE ROBOT PARTS , [Online]. Available: https://www.robotshop.com/products/all-terrain-robot-wheel-130-x-59-mm-pair?gad_source=1&gclid=Cj0KCQjwwO20BhCJARIsAAnTIVRAWm1mUAzE3tXLd9EaFAhswn_iAlR-8LgjyFZGBemg2O3MY8OiRK4aAp9DEALw_wcB. [Accessed 21 July 2024].

[93] Studica Robotics , "125mm All-Terrain Robotics Wheel Set," Studica Robotics , [Online]. Available: https://www.studica.com/studica-robotics-brand/125mm-all-terrain-wheel-set?gad_source=1&gclid=Cj0KCQjwwO20BhCJARIsAAnTIVSS4OGxg_beOnvUx88DJe7LSCH59XCbys_LNsItI-6d4FhJxYCCPgUaAhVbEALw_wcB. [Accessed 21 July 2024].

[94] ViaGasaFamido, "DC12V DIY Encoder Gear Motor for Smart Car Robot with Mounting Bracket 65mm Wheel Kit (60RPM)," ViaGasaFamido, [Online]. Available: https://www.amazon.com/gp/product/B08C5J95RZ/ref=ppx_yo_dt_b_asin_title_o00_s00?ie=UTF8&psc=1. [Accessed 21 July 2024].

[95] ARDUINO Team, "Introducing the Arduino MKR WAN 1300 and MKR GSM 1400!," 25 9 2017. [Online]. Available: https://blog.arduino.cc/2017/09/25/introducing-the-arduino-mkr-wan-1300-and-mkr-gsm-1400/. [Accessed 13 7 2024].

[96] ESP, "ESP32-WROOM-32 Datasheet.," [Online]. Available: https://www.espressif.com/sites/default/files/documentation/esp32-wroom-32_datasheet_en.pdf. [Accessed 23 7 2024].

[97] C. Dunn, "How to Build a Raspberry Pi Object Identification Machine," 14 2 2021. [Online]. Available: https://www.tomshardware.com/how-to/raspberry-pi-object-identification. [Accessed 13 7 2024].

[98] Adafruit, "Adafruit 9-DOF Absolute Orientation IMU Fusion Breakout - BNO055," [Online]. Available: https://www.adafruit.com/product/2472. [Accessed 14 7 2024].

[99] AMS, "ams AS5048B High Resolution Position Sensor Position Sensors - ams-osram - ams," [Online]. Available: https://ams-osram.com/products/sensors/position-sensors/ams-as5048b-high-resolution-position-sensor. [Accessed 14 7 2024].

[100] SparkFun, "Ultrasonic Distance Sensor - HC-SR04 - SEN-15569 - SparkFun Electronics," [Online]. Available: https://www.sparkfun.com/products/15569. [Accessed 14 7 2024].

[101] D. Astels, "Overview | Using the Slamtec RPLIDAR on a Raspberry Pi | Adafruit Learning System," [Online]. Available: https://learn.adafruit.com/slamtec-rplidar-on-pi/overview. [Accessed 14 7 2024].

[102] Admin, "How to use TFMini-S LiDAR Distance Sensor with Arduino," [Online]. Available: https://how2electronics.com/how-to-use-tfmini-s-lidar-distance-sensor-with-arduino/. [Accessed 14 7 2024].

[103] J. Hrisko, "Distance Detection with the TF-Luna LiDAR and Raspberry Pi," [Online]. Available: https://makersportal.com/blog/distance-detection-with-the-tf-luna-lidar-and-raspberry-pi. [Accessed 14 7 2024].

[104] R. P. Ltd, "Buy a Raspberry Pi High Quality Camera," [Online]. Available: https://www.raspberrypi.com/products/raspberry-pi-high-quality-camera/. [Accessed 13 7 2024].

[105] J. Silver, "Best Raspberry Pi Camera For Your Project," [Online]. Available: https://randomnerdtutorials.com/best-raspberry-pi-camera-for-your-project/. [Accessed 13 7 2024].

[106] "LASER TREE 455nm 5W Blue Laser Diode," Laser Tree, [Online]. Available: https://lasertree.com/products/laser-tree-455nm-5w-blue-laser-diode?variant=42721566359703&currency=USD&utm_medium=product_sync&utm_source=google&utm_content=sag_organic&utm_campaign=sag_organic&gad_source=1&gclid=Cj0KCQjw-ai0BhDPARIsAB6hmP4cpZiZgyq1g8uj4. [Accessed 8 Jul 2024].

[107] "2pcs 5W 447nm 450nm Blue Powerful 5000mW Laser Diode in 9mm TO-5 Package," Laser Home, [Online]. Available: https://www.ebay.com/itm/134657285374?itmmeta=01J27Z5BJ51T1CR3A36JJQXH2Q&hash=item1f5a331cfe:g:0ugAAOSwwqZktPkL&itmprp=enc%3AAQAJAAAA0F2MGFhrROP3eYRxCdKaW1n8Ub7XxkVmdIk4%2Flcq6o6ZfiGPfyUlqnqWyy%2FbbgEUq%2F6c57hZ0y8ehhbDv%2FHOq%2F5iKBGYaFlBaBmiInoPKFxHpYef. [Accessed 8 Jul 2024].

[108] Ebay, "Sharp GH04C05B9G φ9mm Blue 440nm 445nm 5W Blue Laser Diode," OpticsLD, [Online]. Available: https://www.ebay.com/itm/313800464017?itmmeta=01J27Z5BJ5MA8W85ZX66QC821R&hash=item490ff71691:g:UzwAAOSwF6hlCGhB&itmprp=enc%3AAQAJAAAA4E%2FjkWgOhHuAvVYWdWFFNZ25sgmIyqOW2j05ky3PdFQdDEjdnfr8CdrxopQMIEgXLgT2WdI8mNWp1LO%2BSkYMBhxLrJA6Ca5OzXnucnzpS6ju3U6HwXqX5J. [Accessed 8 Jul 2024].

[109] Amazon, "STEPPERONLINE Nema 17 Stepper Motor Bipolar 2A 59Ncm(84oz.in) 48mm Body 4-lead W/ 1m Cable and Connector compatible with 3D Printer/CNC," STEPPERONLINE, [Online]. Available: https://www.amazon.com/STEPPERONLINE-Stepper-Bipolar-Connector-compatible/dp/B00PNEQKC0/ref=asc_df_B00PNEQKC0/?tag=hyprod-20&linkCode=df0&hvadid=692875362841&hvpos=&hvnetw=g&hvrand=4140014027519187216&hvpone=&hvptwo=&hvqmt=&hvdev=c&hvdvcmdl=&hvlocint=&hvl. [Accessed 18 July 2024].

[110] OpenBuilds, "NEMA 17 Stepper Motor," OpenBuilds, [Online]. Available: https://openbuildspartstore.com/nema-17-stepper-motor/. [Accessed 18 July 2024].

[111] Amazon, "3Pcs DRV8825 Stepper Motor Driver Module Six Different Step Resolutions for 3D Printer RepRap 4 RAMPS1.4 StepStick (3Pcs DRV8825)," WWZMDiB, [Online]. Available: https://www.amazon.com/dp/B0C6P9BCLV?ref=ppx_yo2ov_dt_b_product_details&th=1. [Accessed 18 July 2024].

[112] Amazon, "A4988 Stepper Motor Drive with Heat Sink for Arduino, 3D Printer, CNC Machine or Robotics (3Pcs A4988)," WWZMDiB, [Online]. Available: https://www.amazon.com/WWZMDiB-Stepstick-Stepper-Printer-Suitable/dp/B0BFQZWT6R/ref=sr_1_1_sspa?dib=eyJ2IjoiMSJ9.-DERZWswWeLIrDX-CE6W2dWrIQtjp_cvQ4ctbViX_aBQcn1drgq2zZyAxeP7eJv9NnIKFiEtz_7cwrI6_nU0R8pE1ZxYP5keV-oYCrQiXYDvXAuGAP_NO-GjcuBjev3DPoTrhBnXm1dmw9. [Accessed 18 July 2024].

[113] RBTX, "Autonomous agriculture robot kills weed with laser and drastically reduces weeding costs," RBTX by igus, PONCHON SAS, [Online]. Available: https://rbtx.com/en-US/solutions/ponchon-sas-autonomous-robot-laser-weed-agriculture-delta-robot. [Accessed 7 July 2024].

[114] L. Campbell, "Will Laser-Weeding Robots Change Farming?," 21 1 2022. [Online]. Available: https://modernfarmer.com/2021/12/laser-weeding-robots-laserweeder/. [Accessed 7 7 2024].

[115] R. Saracco, "Robotics and AI for weeding," 5 5 2021. [Online]. Available: https://cmte.ieee.org/futuredirections/2021/05/05/robotics-and-ai-for-weeding/. [Accessed 7 7 2024].

[116] C. BERNIER, "Weeding robots: redefining sustainability in agriculture," 17 7 2023. [Online]. Available: https://howtorobot.com/expert-insight/weeding-robots-redefining-sustainability-agriculture. [Accessed 7 7 2024].

[117] United States Agency for International Development (USAID), "Lithium-Ion Battery Standards," United States Agency for International Development (USAID), [Online]. Available: https://www.usaid.gov/energy/powering-health/technical-standards/lithium-ion-batteries. [Accessed 7 July 2024].

[118] LiPol Battery Co., "What's IEC 62133-2:2017 Certification of Lithium-Ion Battery?," LiPol Battery Co. Ltd., [Online]. Available: https://www.lipolbattery.com/What's-IEC62133-2-2017-Certification-of-Lithium-ion-Battery.html. [Accessed 7 July 2024].

[119] International Electrotechnical Commission, "Battery charge controllers for photovoltaic systems – Performance and functioning," International Electrotechnical Commission, 16 December 2010. [Online]. Available: https://cdn.standards.iteh.ai/samples/15610/04cc35572bec456ba463541a44a22fc3/IEC-62509-2010.pdf. [Accessed 7 July 2024].

[120] United States Agency for International Development, "Photovoltaic System Standards," United States Agency for International Development, [Online]. Available: https://www.usaid.gov/energy/powering-health/technical-standards/photovoltaic-systems. [Accessed 7 July 2024].

[121] IEEE, "IEEE Recommended Practice for," IEEE, 29 January 2004. [Online]. Available: https://ieeexplore.ieee.org/stamp/stamp.jsp?tp=&arnumber=1263344. [Accessed 7 July 2024].

[122] "IEEE Guide: Test Procedures for Direct-Current Machines IEEE std 113-1985, pg 7-27," [Online]. Available: https://ieeexplore.ieee.org/stamp/stamp.jsp?tp=&arnumber=574827. [Accessed 7 July 2024].

[123] "TUV SUD IEC 61508 FUNCTIONAL SAFETY STANDARD," [Online]. Available: https://www.tuvsud.com/en-us/services/functional-safety/iec-61508. [Accessed July 2024].

[124] "IDEC Group Safety Standards," [Online]. Available: https://us.idec.com/RD/safety/law/iso-iec/iec60204. [Accessed July 2024].

[125] H.-D. Reidenbach, "Laser safety," in *Springer Handbook of Lasers and Optics*, 2012, pp. 1569-1600.

[126] IEEE Standards Association, "IEEE SA - IEEE Standard for Design and Verification of Low-Power, Energy-Aware Electronic Systems," [Online]. Available: https://standards.ieee.org/ieee/1801/6767/. [Accessed 7 7 2024].

[127] IEEE Standards Association, "IEEE SA - IEEE Standard for Test Methods for the Characterization of Organic Transistors and Materials," [Online]. Available: https://standards.ieee.org/ieee/1620/3981/. [Accessed 7 7 2024].

[128] IEEE Standards Association, "IEEE SA - IEEE Standard for Rechargeable Batteries for Cellular Telephones," [Online]. Available: https://standards.ieee.org/ieee/1725/4783/. [Accessed 7 7 2024].

[129] IEEE Standards Association, "IEEE SA - ISO/IEC/IEEE International Standard - Software and systems engineering –Software testing –Part 1:Concepts and definitions," [Online]. Available: https://standards.ieee.org/ieee/29119-1/5308/. [Accessed 8 7 2024].

[130] OpenAI, "ChatGPT," OpenAI, [Online]. Available: https://www.openai.com. [Accessed 7 July 2024].

[131] D. R. Grimm, Y.-J. Lee, L. Liu, O. Garcia, K. Balakrishnan and N. F. Ayoub, "The utility of ChatGPT as a generative medical translator," *Springer Link*, vol. 281, no. 8, 2024.

[132] S. M. Derus and A. Z. Ali, "DIFFICULTIES IN LEARNING PROGRAMMING: VIEWS OF STUDENTS," *1st International Conference on Current Issues in Education*, 2012.

[133] D. Goodwin, "Google AI Overviews under fire for giving dangerous and wrong answers," 24 5 2024. [Online]. Available: https://searchengineland.com/google-ai-overview-fails-442575. [Accessed 7 7 2024].

[134] J. Gladd, "How Large Language Models (LLMs) like ChatGPT Work," 8 202. [Online]. Available: https://idaho.pressbooks.pub/write/chapter/how-large-language-models-llms-like-chatgpt-work/. [Accessed 23 7 2024].

[135] A. Zewe and M. I. of Technology, "Beyond Human: MIT Experts Explain Generative AI and the ChatGPT Phenomenon," 9 11 2023. [Online]. Available: https://scitechdaily.com/beyond-human-mit-experts-explain-generative-ai-and-the-chatgpt-phenomenon. [Accessed 23 7 2024].

[136] S. Wolfram, "What Is ChatGPT Doing … and Why Does It Work?," 14 2 2023. [Online]. Available: https://writings.stephenwolfram.com/2023/02/what-is-chatgpt-doing-and-why-does-it-work/. [Accessed 23 7 2024].

[137] PBZ, "Aluminum vs. Steel Patio Furniture," A Paul B. Zimmerman, Inc, [Online]. Available: https://pbzmfg.com/blog/aluminum-vs-steel-patio-furniture/#:~:text=Choosing%20aluminum%20for%20your%20outdoor,as%20the%20lightest%20steel%20material.. [Accessed 22 July 2024].

[138] Raspberry Pi Ltd., "Raspberry Pi Documentation," Raspberry Pi Ltd., 2024. [Online]. Available: https://www.raspberrypi.com/documentation/computers/raspberry-pi.html#recommended-power-supplies. [Accessed 22 July 2024].

[139] Texas Instruments, "TPS40200-Q1 Wide-Input-Range Nonsynchronous Voltage-Mode Controller," Texas Instruments, January 2016. [Online]. Available: https://www.ti.com/lit/ds/symlink/tps40200.pdf?ts=1721523802946&ref_url=https%253A%252F%252Fwww.ti.com%252Fproduct%252FTPS40200%253Fbm-verify%253DAAQAAAAJ_____5q3bdpSseRl7YiuRc1I4bw_vkjKXNKoqEkAVdKoRbW_-xv6562N4HyDfxTcCk5qhXkaEx6ug9YiTBP88PK4Uz53j4lZg-yIA. [Accessed 22 July 2024].

[140] Infeon Technologies, "BTS 7960 High Current PN Half Bridge," December 2004. [Online]. Available: https://image.dfrobot.com/image/data/DRI0018/BTS7960.pdf.

[141] "Collimating Lens," IADIY, [Online]. Available: https://www.iadiy.com/collimating-lenses. [Accessed 20 July 2024].

[142] "Double Convex Lens," WTS Photonics, [Online]. Available: https://www.wts-photonics.com/high-presion-double-convex-lenses-and-bi-convex-lenses_p70.html. [Accessed 23 July 2024].

[143] A. Masley, "Light Intensity - IB Physics," 2019. [Online]. Available: https://www.youtube.com/watch?app=desktop&v=fGynXsoSA3U. [Accessed 20 July 2024].

[144] Z. Ma, S. Li, M. Zhang, S. Jiang and Y. Xiao, "Light Intensity Affects Growth, Photosynthetic Capability, and Total Flavonoid Accumulation of Anoectochilus Plants," *Ashs*, vol. 45, no. 6, pp. 863-867, 2010.

[145] R. Paschotta, "Optical Intensity," *RP Photonics*, vol. 10, no. 61835.

[146] O. 4. L. E. Laboratory, "Experiment #1: The HeNe Laser and Gaussian Beam Propagation," The College of Optics and Photonics University of Central Florida, Orlando.

[147] Makerguides, "How to control a stepper motor with DRV8825 driver and Arduinos," Makerguides.com, [Online]. Available: https://www.makerguides.com/drv8825-stepper-motor-driver-arduino-tutorial/. [Accessed 22 July 2024].

[148] M. McCauley, "AccelStepper library for Arduino," AirSpayce Pty Ltd., 2021. [Online]. Available: https://www.airspayce.com/mikem/arduino/AccelStepper/index.html. [Accessed 22 July 2024].

[149] micro-ROS, "micro-ROS," [Online]. Available: https://github.com/micro-ROS. [Accessed 23 7 2024].

[150] RoboFoundary, "ESP32 — micro-ROS actually working over WiFi and UDP Transport," 29 8 2023. [Online]. Available: https://robofoundry.medium.com/esp32-micro-ros-actually-working-over-wifi-and-udp-transport-519a8ad52f65. [Accessed 23 7 2024].

[151] ROS Wiki, "slam_toolbox - ROS Wiki," [Online]. Available: https://wiki.ros.org/slam_toolbox. [Accessed 23 7 2024].

[152] TensorFlow 2 Object Detection, "TensorFlow 2 Object Detection API tutorial — TensorFlow 2 Object Detection API tutorial documentation," [Online]. Available: https://tensorflow-object-detection-api-tutorial.readthedocs.io/en/latest/. [Accessed 22 7 2024].

[153] OpenCV, "OpenCV library," 2019. [Online]. Available: https://opencv.org/. [Accessed 22 7 2024].

[154] learn.adafruit.com, "Overview | Running TensorFlow Lite Object Recognition on the Raspberry Pi 4 or Pi 5 | Adafruit Learning System," [Online]. Available:

https://learn.adafruit.com/running-tensorflow-lite-on-the-raspberry-pi-4/overview. [Accessed 22 7 2024].

[155] MakerFocus, "MakerFocus TFmini-S Lidar Single-Point Micro Ranging Module Compatible with Pixhawk Arduino," [Online]. Available: https://www.makerfocus.com/products/tfminis-lidar-single-point-micro-ranging-module?variant=31319463166029. [Accessed 14 6 2024].

[156] L. TREE, "LASER TREE 455nm 5W Blue Laser Diode," [Online]. Available: https://lasertree.com/products/laser-tree-455nm-5w-blue-laser-diode. [Accessed 14 6 2024].

[157] L. Tree, "Laser Tree 639nm 2100mW High Power Red Laser Diode with FAC Linear," [Online]. Available: https://lasertree.com/products/laser-tree-639nm-2100mw-high-power-red-laser-diode-with-fac-linear?currency=USD&variant=43018420682903&utm_source=google&utm_medium=cpc&utm_campaign=Google%20Shopping&stkn=0333ab05951a&gad_source=1&gclid=CjwKCAjw1K-zBhBIEiwA. [Accessed 14 6 2024].

[158] L. Tree, "Laser Tree 530nm 1400mW High Power Green Laser Diode," [Online]. Available: https://lasertree.com/products/laser-tree-530nm-1400mw-high-power-green-laser-diode?currency=USD&variant=43287566647447&utm_source=google&utm_medium=cpc&utm_campaign=Google%20Shopping&stkn=0333ab05951a&gad_source=1&gclid=CjwKCAjw1K-zBhBIEiwAWeCOF1in9hM1hX. [Accessed 14 6 2024].

[159] HUSETOO, "40W 12V DC Motor with High Torque, Metal Gear, and Bearings, Upgrade Bracket (2-Pack)," [Online]. Available: https://www.amazon.com/Torque-Bearings-Upgrade-Bracket%EF%BC%89-Motors-2Pack/dp/B0BW73XTKJ/ref=sr_1_6?crid=Y21TU0RXDFRL&dib=eyJ2IjoiMSJ9.N6d-6s-atylgxy_OF9DSAhW4Nn6X_fdBEDdNA75YAsMNeIgsmMY1Qc7vBwzmm9IkgoA3yoR1cgatLxqnz0WR17JZAr0zgNICoZEfE1on_-9xNnalPANWJ. [Accessed 14 6 2024].

[160] LewanSoul, "LewanSoul DIY Robot Chassis Kit, Intelligent Aluminum Alloy Chassis, Unassembled," [Online]. Available: https://www.amazon.com/LewanSoul-Chassis-Intelligent-Aluminum-Unassembled/dp/B08LK1RDXM/ref=sr_1_7?dib=eyJ2IjoiMSJ9.ChfshA6U4JkJ_bQzDBgVrre5OIDqG29jGaTIipcvVXEAwkylVra7OOQArRLGLBKSZeZOTn5erDdVHNd4OcMJzWqYYLRHZhusDXNR7BV3jOq5CRcQ_ewZIGwIFx2M4sYvmpzMzKK9IV. [Accessed 14 6 2024].

[161] R. Ltd, "Buy a Raspberry Pi 5," [Online]. Available: https://www.raspberrypi.com/products/raspberry-pi-5/. [Accessed 14 6 2024].

[162] XZNY, "XZNY LiFePO4 Battery 12V 7Ah Rechargeable Battery, Suitable for Emergency Lighting, RV, Solar, and Marine Applications," [Online]. Available: https://www.amazon.com/XZNY-LiFePO4-Rechargeable-Suitable-Emergency/dp/B09Q8B8MLR/ref=asc_df_B09Q8B8MLR/?tag=hyprod-20&linkCode=df0&hvadid=693464962511&hvpos=&hvnetw=g&hvrand=6665958920215736048&hvpone=&hvptwo=&hvqmt=&hvdev=c&hvdvcmdl=&hvlocint=&hvlocphy=. [Accessed 14 6 2024].

[163] B. Electronics, "BOJACK Electronics Kit with Potentiometer, Tie-Points Breadboard, and Various Electronic Components," [Online]. Available: https://www.amazon.com/BOJACK-Electronics-Potentiometer-tie-Points-Breadboard/dp/B099MQV8ZW/ref=sr_1_1_sspa?crid=1KZMKNSOQP60P&dib=eyJ2IjoiMSJ9.SX_rNAG2gCZaeTO8QQuYqfO1FWiB4_htcMYIndDX0bhYf7upOzLv9RMxzZxVfHRMoLpjvAyNowiCkinQYbyWAZ3MXQQazCKshfthaffD5j_NaZF. [Accessed 14 6 2024].

[164] NERMAK, "Solar Battery Maintainer and Controller, Waterproof for Automotive and Motorcycle Applications," [Online]. Available: https://www.amazon.com/Maintainer-Controller-Waterproof-Automotive-Motorcycle/dp/B0CQMTCDTL/ref=asc_df_B0CQMW1Z5N/?tag=hyprod-20&linkCode=df0&hvadid=693071376145&hvpos=&hvnetw=g&hvrand=7528158914428673620&hvpone=&hvptwo=&hvqmt=&hvdev=c&hvdvcmdl=&hvlocint=. [Accessed 14 6 2024].

[165] Raspberry Pi Foundation, "Getting started with the Camera Module," Raspberry Pi Foundation, [Online]. Available: https://projects.raspberrypi.org/en/projects/getting-started-with-picamera/4. [Accessed 22 July 2024].

Appendix B – Copyright Permissions

For Figure 11 - © Wikimedia Commons / Daniele Pugliesi, M0tty.

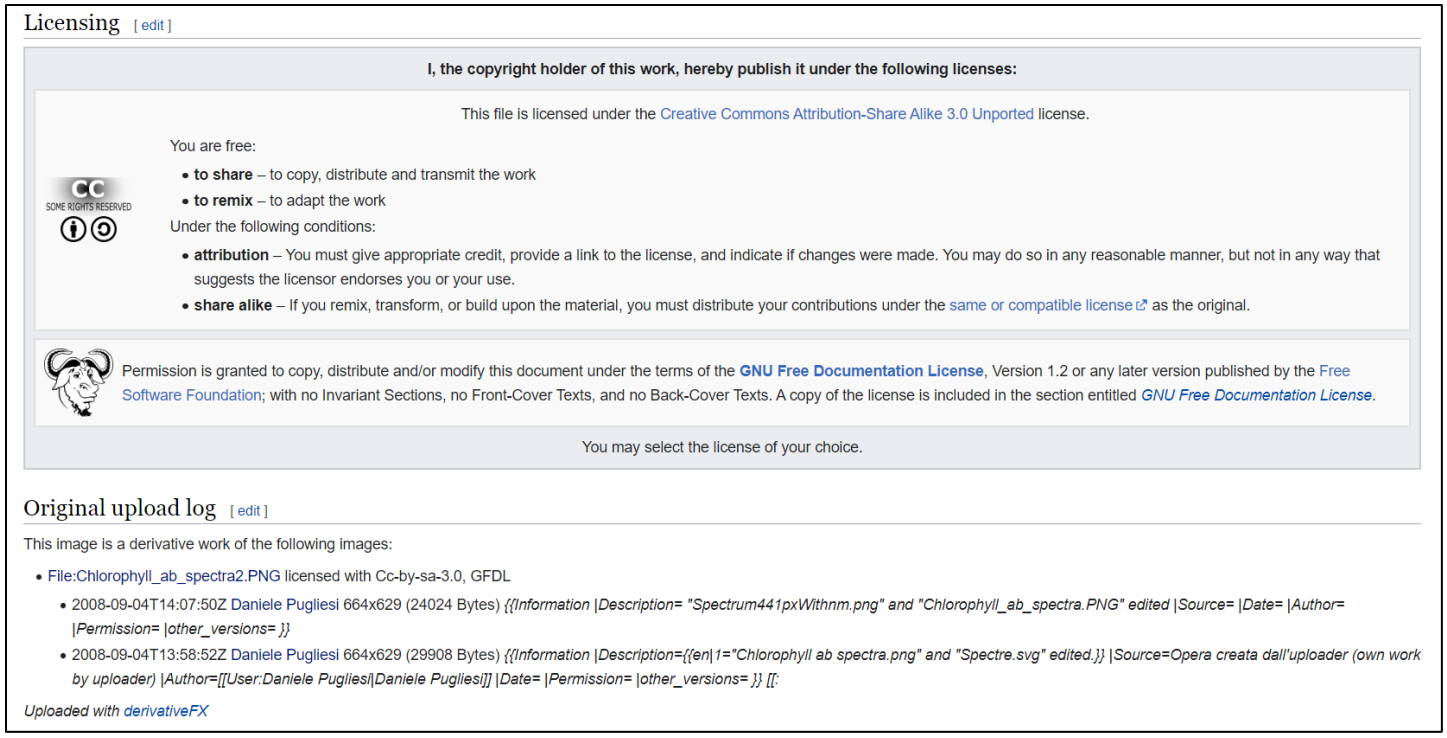

Licensing [edit]

I, the copyright holder of this work, hereby publish it under the following licenses:

This file is licensed under the Creative Commons Attribution-Share Alike 3.0 Unported license.

You are free:

- **to share** – to copy, distribute and transmit the work
- **to remix** – to adapt the work

Under the following conditions:

- **attribution** – You must give appropriate credit, provide a link to the license, and indicate if changes were made. You may do so in any reasonable manner, but not in any way that suggests the licensor endorses you or your use.
- **share alike** – If you remix, transform, or build upon the material, you must distribute your contributions under the same or compatible license as the original.

Permission is granted to copy, distribute and/or modify this document under the terms of the **GNU Free Documentation License**, Version 1.2 or any later version published by the Free Software Foundation; with no Invariant Sections, no Front-Cover Texts, and no Back-Cover Texts. A copy of the license is included in the section entitled *GNU Free Documentation License*.

You may select the license of your choice.

Original upload log [edit]

This image is a derivative work of the following images:

- File:Chlorophyll_ab_spectra2.PNG licensed with Cc-by-sa-3.0, GFDL
  - 2008-09-04T14:07:50Z Daniele Pugliesi 664x629 (24024 Bytes) *{{Information |Description= "Spectrum441pxWithnm.png" and "Chlorophyll_ab_spectra.PNG" edited |Source= |Date= |Author= |Permission= |other_versions= }}*
  - 2008-09-04T13:58:52Z Daniele Pugliesi 664x629 (29908 Bytes) *{{Information |Description={{en|1="Chlorophyll ab spectra.png" and "Spectre.svg" edited.}} |Source=Opera creata dall'uploader (own work by uploader) |Author=[[User:Daniele Pugliesi|Daniele Pugliesi]] |Date= |Permission= |other_versions= }} [[:*

Uploaded with derivativeFX

Appendix C – Software Code

Testing for NEMA 17 stepper motors

```
// Include the AccelStepper Library
#include <AccelStepper.h>

// Define pin connections
const int dirPin = 2;
const int stepPin = 3;

// Define motor interface type
#define motorInterfaceType 1
```

```
// Creates an instance
AccelStepper myStepper(motorInterfaceType, stepPin, dirPin);

void setup() {
  // set the maximum speed
  // initial speed
  myStepper.setMaxSpeed(1000);
  myStepper.setSpeed(75);
}

void loop() {
  // Move the motor one step
  myStepper.runSpeed();
}
```

Testing for RGB Camera [165].

```
from picamera2 import Picamera2, Preview
from time import sleep

picam2 = Picamera2()
picam2.start_preview(Preview.QTGL)
picam2.start()
sleep(5)
picam2.close()
```